MAGYAR ÁLLAMI
EÖTVÖS LORÁND
GEOFIZIKAI INTÉZET

GEOFIZIKAI
KÖZLEMÉNYEK

ВЕНГЕРСКИЙ
ГЕОФИЗИЧЕСКИЙ
ИНСТИТУТ
ИМ Л. ЭТВЕША

ГЕОФИЗИЧЕСКИЙ
БЮЛЛЕТЕНЬ

BUDAPEST

GEOPHYSICAL
T R A N S A C T I O N S
EÖTVÖS LORÁND GEOPHYSICAL INSTITUTE OF HUNGARY

CONTENTS

TARTALOMJEGYZÉK

International deep reflection survey along the Hungarian Geotraverse

Károly POSGAY[*],

Ernő TAKÁCS, István SZALAY[*], Tamás BODOKY[*], Endre HEGEDŰS[*],
J. Ilona KÁNTOR[*], Zoltán TIMÁR[*], Géza VARGA[*],
István BÉRCZI[**], Árpád SZALAY[**], Zoltán NAGY[**], Antal PÁPA[**],
Zoltán HAJNAL[***], Brian REILKOFF[***],
Stephan MUELLER[****], Joerg ANSORGE[****], Remo DE IACO[****],
Isa ASUDEH[+]

Low-frequency seismic reflection investigations of the lithosphere were conducted in SE Hungary with *Hungarian, Canadian and Swiss* cooperation during 1992. The profile PGT-4 (part of the Hungarian Geotraverse Project), starting at the eastern flank of the Algyő High (near the town of Szeged), crossed
—the Hódmezővásárhely-Makó Graben,
—the Pusztaföldvár-Battonya Ridge and
—the Békés Basin (Fig. 1).
The Neogene sediments of both the Hódmezővásárhely-Makó Graben and the Békés Basin have a thickness of 6–7 km. A NE dipping shear zone, which may be traced into the lower lithosphere, marks the eastern margin of the Algyő High.
Integrated interpretation of seismic (related profile PGT-1), regional geothermal, geomagnetic and gravity data reveals an elevation in the lower crust, the crust-mantle and the lithosphere–asthenosphere boundary, as well as magmatic intrusions which protrude as high as the upper crust beneath the Békés Basin. Deep reflection and magnetotelluric data along the PGT-4 indicate an anomalous rise of the lithosphere–asthenosphere boundary: a *domal uplift of the asthenosphere*, beginning at the NE termination of the profile. Beneath the Hódmezővásár-

* Eötvös Loránd Geophysical Institute of Hungary (ELGI), Budapest
** Hungarian Oil and Gas Company LTD (MOL RT), Budapest
*** University of Saskatchewan, Saskatoon, Canada
****Institute of Geophysics, Swiss Federal Institute of Technology (ETH), Zürich
+ Geological Survey of Canada, Ottawa

hely–Makó Graben both the crust–mantle and the lithosphere–asthenosphere boundaries form a minor uplift slightly westward from the Hódmezővásárhely-Makó Graben.

Low-frequency seismic reflection measurements within the Carpathian Basin outline a *sketch of the complete lithosphere*, suggestive of tectonic *development* described by low angle *extensional basin* forming models. Analogously to this Basin and Range type extensional model, the Hódmezővásárhely-Makó Graben and the Dorozsma Graben (to the southwest) were formed as a consequence of major penetrating shear zones and upswell of the lower crust and the lithosphere–asthenosphere boundary.

In addition to this *new tectonic model*, intriguing structures were mapped, at those depths which may be effective targets for *oil and gas* exploration.

1. Introduction

Deep seismic reflection experiments initiated in Hungary in the early 70's utilized low frequencies which penetrated the complete lithosphere and, in some localities, segments of the asthenosphere. One of the main objectives of these investigations was to generate observable signals at frequencies down to 2–4 Hz. Instead of adopting low cut filters, the signal to surface wave amplitude ratios were improved by placing explosive sources in 50–70 m boreholes and implementing specific velocity filtering. Processing with true amplitude recovery was achieved by applying spherical correction. Within the first experiments (line KA in *Fig. 1*), expanding spread survey configurations enabled us to infer that reflections can be received from the upper mantle. Relying on interval velocities derived from seismic signals, we were able to estimate the depth of the lithosphere–asthenosphere boundary [POS-GAY 1975]. Along the deep reflection profile KESZ-1 (Biharkeresztes area, near Debrecen, Fig. 1) seismic signatures suggested a deep fracture zone dissecting the entire lithosphere [POSGAY et al. 1981, POSGAY et al. 1986], and located in a region coinciding with a known major tectonic line of significant strike-slip component [GROW et al. 1989]. The results of the southern part of the reflection profile PGT-1 [POSGAY et al. 1990] indicated an upswelling of the crust-mantle and the lithosphere–asthenosphere boundaries beneath the Békés Basin [POSGAY et al. 1995].

Most recently these investigations were extended through an international seismic experiment with the collaboration of Hungarian, Canadian and
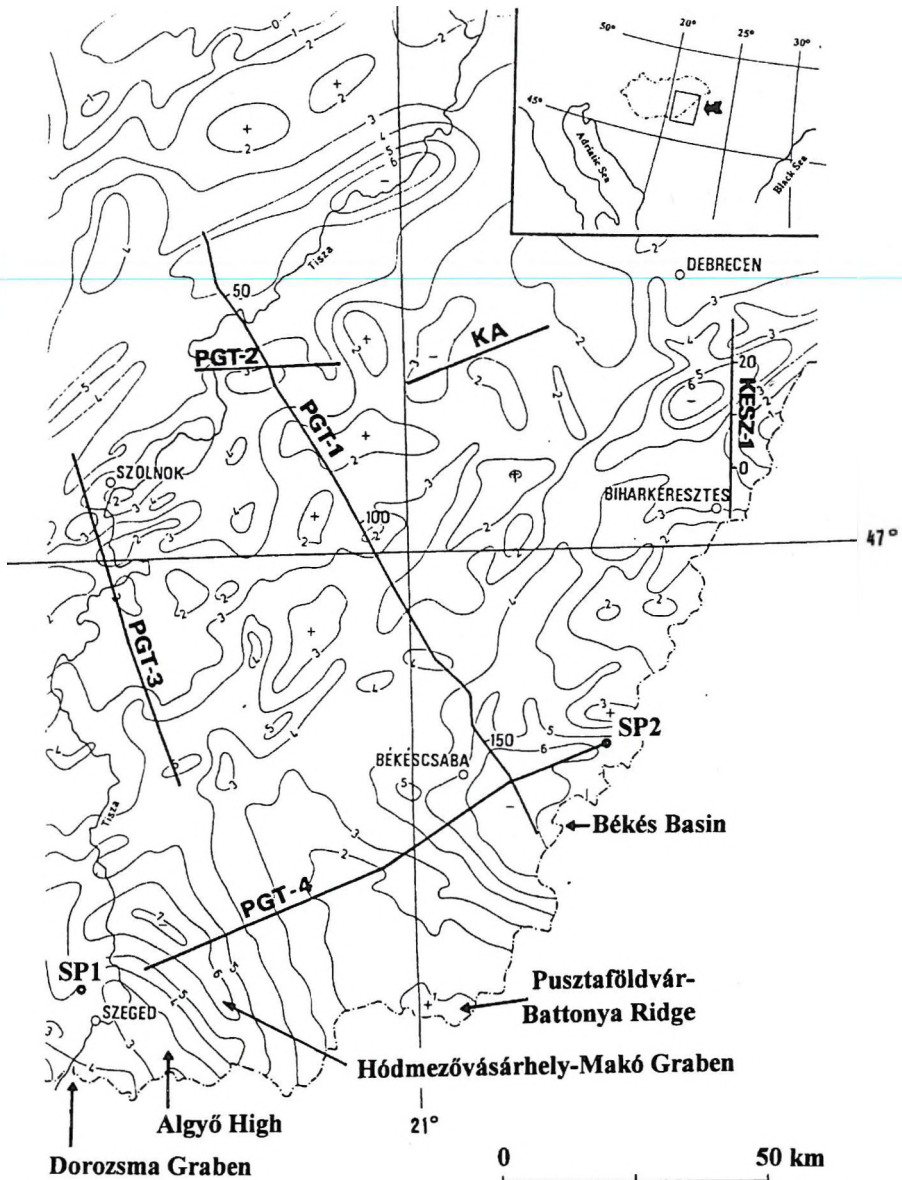
Fig. 1. Location of the deep seismic reflection lines in SE Hungary. Also shown is the contour map of the basement (pre-Tertiary rocks) compiled by KILÉNYI et al. [1991]. Contour lines of the basement in km

1. ábra. DK Magyarországon végzett mélyreflexiós kutatások helyszínrajza a pre-tercier medencealjzat [KILÉNYI et al., 1991] mélységtérképén. A szintvonalak értékközét km-ben írtuk fel

Swiss investigators. Efforts were made to further increase the penetration of deep reflection measurements by shifting the frequency range (approx. one octave) further towards lower frequencies. The data acquisitions were along the reflection profile PGT-4 (Fig. 1). This profile passes over two sub-basins of the inner Carpathians: the Hódmezővásárhely–Makó Graben and the Békés Basin, as well as the domal uplift separating them. The location of the survey line was chosen to map deep structures beneath this rapidly-developed region of the inner Carpathians. A special aim of the study was to gain a better insight on the origin and formation of the sedimentary sub-basins, their associated thermal and tectonic processes, injection of fluids, and the development structural traps within the lower segments of these features.

Researchers from a number of institutions contributed to the planning, execution, processing and interpretation of the data set:

— Eötvös Loránd Geophysical Institute (Hungary).

— LITHOPROBE, Canada,

— Department of Geological Sciences, University of Saskatchewan (Canada),

— Institut für Geophysik, Eidgenössische Technische Hochschule (Switzerland),

— Continental Geoscience Division, Geological Survey of Canada.

2. Seismic data acquisition and processing

The deep reflection data acquisition along seismic profile PGT-4 (Fig. 1) was conducted in September and October 1992. Seismic sources consisted of 50 kg chemical explosives, detonated in 70 m boreholes. The seismic signals were observed in three, coeval but different survey and recording configurations (*Fig. 2*).

In the first survey format 195 PRS (Portable Recording System, Canada) type recording units were deployed. Spacing of the detectors was 100 m. Each twenty first unit had three-component signal detection capability (PRS-4). The seismometers of the PRS units had an unattenuated natural frequency of 2 Hz. The low-frequency transmission limit of this recording equipment started practically at 0 Hz. The digital sampling frequency was 120 Hz with an observation time of 60 s. To achieve a more favourable signal to noise ratio field operations were performed at nights only. During this
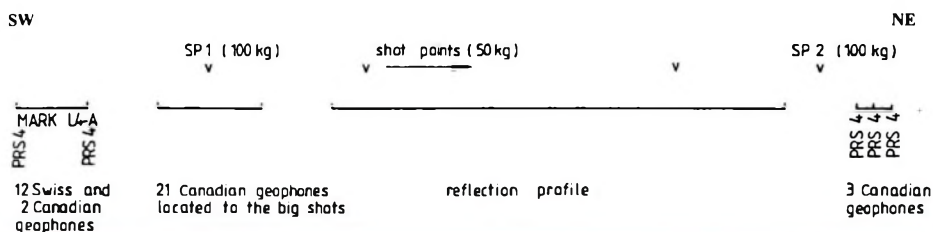
Fig. 2. Reflection survey configuration of deep reflection profile PGT-4 along the Hungarian Geotraverse. Shots were observed in 3 different arrangements

2. ábra. A Magyar geotraverz menti, PGT-4 mélyreflexiós szelvény észlelési vázlata. A robbantásokat 3 rendszerben észleltük

time-period the spread remained stationary, with detonations at alternate source locations. A total of 288 shots were observed along 15 spreads.

In the second survey arrangement observations were conducted with a 160 channel MDS-18 type (Halliburton Geophysical Services, USA) telemetric instrument and detector array spacing of 50 m. Each detector array was formed by 5 seismometers, having an unattenuated natural frequency of 4.5 Hz. The digital data sampling rate was 4 ms (high cut filter of 93 Hz), the recording time 48 s. Survey spreads of this data acquisition format were laid out parallel with the previous configuration.

The third data collection was provided by two stationary seismic arrays at the west and east ends of the survey line. At the west end 2 PRS-4 units and 12 L4-A detectors (MARK Products, USA) were deployed with ELGI's telemetric system; at the east end 3 PRS-4 units provided the data acquisition. The ELGI system (low-frequency transmission characteristics: at 1 Hz was –3 dB) recorded 48 s of data with a sampling rate of 8 ms. All PRS-4 units observed 100 s of data. The survey was completed with the detonation of 100 kg charges at both ends of the profile (Fig. 2).

The different data sets were processed and interpreted in the laboratories of the cooperating institutions. ELGI's staff processed the data observed by the first and second systems, with special attention to structures of Neogene sediments and of the underlying lithosphere. This presentation relies only on results generated by the Hungarian participants. Processing and consequent presentation of the results of the first system were provided by the Canadian contributors in a special issue of Tectonophysics [HAJNAL et al. 1996].

Synthesis of the stationary and transverse data — gathered in the third system — was the task of the Swiss members. The results are still being worked on.

In the course of processing reflection data at ELGI's laboratory, an attempt was made to obtain true amplitude images (no automatic amplitude control was applied). These data were subjected to velocity and wide-band (2–5, 29–32 Hz) filtering, spherical divergence correction and editing. (Efforts were directed towards suppressing surface waves through specially developed coherent noise adaptive filtering and through a more careful cutting of the surface wave prior to summing, thereby to avoid the weakening of low frequency deep reflections by low-cut filtration). Velocity depth functions of the Neogene sedimentary complexes were established from refraction arrivals — appearing in the 18 km long spreads — and utilization of the areal velocity–depth functions of hydrocarbon exploration, from the same area of consideration. Where wireline well logging data were not available, and in the crystalline crust and the upper mantle, interval velocities were determined from the expanding spread data of profile KESZ-1 [POSGAY et al. 1981, POSGAY et al. 1995]. Stacked data were subjected to f–k domain filtration, f–x deconvolution and the weighted 2D median filtering. One of the post stack processing steps was the application of 45° finite-difference time migration.

The first 6 s of the information of the second system was processed with frequency band limits of 4-60 Hz (Figs. 3–6). No f–k domain filtering was applied and a minimum phase predictive deconvolution filtering was implemented to replace f–x deconvolution and weighted 2D median filtering.

3. Regional structural sketch

The pre-Neogene floor of the Carpathian Basin is constituted by tectonic 'terranes' formed in various parts of the Tethys sea. The region of this investigation falls on the Tisza terrane. The origin and present site of this unit were established through concentrated paleogeographic, biostratigraphic, paleomagnetic, paleokinematic, sedimentologic and facies studies [KOVÁCS 1982, BALLA 1984, CSONTOS et al. 1992]. Although there are a number of contentious issues still remaining to be solved, all the investigators agree that the Tisza terrane more likely originates from the European (northern) side of the Tethys, at the time of the Alpine-Carpathian orogeny [STEGENA et al. 1975, MÁRTON 1981, HORVÁTH and ROYDEN 1981]. In that part of the Tisza terrane which falls within the survey area, the

pre-Neogene basement includes continuation of the Codru nappe system, which is exposed in the outcrops in the Apuseni Mountain of the Transylvanian Middle Range [SZEDERKÉNYI et al. 1991]. The upthrusts of these units occurred in the upper Cretaceous (Middle-Upper Turonian, GYÖRFI 1994), with a N vergence, during the impact of the Alpine compressional phases. On the basis of the stratigraphic and facies character of these strata, five structural units can be distinguished. They are, from the bottom upwards: Mecsek–northern part of the Great Hungarian Plain zone, Villány–Bihar zone, Papuk–Békés–Lower Codru zone, Northern Bácska–Upper Codru zone, and Nagybihar zone. These structural units contain both Mesozoic and metamorphic Paleozoic and older series, except the Nagybihar zone, where no Mesozoic formations are known.

The pre-Neogene basement of the Carpathian Basin was formed in the Paleogene. Along the boundaries of the developing terranes (and within their interior as well) major shear zones were formed as a consequence of the irregular transpressional movements between the various units. Results of deep seismic measurements reveal that these wrench faults dissect the entire crust and in some cases penetrate the lithospheric segment of the mantle [POSGAY and SZENTGYÖRGYI 1991].

At the end of Paleogene—beginning of Miocene, the Tisza terrane may have reached its present location [CSONTOS et al. 1992]. Tectonic processes leading to the formation of the Carpathian Basin (Pannonian Basin system) were initiated in the Late Oligocene and/or in the Early Miocene and culminated during the Middle Miocene [CSONTOS et al. 1991, HORVÁTH 1993]. The 'back arc' extension of the Carpathian Basin is contemporaneous with the formation of the Outer-Carpathian flysch belt. The synrift phase (active extension) within the Carpathian Basin — according to one estimate — started from 22 Ma [GROW et al. 1994], the other estimate [TARI et al. 1992] is 17.5 Ma, and extended either to 12 Ma [HORVÁTH and POGÁCSÁS 1988], or to 10.5 Ma [TARI et al. 1992, HORVÁTH et al. 1988]. The postrift phase is still going on.

Numerical modelling of the evolution of the Great Hungarian Plain shows that a moderate crustal extension (stretching parameter less than 2.2), combined with a major thinning (or heating) of the mantle lithosphere (the stretching parameter is bigger by one order of magnitude), has controlled the formation of the basin [HORVÁTH et al. 1988]. Modelling of the subsidence of the sedimentary sequences of the Hódmezővásárhely-I deep borehole

provided figures between 11 Ma and 0 Ma with values of $\beta_c = 2.2$ for the crust, and $\beta_m = 19$ for the mantle lithosphere [HORVÁTH 1986].

4. The Neogene complex

The depth section derived from data recorded with PRS stations — in the first observation system — is shown in *Encl. 1*. One possible interpretation of it is presented in *Encl. 2*. The depth section obtained from data of the MDS-18 equipment — second system — is provided in *Encl. 3*. Interpretation of these data is given in *Encl. 4* with some interpretive concepts taken from Encl. 2. The differences in instrument responses and spread parameters are reflected in the sections. The PRS section gives a more conspicuous image of the deep structure, while the MDS section highlights the sedimentary strata, the floor of the basin and the fractures within the sub-basin sequences. Magnetotelluric results are also given in Encls. 2 and 4. Crosses in the vicinity of the bottom of the Neogene basin are indicative of the high resistivity beneath the basin.

An accurate correlation of Neogene sediments, deposited in the Hód-mezővásárhely–Makó Graben and in the Békés Basin, would be of interest for the reconstruction and comparison of the development of these two basins. However, sediments deposited at greater depths cannot be directly correlated along the profile because the Pusztaföldvár–Battonya pre-Neogene ridge separates them (*Fig. 3*). A number of relevant studies based on earlier data sets are, however, available in the literature. Incorporation of these concepts into the present synthesis is revealed in *Fig. 4*. Age data received from seismo-, sequence- and magnetostratigraphy, as well as radiometric age determinations were marked at the end of the profile, based on data from VAKARCS et al. [1994]; at the crossing of PGT-1 and PGT-4 the information is from MATTICK et al. [1994]. The interpretation at the deep drilling site 1 is taken from MATTICK et al. [1988]. As the scope of understanding on the sedimentary infill within the basins has increased, so the regional correlation of individual complexes has also progressed. It is now recognised that sedimentation was provided to the basins from a variety of directions NE, N, NW, W and S [MATTICK et al. 1994]. In that it was unlikely that there would be any direct correlation of all the phases within the two basins, direct correlation was not attempted. As a consequence of these complexities the most comprehensive interpretation of the sedimentary sequences along
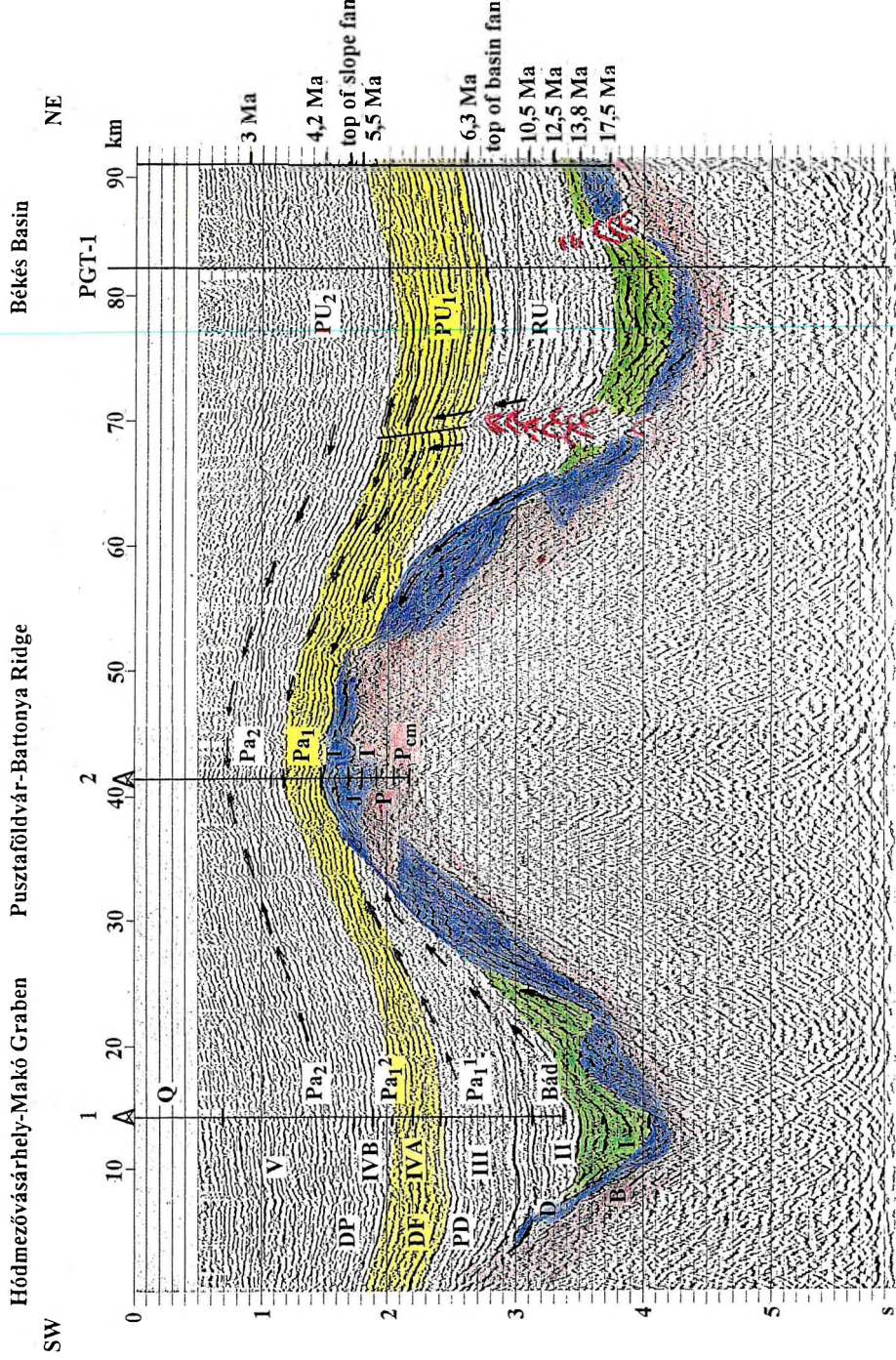
Hódmezővásárhely-Makó Graben   Pusztaföldvár-Battonya Ridge   Békés Basin

SW   NE

3 Ma
4,2 Ma
top of slope fan
5,5 Ma
6,3 Ma
top of basin fan
10,5 Ma
12,5 Ma
13,8 Ma
17,5 Ma

Fig. 4. Interpretation of the section of Fig. 3. Delta sediments are indicated in yellow, a complex interpreted as Lower Badenian–Lower Miocene in green, and the Mesozoic sediments of the pre-Neogene basement in blue. Black arrows show the assumed direction of oil and gas migration. It can be assumed that from high pressure beds of the Békés Basin hydrocarbon migrated in fractured, fissured reservoirs formed on elevated parts of the pre-Neogene basement, further on, in reservoirs formed in Neogene sediments

4. ábra. A 3. ábrán látható szelvény értelmezése. A delta üledékeket sárga, egy értelmezésünk szerinti alsóbádeni–alsómiocén összletet zöld és a preneogén medencealjzat mezozoós üledékeit kék színnel jelöltük. Fekete nyilakkal a olaj és gáz migráció feltételezett irányát érzékeltettük. Feltételezhető, hogy a Békési medence nagynyomású rétegeiből szénhidrogén migrált a preneogén medencealjzat magasabb részein kialakult töréses, repedezett, továbbá a neogén üledékekben kialakult tárolókba.

PGT-4 and more specifically within the two basins demanded the establishment of local stratigraphic concepts. In *Table I* the names generally accepted in seismostratigraphic investigations are shown together with the international chronostratigraphic boundaries most widely known in Hungary, and with those used in the practice of hydrocarbon exploration.

The last substantial phase of basin infill — the *Late Progradational Unit* (PU_2, MATTICK et al. 1994) — corresponds to the *Delta Plain Facies*, i.e. to the sequencies *IV.B and V* of MATTICK et al. [1988]. Sediments deposited during this period (over 4 Ma) are present along the whole length of the profile (Encls. 1 - 4, also Figs. 3 and 4).

In the middle of the Pannonian epoch (6–7 Ma) delta sediments began to fill in the Békés Basin [POGÁCSÁS et al. 1994] and the Hódmezővásárhely–Makó Graben. At the beginning of the epoch the decrease of water depth may have exceeded 200 m. A relatively intensive sedimentation in the Hódmezővásárhely–Makó Graben started somewhat earlier than in the Békés Basin [VAKARCS et al. 1994]. The *Early Progradational Unit (PU_1,* MATTICK et al. 1994) was interpreted by us as a contemporaneous deposit to the *Delta Front Facies* or *sequence IV.A* [MATTICK et al. 1988]. Reflection signatures which originated from this sedimentary interval of the subsurface appear with significant amplitudes and characteristic stratal termination patterns and stratal discontinuities. In Encls. 2 and 4 as well as in Fig. 4 these band reflections are marked in yellow. The lower levels of the sequence onlap the Pusztaföldvár–Battonya Ridge. The ridge may have subsided below the interior lake level approximately 6 million years ago. Submersion of portions of the basins must have progressed at a quicker pace since that period as a number of equivalent strata occur in the basins at a greater depth than over the ridge.

According to the results of seismostratigraphic, sequence-stratigraphic, magnetostratigraphic investigations and radiometric age determinations [VAKARCS et al. 1994] the shallow sea of the inner Carpathians was isolated from the world oceans and reduced to a lake at the boundary of the Sarmatian and Pannonian stages (11.5 Ma). At that time the water depth began to increase and progressively reached 800 to 1000 m. At the end of the Sarmatian and the beginning of the Pannonian stage the subsidence of the Hódmezővásárhely–Makó Graben and of the Békés Basin was quicker than the accumulation of sediments, thus it was relatively starved of sedimentary fill [POGÁCSÁS et al. 1989, KÓKAI and POGÁCSÁS 1991]. The *Retrogradational Unit* (*Ru,* MATTICK et al. 1994), which contains readily traceable reflection

horizons, was correlated by us to the earlier described *Deep Basin Facies* and *Prodelta Facies* [MATTICK et al. 1988], i.e. approximately corresponding to *sequences III and II* .

An extended (time)segment of the (MDS-18) seismic section images the central region of the Békés Basin (*Fig. 5*). Interpretation of this partial section reveals a number of seismic signal characteristics some of which are regional in nature; the others are confined to a specific segment of the subsurface (*Fig. 6*). The prevailing, laterally well correlatable subparallel reflections, with visible decrease in frequency content and gentle overall easterly dip — down to 2.75 s travel times on the southwest and 4 s arrival times on the northeast — are clear manifestations of the characteristic seismic images of the Neogene sediments. In the lower central regions of the sections (Figs. 5, 6), approximately 70 km southwest from the northeast end of the survey line, just below 2.5 s travel time, extending below 4 s, there are a number of directly recognizable congruous, highly curved, laterally limited and locally distinct reflection patterns. The nature of these reflectivity patterns and the draping of the overlying sedimentary strata are suggestive of a *young magmatic intrusion* which locally protruded the basin. Originating as a consequence of differential compaction a steeply east dipping *listric fault* and a *roll-over structure* are traceable from 1.8 s to a significant depth, along the NE side of the magmatic intrusion. Based on the geochronological age of the affected sediments the inferred age of the strata directly overlying the magmatic body is 6–7 Ma.

In the Apuseni Mountain (an area 60–150 km eastward from the investigated anomaly) rhyolitic volcanism was active in the Upper Badenian, dacitic and andesitic in the Sarmatian, while basaltic at the beginning of the Lower Pannonian. In the eastern part of the Pannonian Basin there are

Table I. International chronostratigraphic boundaries best known in Hungary and used in the practice of oil and gas exploration [HORVÁTH 1986], and nomenclature established in sequence-stratigraphical investigations [MATTICK et al.1988, 1994]. As our interpretation shows, in Encls. 2 and 4 it is assumed that the synrift sediments deposited in the Lower–Miocene and at the beginning of the Middle–Miocene, and the postrift phase began 10–15 million years ago

I. táblázat. A Magyarországon legismertebb nemzetközi, továbbá a szénhidrogénkutatás gyakorlatában használt korbeosztások [HORVÁTH 1986], és a szekvenciasztratigráfiai vizsgálatoknál kialakult elnevezések [MATTICK et al. 1988, 1994]. A 2. és 4. mellékleteken látható értelmezésünk szerint feltételezzük, hogy a szinrift üledékek az alsó miocénben és a középső miocén elején keletkeztek és a posztrift fázis 10–15 millió évvel ezelőtt kezdődött

BASIN DEVELOPMENT
- OUR: POSTRIFT FACIES, ?, SYNRIFT FACIES
- PUBLISHED: POSTRIFT FACIES, ?, SYNRIFT FACIES

SEQUENCE STRATIGRAPHIE

MATTICK ET AL. 1994: PU2, PU1, RU, BRU — PROGRADATIONAL UNIT, RETROGRADATIONAL UNIT, BASINALLY RESTRICTED UNIT

MATTICK ET AL. 1988: SEQUENCE V, SEQUENCE IV B, SEQUENCE IV A, SEQUENCE III (?), SEQUENCE II, SEQUENCE I

DELTA PLAIN FACIES D P, DELTA FRONT FACIES D F, PRO DELTA FACIES P D (?), DEEP BASIN FACIES D, BASAL FACIES B

GENERAL FACIES: FLUVIATILE, CONTINENTAL, LACUSTRINE-FLUVIATILE, FRESHWATER, BRACKISH, MARINE

ADOPTED IN HUNGARY: QUARTER — 2.4; UPPER PANNONIAN, Pa_2 — 8; Pa_1^2 — 10; Pa_1^1, LOWER PANNONIAN — 12; SARMATIAN — 14; BADENIAN; KARPATHIAN — 17, 17.5; OTTNANGIAN — 19; EGGENBURGIAN — 22

STAGES

C PARATHETIS: ROMANIAN, DACIAN, PONTIAN, PANNONIAN, SARMATIAN, BADENIAN, KARPATHIAN, OTTNANGIAN, EGGENBURGIAN

MEDITERRANEAN: CALABRIAN, PIACENZIAN, ZANCLEAN, MESSINIAN, TORTONIAN, SERRAVALLIAN, LANGHIAN, BURDIGALIAN, AQUITANIAN

EPOCHS: QUARTER; PLIOCENE; MIOCENE (LATE, MIDDLE, EARLY)

TIME (Ma): 1, 5, 10, 15, 20

ignimbrites and pyroclastic of rhyolitic composition (11–12 Ma), in its central and southern parts submarine basalts are encountered [7–10 Ma, PÓKA 1988]. According to KŐRÖSSY [1992] products of basaltic volcanism, recognized in boreholes, around Kecel (~ 150 km to the west of the anomaly), formed a more than 600 m thick pyroclastic complex with basaltic beds and veins. Within this sequence volcanic rocks alternate with fossiliferous Lower Pannonian marl and argillaceous marl. The respective ages of these volcanics, as determined by the K/Ar method, are 8.13± 0.71 and 8.47±0.77 Ma [BALOGH and JÁMBOR 1987]. Supported by the above evidence the magmatic intrusion in the Békés Basin was interpreted as *Upper Miocene (Lower Pannonian) basalt*.

The comparable characteristic upwarping of the reflection horizons, at about profile kilometer 85, between 3.3 and 3.5 s (smaller sets can be observed on Encls. 1 through 4) is also suggestive of magmatic origin. Seismic patterns of overlying younger sedimentary horizons, indicative of a listric fault, are also present on the SW side of the magmatic body (Encls. 3 and 4). At both locations of the section, seismic signatures traced the intrusive structures down into the crust.

The *time of synrift formation* in the basin [GROW et al. 1994 and in Table I] is coeval with the deposition of the *Basinally-Restricted Unit (BRU*, MATTICK et al. 1994), or the *Basal Facies* of the Hódmezővásárhely-Makó Graben [*sequence I,* MATTICK et al. 1988]. Encls. 2 , 4 and Fig. 4 show our interpretation which somewhat deviates from the published basin develop-ment models (Table I). It is assumed that the Middle Miocene (Upper Badenian) beds intersected by the deep drilling, denoted by 1, had already been formed as a postrift facies. (If too high velocities were used for depth determination, this error may have contributed to the deviating interpretation; if, however, our notion is correct, then the beginning of the postrift facies formation may be put between 10 and 15 Ma). According to our model, in the deep part of both basins *Lower Miocene* (perhaps Paleogene) sediments may also have accumulated under the Badenian beds. This synrift formation is characterized by a slightly fractured texture and has a significant thickness of about 1500 m. Seismically it is manifested by high amplitude and low frequency. In enclosures 2 and 4, as well as in Figs. 4 and 6 this series is shown in green. On the basis of magnetotelluric studies the resistivity of the previous sedimentary zone is assumed to be over 200 Ωm [VARGA and NEMESI 1994]. On the basis of an integrated seismic and magnetotelluric
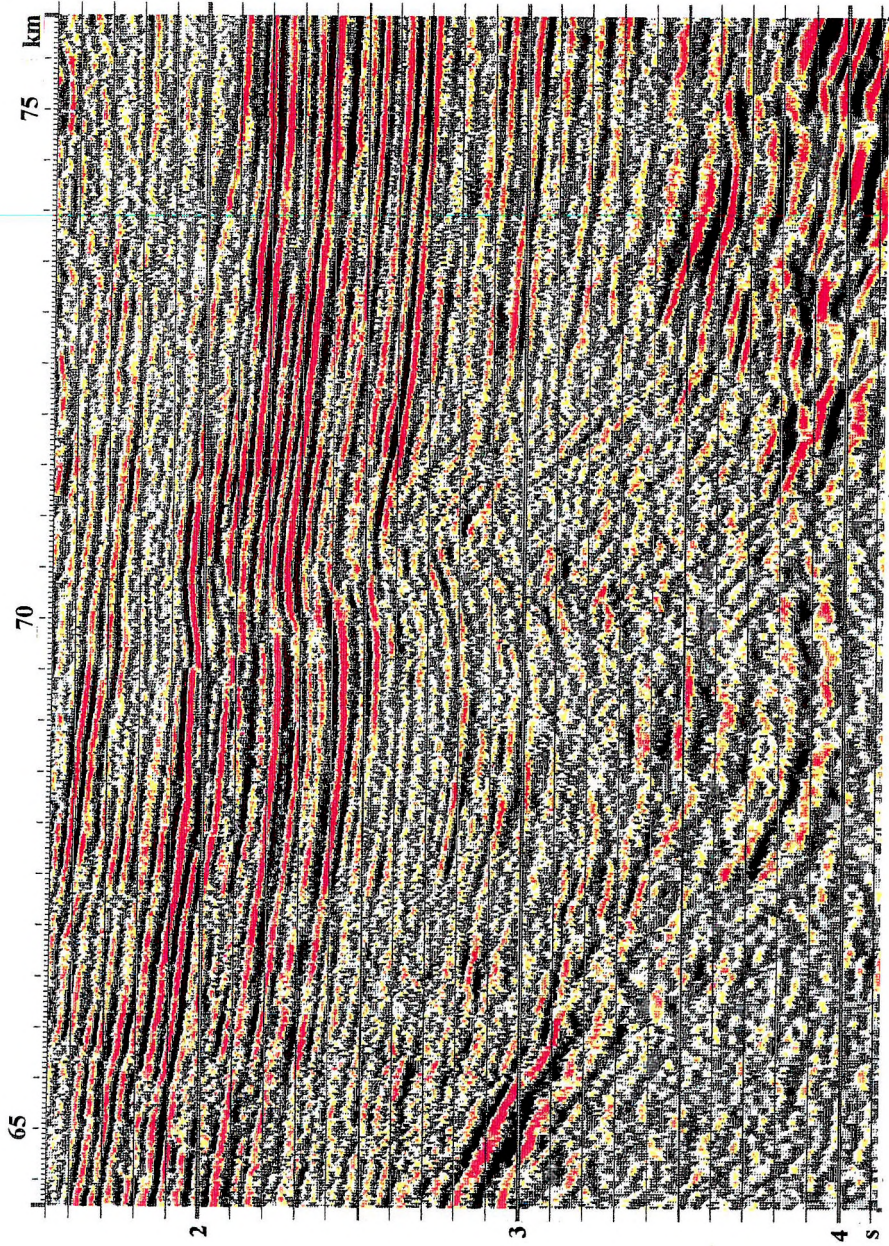
Fig. 5. Part of the time section from data recorded — based on the chapter 'Seismic data acquisition and processing' in the second survey arrangement — by MDS-18 telemetric seismic equipment

5. ábra. A — „Seismic data acquisition and processing" c. fejezet szerinti — második rendszerben, MDS-18 tipusú telemetrikus szeizmikus berendezéssel regisztrált adatokból kapott időszelvény egy részlete
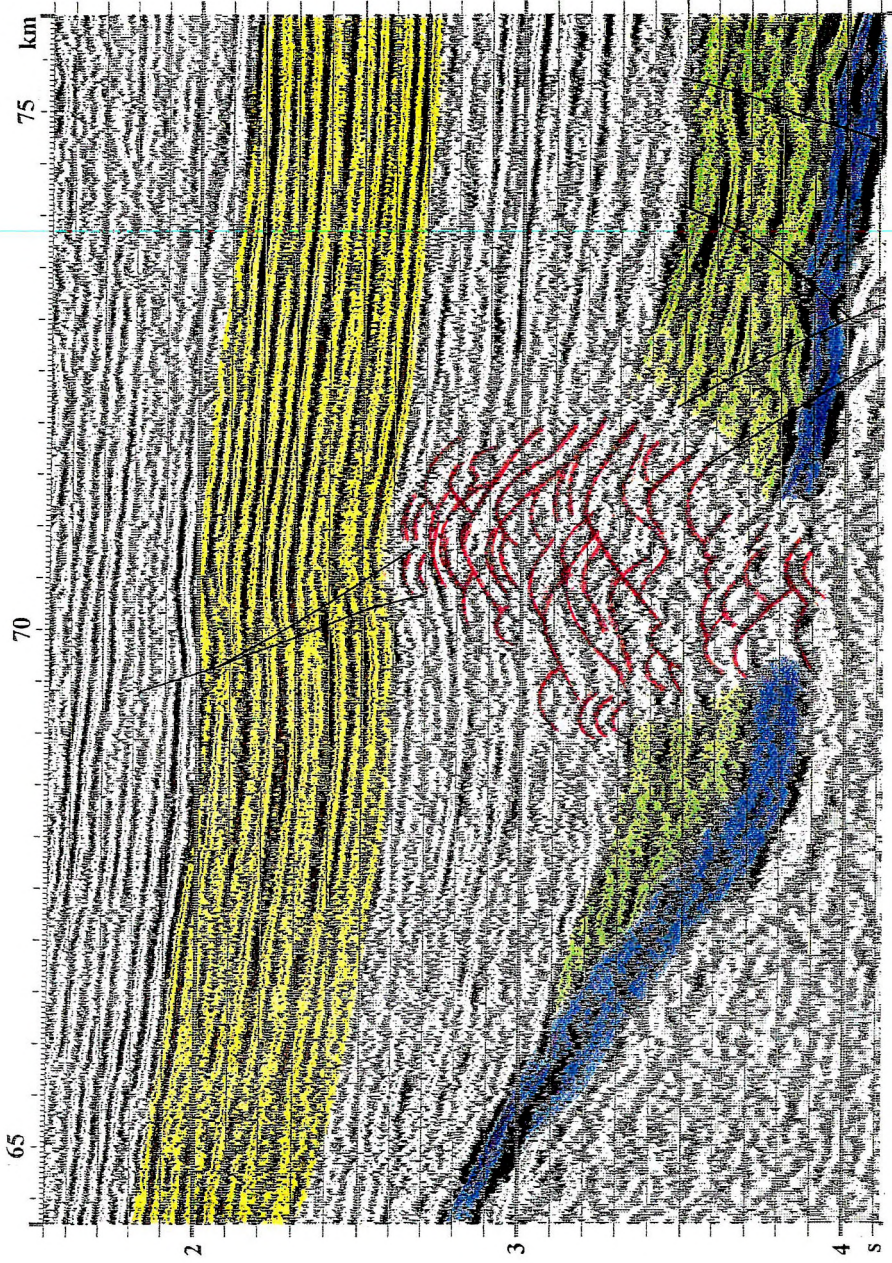
Fig. 6. Interpretation of the section part in Fig. 5. Delta sediments are indicated in yellow, the series interpreted as Lower Badenian–Lower Miocene in green, layers assumed to be Mesozoic in blue and the magmatic intrusions in red. Above the basic intrusion of assumed Lower Pannonian age a listric fault has formed which is dipping towards the side of the intrusion facing the basin

6. ábra. Az 5. ábrán látható szelvényrészlet értelmezése. A deltaüledékeket sárga, az alsó-bádeni–alsó-miocénnek értelmezett rétegsort zöld, a mezozoósnak feltételezett rétegeket kék és a magmatikus benyomulásokat piros színnel jelöltük. A feltételezett alsó-pannon korú bázikus benyomulás felett lisztrikus vető alakult ki, mely a benyomulás medence felé eső oldala felé lejt
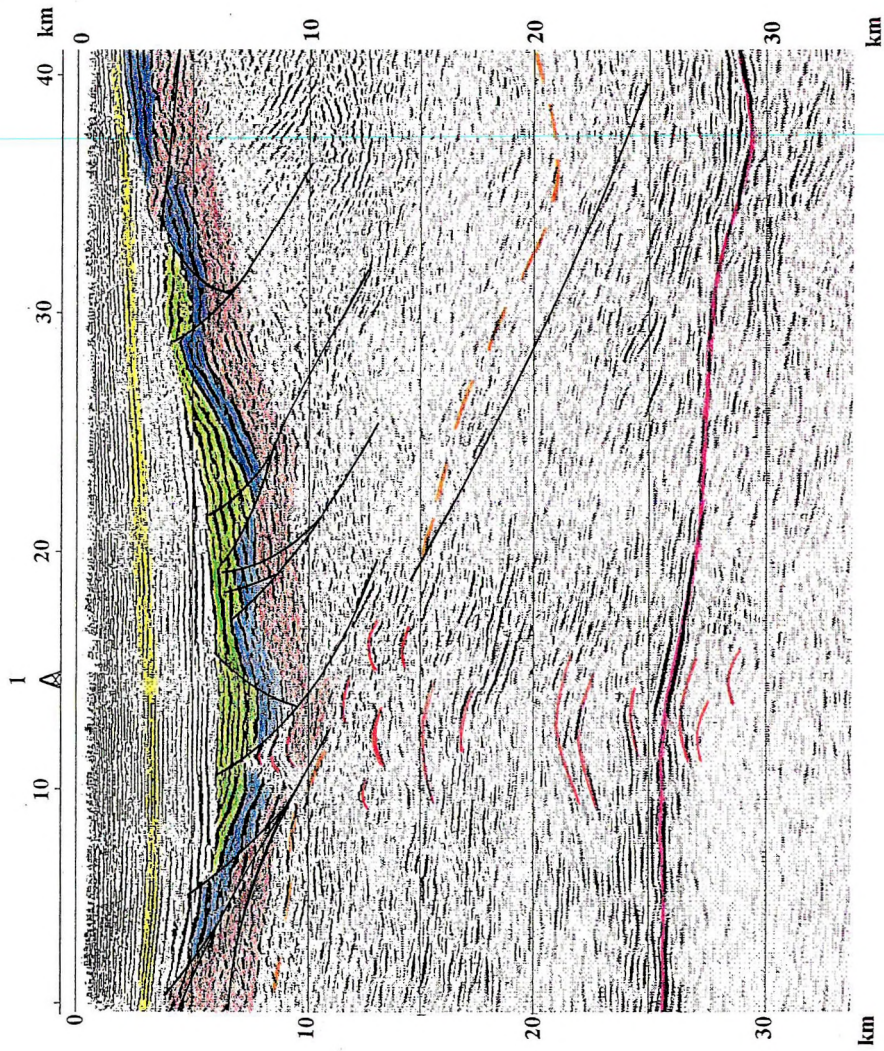
Fig. 7. Results shown in Encls. 1 and 3 may suggest an evolution of the Hódmezővásár-hely–Makó Graben slightly deviating from that presented in Encls. 2 and 4. Between profile kilometers 29 and 34 a *third graben* may also have formed, containing synrift sediments as well

7. ábra. Az 1. és 3. mellékleten ábrázolt eredmények alapján a Hódmezővásárhely–Makói ároknak — a 2. és 4. mellékleten ábrázoltaktól — kissé eltérő kifejlődése is elképzelhető. Lehetséges, hogy a 29 és 34 szelvénykilométer között egy harmadik árok is kialakult és ebben is találhatók szinrift üledékek és az itt észlelt amplitúdó anomália ezekből származik

interpretation these deposits may represent *thick beds of limestone*, or *sandstone with quartz cement*.

In the Hódmezővásárhely–Makó Graben the younger sediments of the synrift complex onlap on older deposits. Such a regression of the series of strata towards the basin, as they turn 'younger', may indicate that the subsidence of the graben must have declined at that time. No such phenomenon was observed in the Békés Basin.

Fractures crossing the synrift sediments in the two basins are different. The Hódmezővásárhely–Makó Graben was bisected during the Lower Miocene. The relief of the ridge separating the *two portions* can be estimated to extend several hundred meters (in the section). In the development of both graben parts the deep fracture zones and the attached smaller faults on their SW side (in the section) may also have played a significant role. At the time of the Lower Badenian the sea may have risen over the ridge thereby initiating a sedimentary basin.

The results shown in Encls. 1 and 3 may suggest evolution of the Hódmezővásárhely–Makó Graben (slightly deviating from that presented in Encls. 2 and 4). Between profile kilometers 29 and 34 a *third graben* may also have formed, containing synrift sediments as well (*Fig. 7*).

In the synrift period, faults dipping towards the basin's interior were formed in the Békés Basin. The fault zone with a throw of many hundred meters that can be detected between profile kilometers 85 and 87 has offset even the Lower Miocene beds. Such a significant throw can be inferred from both the seismic pattern and the changes in the depth of the high-resistivity layer detected by magnetotelluric measurements (Encls. 2 and 4).

5. Amplitude anomalies observed in the pre-Neogene basement

On the deep reflection profile PGT-4 along the Hungarian Geotraverse surveyed with the MDS-18 instrument between profile kilometers 29 and 32 and between 57 and 60 km a nearly horizontal amplitude anomaly protruding laterally was observed. The part of the section shown in *Figs. 8* and *9* was prepared by filtering between 2 and 40 Hz. The amplitude anomaly observed between profile kilometers 57 and 60 was studied in more detail.

When this portion of the data is filtered with a 10 Hz low-cut filter the anomalies are no longer apparent (*Fig. 10*). The anomalously high amplitude levels must therefore receive contributions from frequency components

between 2 and 10 Hz. This amplitude behaviour is a clear indication that *exploration of the deeper part of the sedimentary segment requires specially designed low-frequency survey methods.* The anomaly — presumably below the surface of the Mesozoic basement (about 2.1 s) — was observed at a two-way travel time (TWT) of 2.4 s. TAKÁCS [1996] conducted amplitude versus offset (AVO) modelling of this anomaly (Fig. 13) with a number of velocity estimates *(Fig. 11)*. True amplitude recovery of the original seismic data was established by utilizing the PROMAX data enhancement software system (Advance Geophysical Corporation Products, USA) and through the implementation of processing steps of offset dependent amplitude recovery, surface-consistent amplitude correction, surface-consistent deconvolution and Q compensation. The modelling was carried out with a program especially designed for this purpose.

The values of the best fit velocity model ranges from 3300 m/s to 5600 m/s (Fig. 11) in the travel time interval of 2–2.6 s. The match between the computed synthetic traces *(st)* and the observed traces *(mt)* is excellent. A reasonably high reflection coefficient *(rc)* value of -0.074 was required to find the best correlation between the two seismic trace sets at 2.39 s TWT.

Preliminary interpretation of the derived low-velocity field (2.39 s – 2.575 s) is that the lowest velocity zone (4400 m/s) represents calcareous rocks with gas saturated secondary porosity. The increase to 4800 m/s and the location of the reflection coefficient +0.044 are indicative of the gas–fluid contact. The point at +0.077 reflection coefficient marks the ending of fracture porosity. The equivalent seismic section and amplitude anomalies are shown in *Fig. 12*, where red represents the zone of predicted gas saturation, blue is indicative of the fluid-bearing zone.

Maintaining the modelling generated *P*-wave velocities constant, the matching of the observed amplitude variations with their theoretical equivalent required [TAKÁCS 1996]: for the upper layer (4400 m/s) a Poisson's ratio of 0.115 and for the zone beneath it 0.333 *(Fig. 13)*. According to HARVEY [1993] and OSTRANDER [1984], the distinctly low value is a further indication of gas saturated rock whereas the higher ratio represents fluid saturation.

A comparable anomaly, associated with oil-water contact [ALBU and PÁPA 1992], was detected at the northern margin of the Békés Basin in a fractured metamorphic basement reservoir.

Below a depth of 1800 m most reservoirs are overpressured in the Békés Basin. SPENCER et al. [1994] postulate that the carbon dioxide orginating from the metamorphosis of the calcareous rocks in the deeper part of the
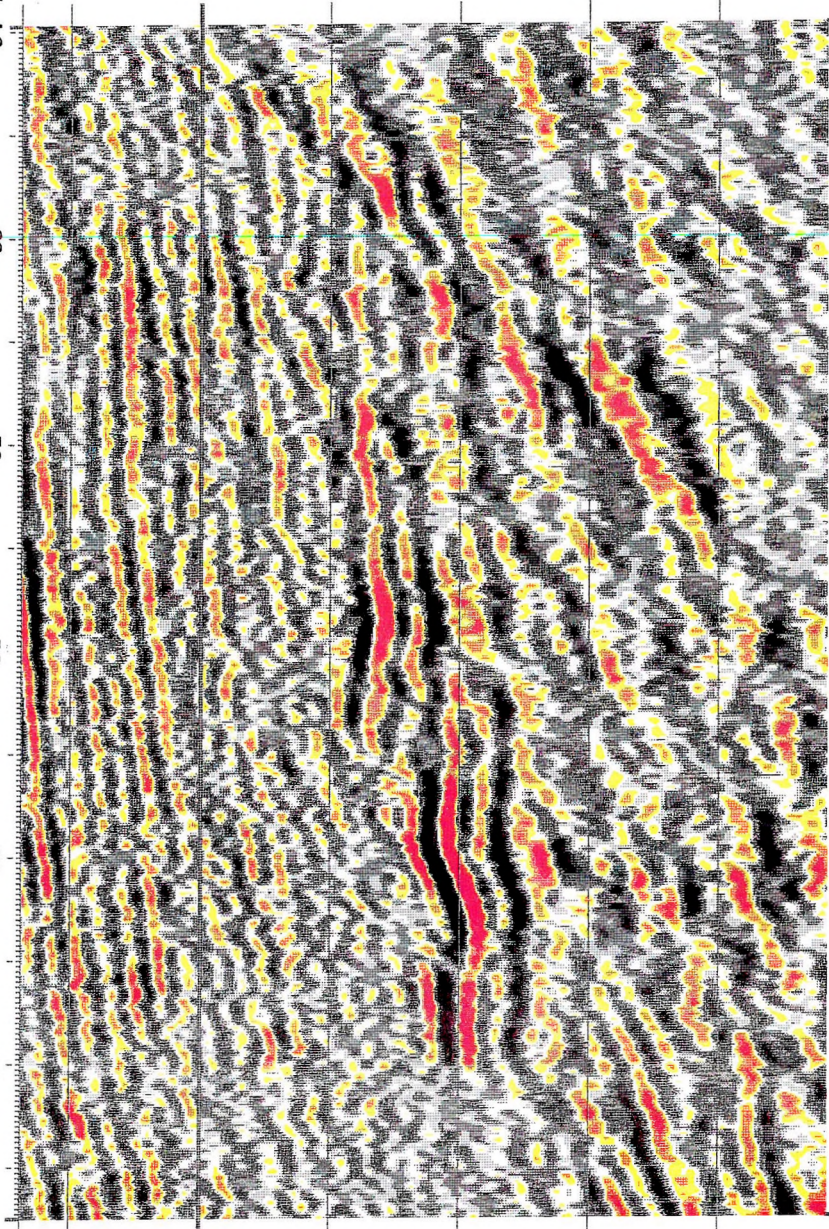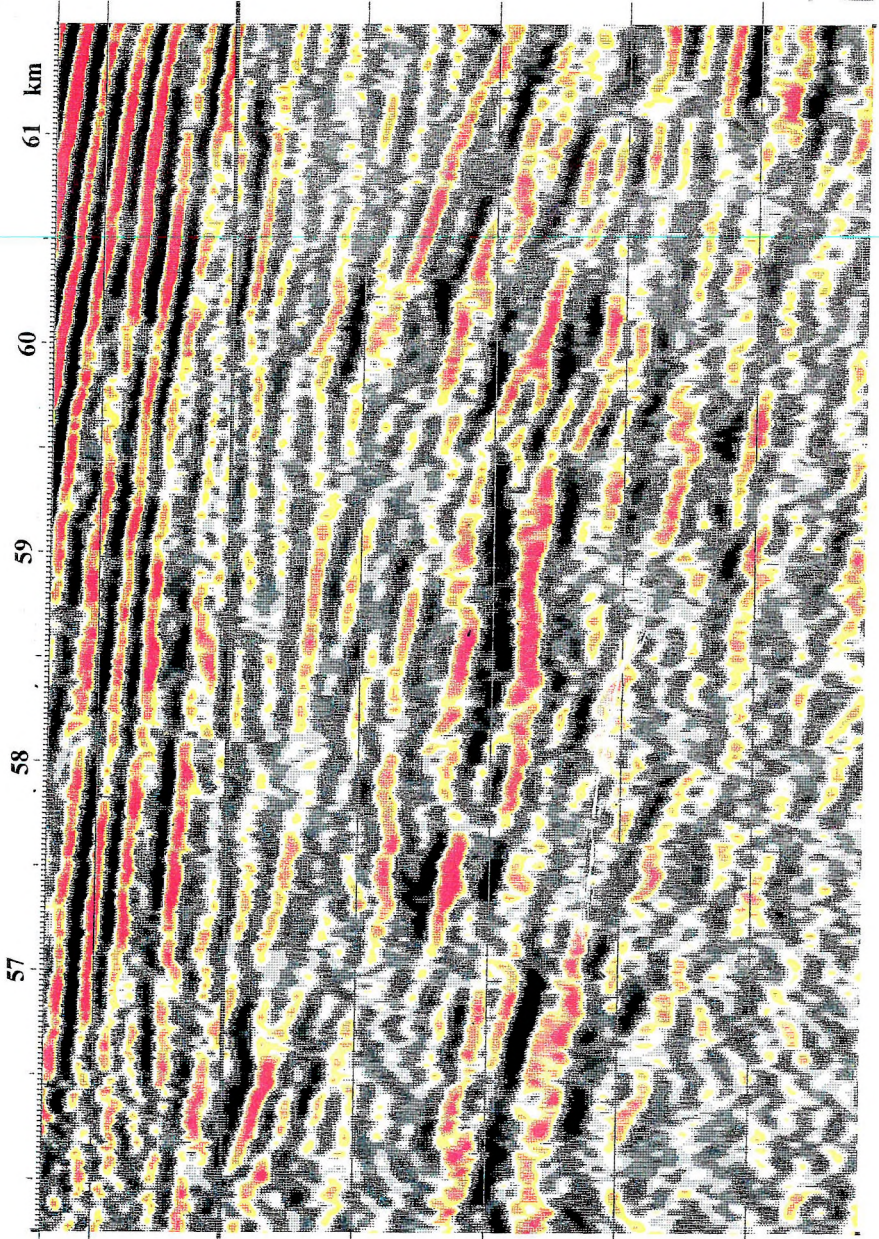
Fig. 8. Amplitude anomaly observed between profile kilometers 29 and 32 of the deep reflection line PGT-4 by low-frequency recording. For the detail of the section given here 2–40 Hz band-pass filtering was used

8. ábra. A PGT-4 mélyreflexiós vonal 29–32 szelvénykilométere között, kis-frekvenciás metodikával észlelt amplitúdó anomália. A szelvényrészlet 2–40 Hz közötti szűréssel készült

Fig. 9. Amplitude anomaly observed between profile kilometers 57 and 60 of the deep reflection line PGT-4 — from the depth of the basement of assumed Mesozoic age — using low-frequency recording. For the detail of the section given here 2-40 Hz band-pass filtering was used

9. ábra. A PGT-4 mélyreflexiós vonal 57-60 szelvénykilométere között, kis-frekvenciás metodikával — a feltételezhetően mezozoós korú medencealjzat mélységéből — észlelt amplitúdó anomália. A szelvényrészlet 2-40 Hz közötti szűréssel készült
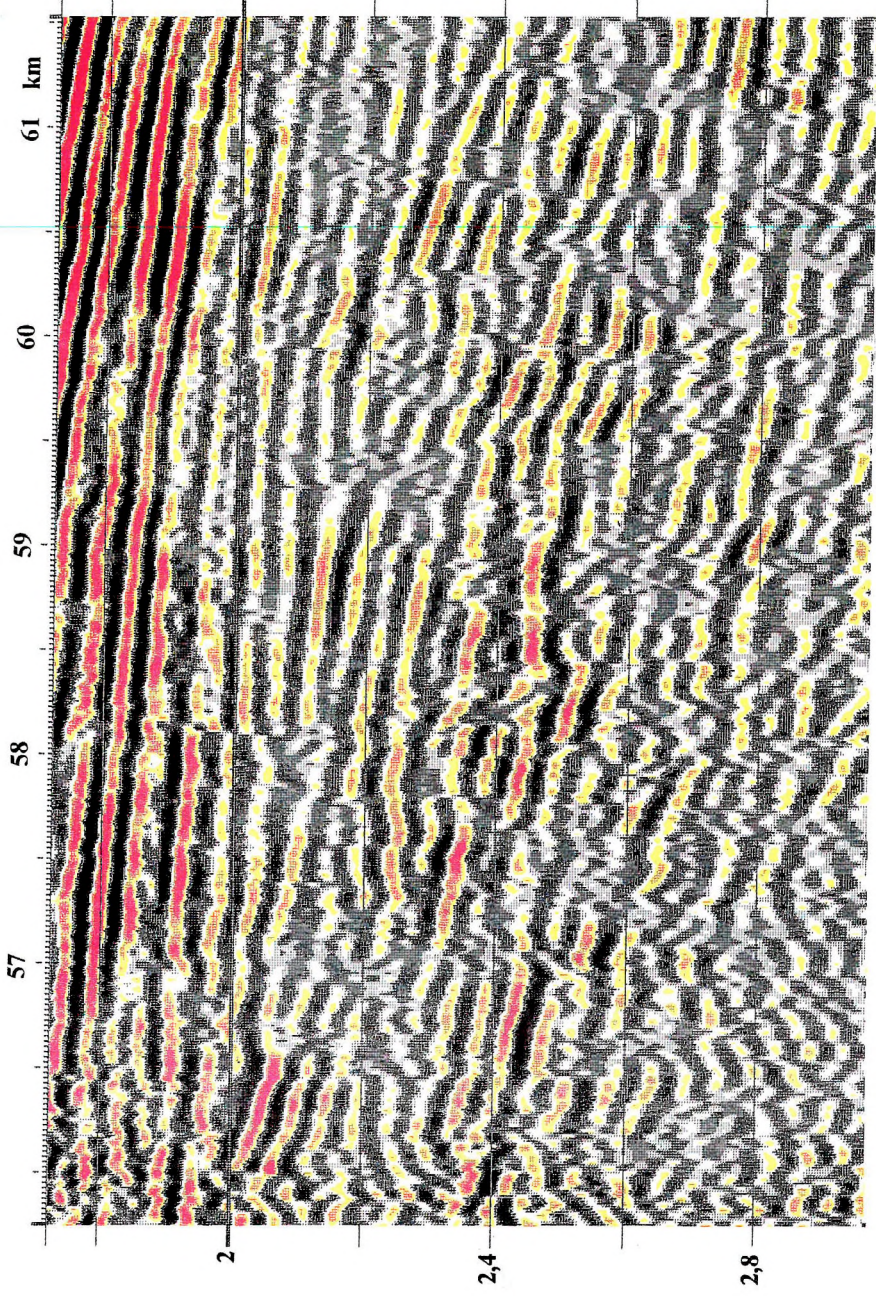
Fig. 10. Detail of the section shown in Fig. 9 after low-cut filtering at 10 Hz. The amplitude anomaly is absent. The difference of the two figures suggests that exploration of pre-Neogene basement structures requires specially designed low-frequency surveying

10. ábra. A 9. ábrán látható szelvényrészlet 10 Hz-es alulvágás után. Az amplitúdó anomália nem figyelhető meg. A két ábra különbségéből arra következtettünk, hogy a kisfrekvenciás metodika a pre-neogén medencealjzat szerkezeteinek felkutatásában is előnyös
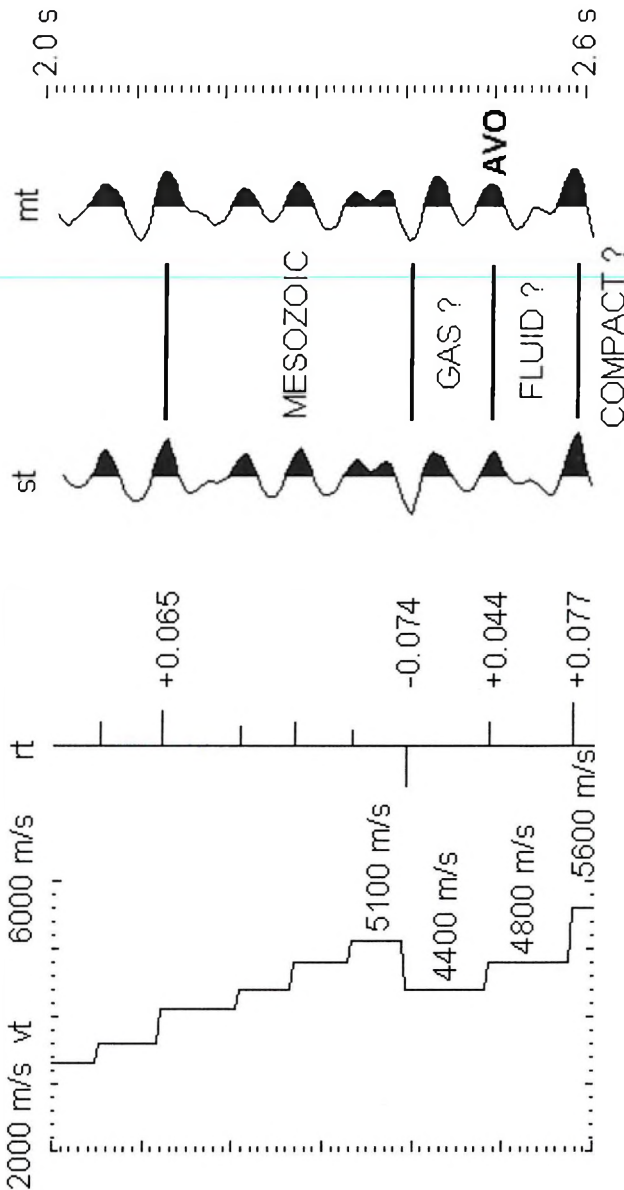
Fig. 11. Result of seismic trace modelling: *vt*—velocity model; *rc*—reflection coefficient; *st*—synthetic trace; *mt*— measured trace [TAKÁCS 1996]

11. ábra. Szeizmikus csatorna modellezés eredménye: *vt*—a sebesség modell; *rc*—a reflexiós tényező; *st*—a szintetikus csatorna; *mt*—a mért csatorna [TAKÁCS 1996]

basin may also contribute to the excessive formation pressure. In porous rocks the velocity of seismic waves decreases substantially when the pressure of fluid, filling up the pores, approximates the rock matrix pressure. Such a decrease is even more conspicuous in fractured rocks [CHRISTENSEN 1989]. For identical pressure conditions and identical pore volume the higher the aspect ratio of pores, the more significant is the decrease in velocity. On this basis the relatively low velocities and the velocity inversion, in segments of the PGT-4 profile, may be ascribed not only to formation saturation, but also to the substantial pressure.

The amplitude anomaly (on PGT-4 between 57 and 60 km) is located on the east flank of the elevated Pusztaföldvár–Battonya Ridge at a depth of 2.5–3 km. In the neighbouring Békés Basin the thickness of Neogene sediments is about 8 km (Fig. 4). It is probable therefore that hydrocarbon migrated from the high pressure beds within the Békés Basin into the reservoir space — due to fractures and faults — formed on the upper segment of the pre-Neogene basement (Fig. 4). Thus, the anomalous reflection amplitude of the seismic section may have been caused by *carbon dioxide and water*, or *hydrocarbon gas and hydrocarbon fluid*, or any other combinations of them.

To support the interpretation of the above analysis, the amplitude anomaly of the PGT-1 (Fig. 1) survey is also commented on. Acoustic logs and areal magnetotelluric surveys were available for the modelling of these seismic data. The amplitude anomaly *(Fig. 14)* with 6–10 dB above the background was observed at a depth of 5–5.5 km *(Fig. 15)*. To determine the character and regional extent of the anomaly the deep reflection cross-line — PGT-2 — was also surveyed *(Fig. 16)*. Subsequently, seismic modelling was conducted by TAKÁCS [1996], and magnetotelluric soundings by VARGA [1992].

Direct sonic and density data were utilized from borehole W-2 (Fig. 14). Additional sonic and density information for deep wells W-1 and W-3 were assembled from an assortment of comparable data from boreholes in nearby localities. Synthetic seismic traces produced from these data were compared to corresponding traces of the profile S-1 (Fig. 14) [SZEIDOVITZ 1990]. Composite subsurface sections *(Fig. 17)* were prepared by applying interval velocities calculated from VSP data of borehole W-4 (Fig. 14). By refining the parameters of the above initial model, an amplitude anomaly was generated which was directly comparable to the observed traces of profile PGT-1.
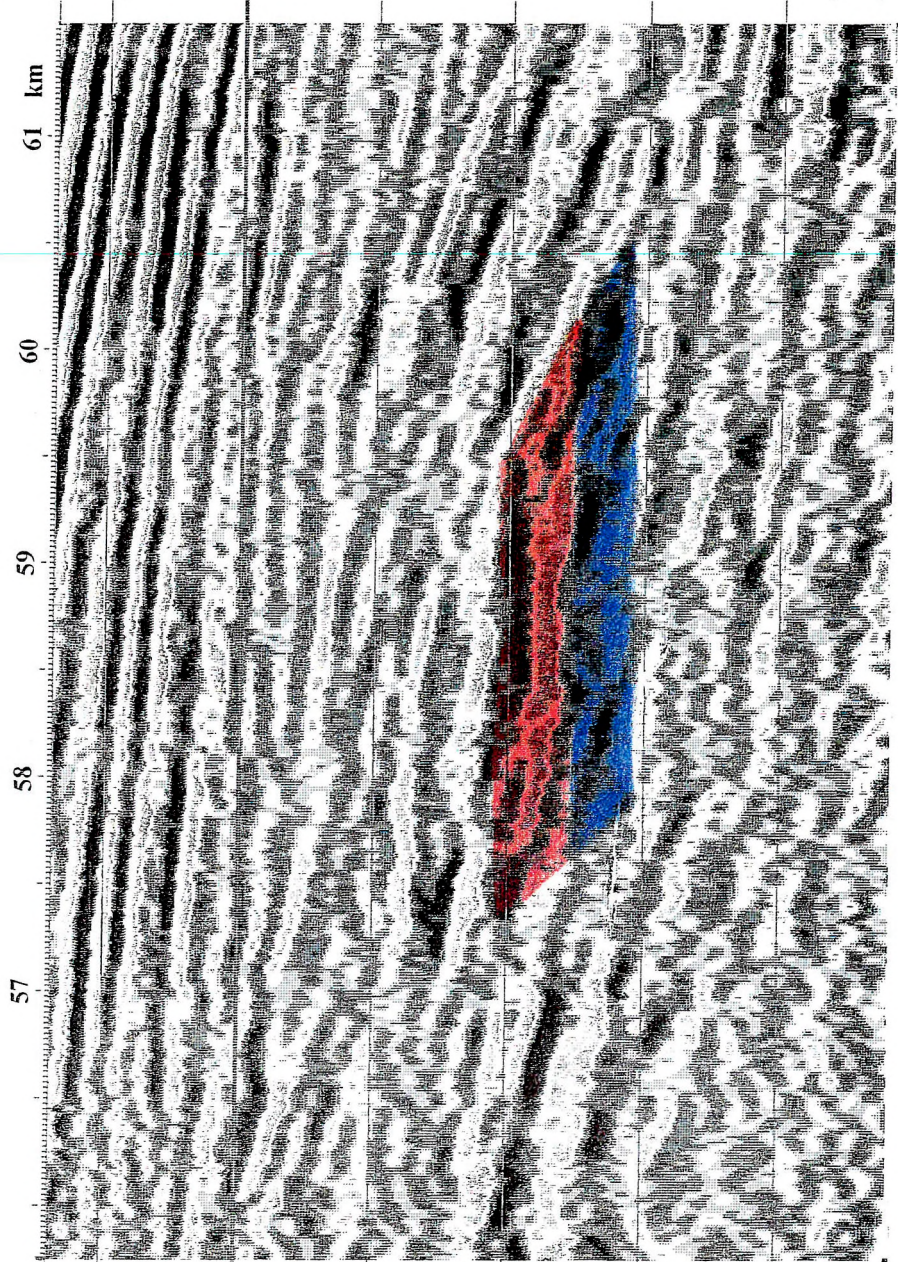
$Vp1 = 4400$ m/s $\quad \rho1 = 2.2$ g/ccm $\quad \sigma1 = 0.115$

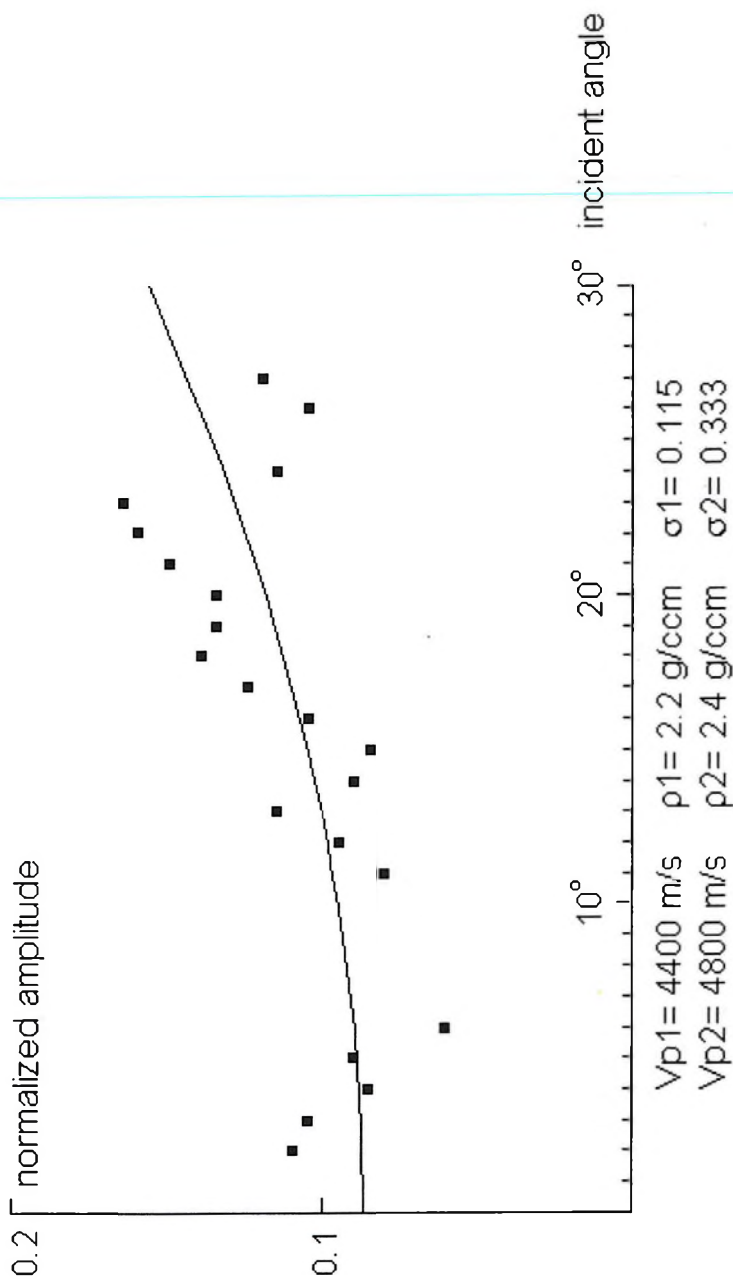$Vp2 = 4800$ m/s $\quad \rho2 = 2.4$ g/ccm $\quad \sigma2 = 0.333$

Fig. 13. Result of the AVO analysis of the amplitude anomaly [TAKÁCS 1996]. The Poisson ratio for the upper layer (σ_1) is anomalously low (0.115), which may correspond to rock with gas saturated pore volume. The Poisson ratio for the lower layer ($\sigma_2 = 0.333$, in extremity) may indicate a porous zone saturated with fluid

13. ábra. Az amplitudó anomália AVO analizisének eredménye [TAKÁCS 1996]. A felső réteg Poisson aránya (σ_1) anomálisan kicsire (0,115) adódott, ami megfelelhet a gázzal telített pórustérfogatú kőzetnek. Az alsó rétegre kapott Poisson arány ($\sigma_2 = 0,333$, határesetben) jelezhet folyadékkal telített porózus zónát
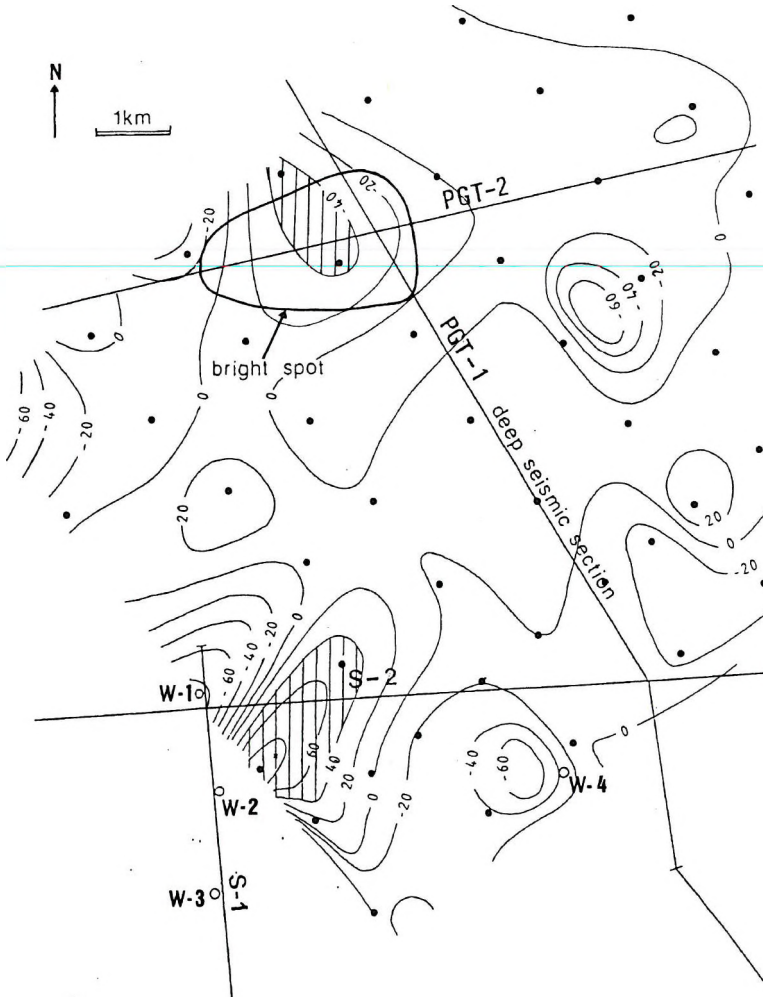
Fig. 14. Sketch of the amplitude anomaly observed on the seismic deep reflection profiles PGT-1 and PGT-2 and contour map of estimated probability of oil and gas occurrence, plotted by applying multi-variable statistical analysis of magnetotelluric data [NAGY 1992)] The seismic amplitude anomaly shows fairly good agreement with a probability maximum. *PGT*—is used to mark the deep reflection profiles; *S*—seismic profiles of hydrocarbon exploration; •—magnetotelluric measuring points; *W*—deep wells

14. ábra. A PGT-1 és PGT-2 szeizmikus, mélyreflexiós szelvényeken észlelt amplitúdó anomália vázlata és a szénhidrogén előfordulás becsült valószinűségének — a magnetotellurikus adatok sokváltozós statisztikai analízise alapján szerkesztett — szintvonalas térképe. A szeizmikus amplitúdó anomália elég jó egyezést mutat egy valószinűség maximummal. *PGT*— mélyreflexiós szelvények; *S*—szénhidrogénkutató szeizmikus szelvények; •—magnetotellurikus mérési helyek; *W*—mélyfúrások

NW

SE

0   1 km

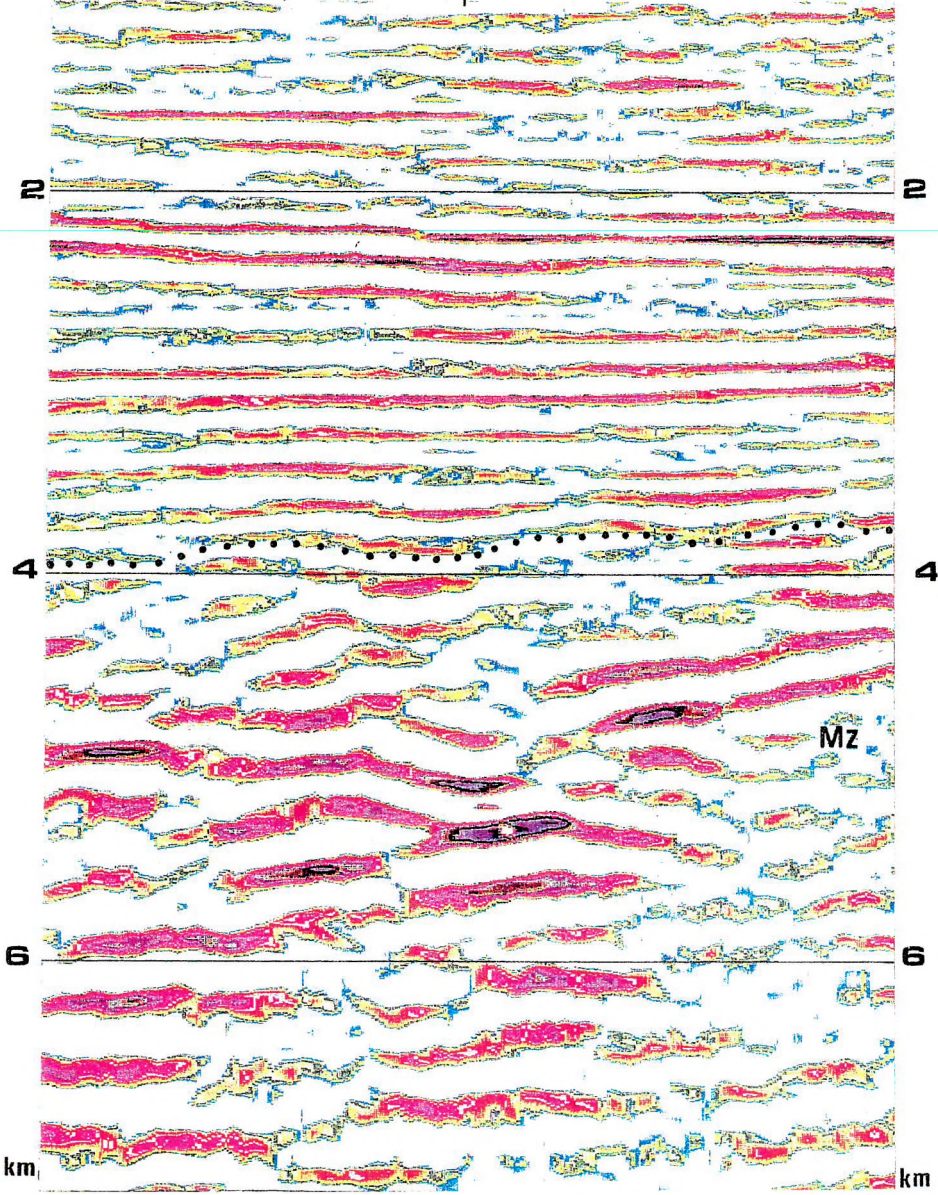PGT 2

2   2

4   4

Mz

6   6

km   km

Fig. 15. Detail of the migrated depth section of geotraverse PGT-1 for lithosphere investigation. An amplitude anomaly with 6–10 dB above background was observed at a depth of 5–5.5 km. Dotted line indicates the surface of the basement, presumably of Mesozoic age

15. ábra. A PGT-1 litoszférakutató geotraverz migrált mélységszelvényének részlete. 5–5,5 km mélységben, a környezetéből 6–10 dB kiugró amplitudó anomáliát észleltünk. Pontozással a mezozoósnak értelmezett medencealjzat felszínét jelöltük
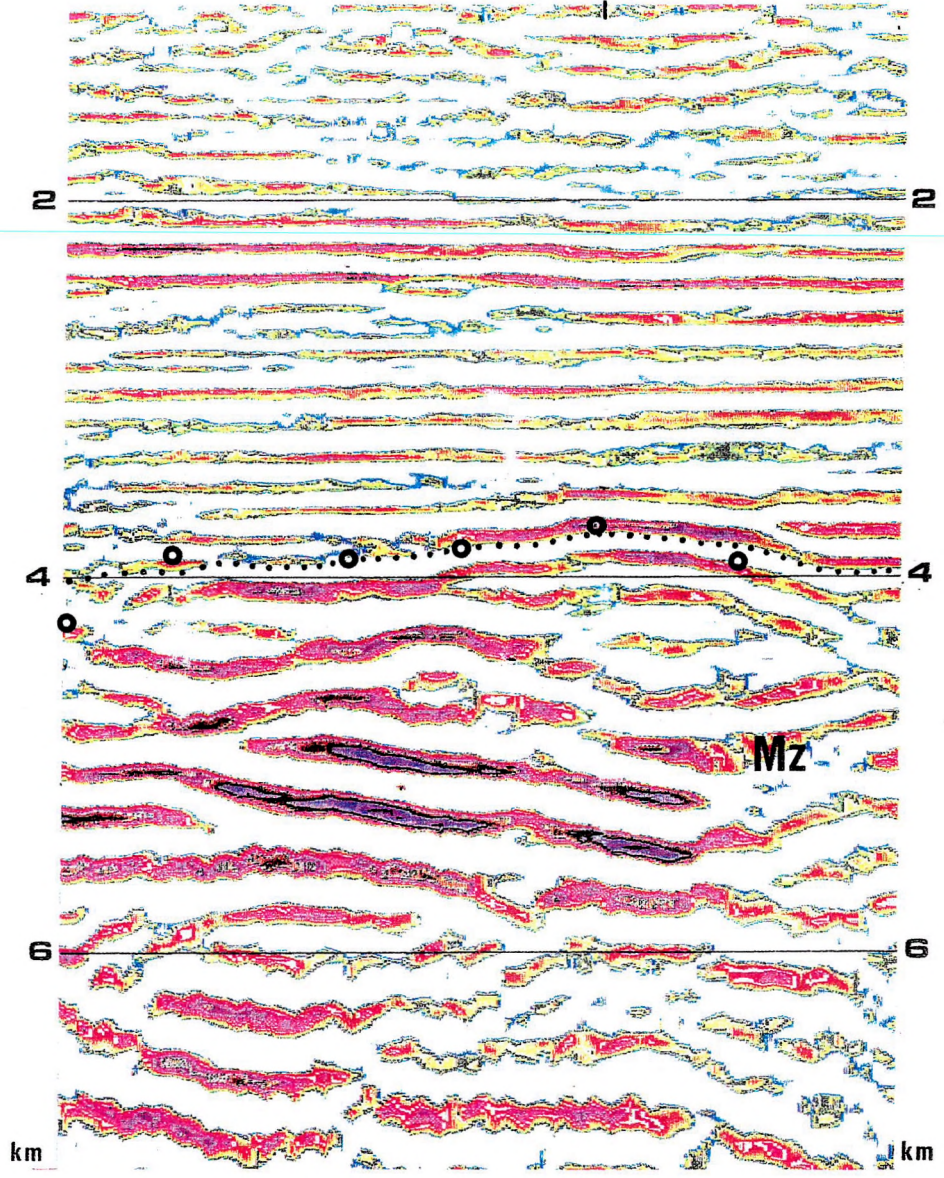
Fig. 16. Detail of the migrated depth section of geotraverse PGT-2 for lithosphere investigation. Dotted line indicates the surface of the basement, presumably of Mesozoic age, bigger points the surface of the high resistivity (100–200 Ωm) basement, determined by magnetotelluric measurements [VARGA 1992]

16. ábra. A PGT-2 jelű mélyreflexiós geotraverz migrációval készített mélységszelvényének részlete. Sűrű pontozással a mezozoósnak értelmezett medencealjzat felszínét, nagyobb pontokkal a nagyellenállású (100–200 Ωm) aljzat — magnetotellurikus mérésekkel meghatározott [VARGA 1992] — felszínét jelöltük
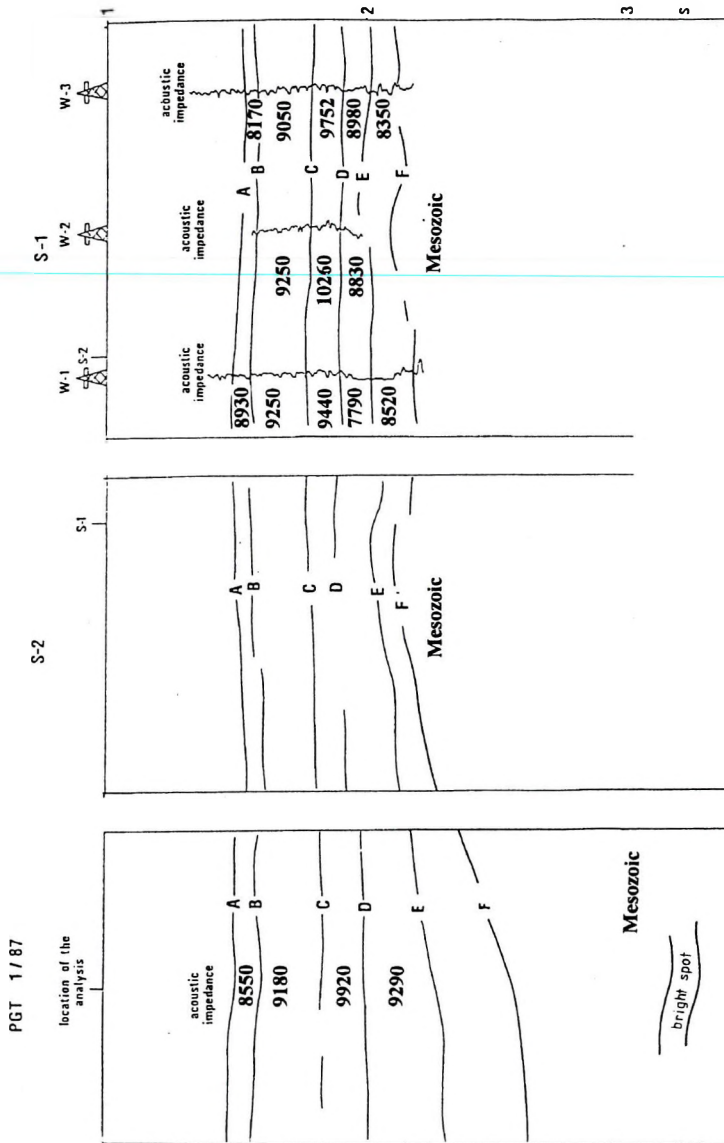
Fig. 17. Composite sections determined with the help of geophysical well logging in oil and gas exploration wells, seismic data, and the deep reflection geotraverse PGT-1 [TAKÁCS 1996]. Here the marker horizons and the acoustic impedance values taken on between them, as well as the acoustic impedance logs at the locations of deep drilling are indicated

17. ábra. Szénhidrogénkutató mélyfúrásgeofizikai és szeizmikus adatok, továbbá a PGT-1 mélyreflexiós geotraverz alapján meghatározott kompozit szelvények [TAKÁCS 1996]. Ezeken a markerszintek és a közöttük felvett akusztikus impedanciaértékek, továbbá a mélyfúrások helyén az akusztikus impedancia szelvények is feltüntetésre kerültek

The final acoustic impedance values, the reflection coefficient series, the synthetic and observed traces are shown in *Fig. 18*. Marker *E* is interpreted as a Middle Miocene complex, *F* as the pre-Neogene basement contact. In the upper several hundred milli-seconds depth interval of this pre-Neogene basement, presumably of Mesozoic age, there are no significant variations in impedance or reflection coefficients. These synthetic values were derived to match the observed weak arrivals, seen between 4 km depth and the amplitude anomaly at the intersection of profiles PGT-1 and PGT-2 (Figs. 15 and 16). There is an abrupt change in the reflection wave form at this depth. The higher frequency and subparallel Neogene reflections are replaced by low-frequency wave forms.

The equivalent model to the amplitude anomaly at the intersection of the two seismic profiles is given in *Fig. 19*. This theoretical response suggests two fluid layers under the gas-saturated zone. The low reflection coefficient (0.043) is attributed to the karstic characteristics of the presumed Mesozoic limestone and dolomite caprock. At the gas–fluid contact the reflection coefficient is significant (0.098). The reflection coefficient at the contact of the two fluids is also significant (0.074). The gradual decrease in porosity with increasing depth is associated with the reflection coefficient of 0.033.

Along PGT-2, magnetotelluric (MT) measurements [VARGA 1992] indicated a highly resistive pre-Tertiary basement at about 4 km depth below the low-resistive (2–6 Ωm) Neogene strata (circles in Fig. 16). This above depth is coincident with the sudden change in character of the seismic reflection images. Within the pre-Tertiary basement no highly conductive zone was detected.

The results of the areal magnetotelluric surveys have also been inter-preted with the aim of evaluating the amplitude anomalies from the aspect of oil and gas prospecting. The principle of evaluation is the recognition that vertical migration of oil and gas fluids causes characteristic changes in the geoelectric parameters of the rocks around the periphery of oil and gas deposits [HUGHES et al. 1985, KARUS et al. 1985]. Thus the detection and recognition of the geoelectric parameters by magnetotelluric surveys is suitable for tracing oil and gas deposits [NAGY 1992]. The problem to be solved is to distinguish significant characteristics for oil and gas deposits in measured electromagnetic (EM) data. The WEGA-D system established by DZWINEL [1983] provides the solution of the problem in the case of a particular EM dipole source field generation. During the 1980's the capabili-ties of this system were tested in the Carpathian Basin, too [DZWINEL and
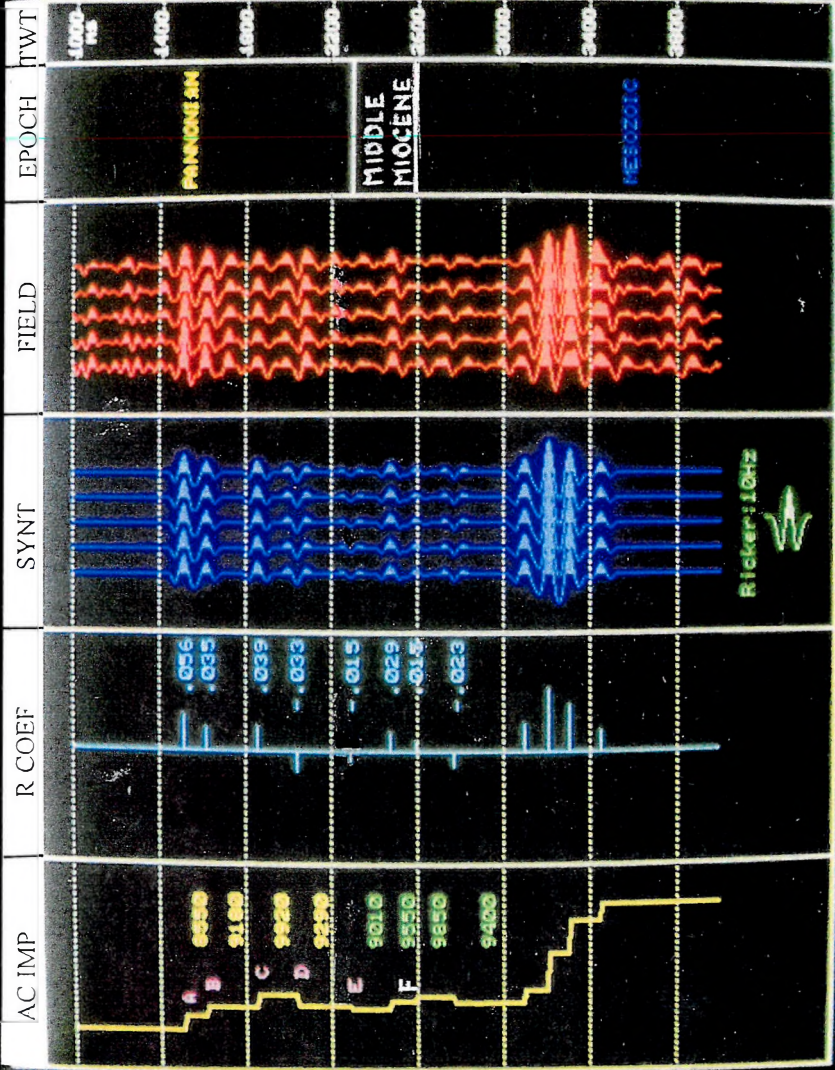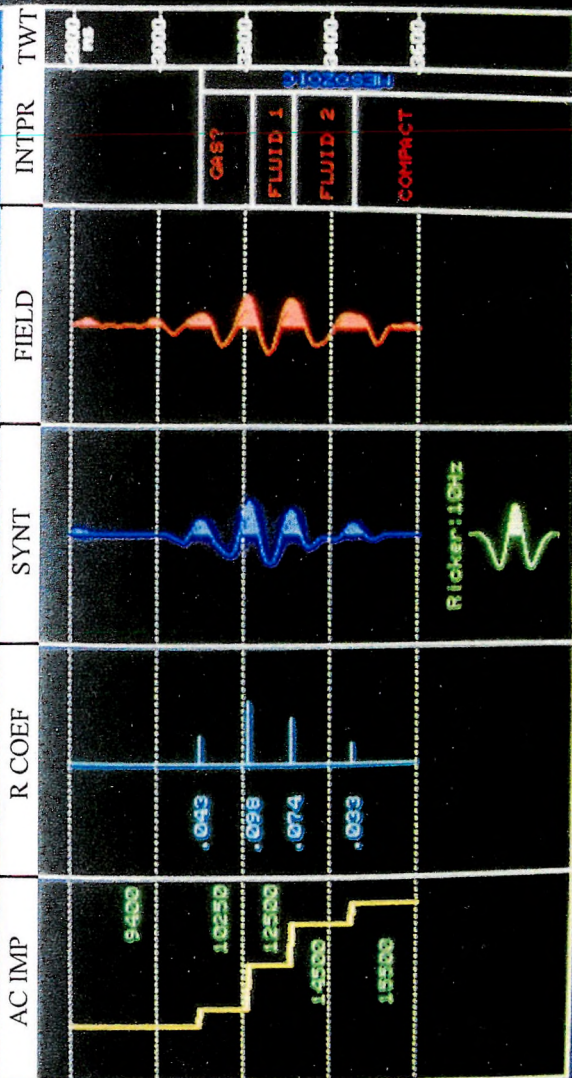
Fig. 19. Impedance model, values of reflection coefficients, detail of the synthetic and the field trace, and a possible interpretation at the depth of the amplitude anomaly. Significant reflection coefficient can be assumed at the gas-fluid and at the fluid-fluid boundary [TAKÁCS 1996]

19. ábra. Az amplitúdó anomália mélységében látható az impedanciamodell, a reflexiós tényező értékek, a szintetikus és az észlelt csatorna részlete, továbbá egy értelmezési lehetőség. Jelentős reflexiós tényező a gáz-folyadék és a folyadék-folyadék határon tételezhető fel [TAKÁCS 1996]

NAGY 1985]. In EM measurements, impedance and phase data determined at a number of frequencies from EM field vectors running in various directions form a characteristic multi-dimensioned vector for each field measurement site. Multi-dimensional vectors are carriers of the information searched for. The data of reference measurements performed on productive and non-productive wells serve as a basis for cluster analysis to be carried out to distinguish significant information characteristic of oil and gas deposits. Pattern recognition on the basis of cluster separation considers the multi-dimensional vectors belonging to the weight centre of clusters as such information that characterizes the occurrence or lack of oil and gas deposits. Weight centres of separated clusters determine the probability values of $p = +100\%$ and -100% for occurrence, respectively. On the basis of deviations of the multi-dimensional information vectors characteristic of the field sites of the survey from the vectors characteristic of the weight centres (point of gravity) of the clusters, probability values — diagnostic for the occurrence of hydrocarbons — are estimated in per cent.

Similar multivariable statistical analysis is applicable for the data of magnetotelluric surveys, too. Fig. 14 shows the locations of MT field sites (black dots) in the vicinity of the seismic amplitude anomaly and the contour map of estimated probability of hydrocarbon occurrence — plotted on the basis of the statistical analysis of MT data with multiple variables. Borehole W2 intersected a gas-producing bed of Miocene age at a depth of about 2600 m. On the map a probability anomaly of $+70\%$ is found near the well site, while close to the non-productive wells the probability reduces to negative values. The seismic amplitude anomaly reveals a probability maximum of $+40\%$ in fairly good agreement with the MT probability anomaly, thus the combined synthesis of the two geophysical data sets supports the interpretive inference of *oil and gas occurrence within the pre-Tertiary basement.*

The amplitude anomaly observed within PGT-4 (region of profile kilometer 60, see Encls. 2 and 4) may originate from — similarly to conditions resolved at the intersection of profiles PGT-1 and PGT-2 — the presence of Mesozoic calcareous rocks. At the depth of the amplitude anomaly observed around profile kilometer 30 of PGT-4, Mesozoic calcareous rocks can be assumed, too (Encls. 2 and 4). If a partial graben formed also between profile kilometers 29 and 34 at the formation of the Hódmezővásárhely–Makó Graben with synrift sediments deposited in it, then it can be imagined that the amplitude anomaly observed here has been caused by them (Fig. 7).

Particularly on PGT-4, the marginally explored basement depth and the seismic acoustic parameter environment *are indicative of oil and gas accumulation* in producing areas of the Carpathian Basin.

6. Structure of the consolidated lithosphere

The pre-Neogene basement is delineated by the striking change in the geophysical parameters beneath orderly arranged signatures of the overlying younger clastic deposits. These juvenile strata are seismically associated with comparatively flat seismic horizons, and large signal amplitudes characteristic of young sediments that can be correlated over long distances. With increasing depth the above features are replaced by a character suggestive of predominantly folded and faulted tectonic pattern (Encls. 1 through 4). The average level of amplitudes is also reduced. Electrically, the conductive young sedimentary series are replaced by series whose resistivity is substantial increased. Beyond the sedimentary cover the upper crust is characterized by shorter irregular reflectivity patterns. Passing from the upper towards the lower crust, coherent reflectivity can be traced over longer distances outlining the previous lamellae characteristic of the lower crust.

Over a substantial portion of PGT-4, the bottom of the crust is imaged by prominent reflections of high amplitude traceable for long distances. In the mantle lithosphere (lithospheric part of the mantle) the average signal amplitudes are reduced. Due to the lack of velocity determinations with increasing depth of penetration (along the PGT-4), the bottom of the lithosphere can only be inferred from fragmented reflections and further decrease of their average amplitudes. From magnetotelluric surveys the surface of a deep, highly conductive layer is inferred as the asthenosphere. Magnetotelluric studies in addition indicate a small quantity of melt around the upper levels of the asthenosphere by a significant increase in conductivity (the depth of this interface is marked with crosses on Encls. 2 and 4). The Békés Basin is coupled with the highest conductivity region within the Hungarian segment of the Carpathian Basin. Since the interpretation of the magnetotelluric data assumed 2D-structures, the derived depth values are only estimates [ÁDÁM et al. 1993].

Key-factors in establishing an overall interpretation of the PGT-4 related information (Encls. 1–4) were:

— the fault zones extending from shallow to considerable crustal depth,

— the extended crust beneath the Békés Basin,

— the relatively thick lithosphere beneath the Hódmezővásárhely–Makó Graben

— the projected thinning of the lithosphere in the NE part of the profile.

At the SW end of the section, from the eastern flank of the Algyő High, zones of reduced amplitude descend to the NE. These zones are defined by numerous, subparallel reflecting surfaces (Encls. 1–4) outlining a number of significant *shear zones* of varying thickness. Along the intersecting PGT-1, the projections of these shear zones also have smaller seismic amplitude and from the 7 km thick fracture zone beneath the Szolnok–Máramaros flysch strike-slip movements can be inferred [POSGAY and SZENTGYÖRGYI 1991, POSGAY 1993]. It is assumed that in the ruptured fragmentary zones the reflecting surfaces are also destroyed/interrupted, hence in such a zone a smaller number of shorter reflecting surfaces are preserved. This may be why only shorter arrivals of lower energy are found in the zones under consideration. From reflections in the shear zone, which reflections run parallel to it, it has been concluded that glide zones generated by tectonic displacements are also reflectors. Several of these shear zones can be traced, with slight local displacements, to the bottom of the lithosphere. These local disruptions may be correlated with local causes (e.g. magmatic intrusions). The extent of the zone perpendicular to the plane of the profile (in rough approximation) may be of tens of kilometers. Displacements along the zone of considerable thickness and width could be influenced only locally by smaller objects, but could not essentially be prevented. Several of these fractured zones can be visually traced on the section, and are marked by continuous lines on Encls. 2 and 4.

At the SW, 0 and 15 km of the profile, curving series of reflections are evident at a depth of 9–11 km (Encls. 1–4). This inferred Dorozsma fractured zone extends beneath the Algyő High and southwestwards to the Dorozsma Graben (Fig. 1). This projected fractured zone may have played a major role in the development of the Dorozsma Graben, thus the tectonic evolution of the Hódmezővásárhely–Makó Graben, the Dorozsma Graben, and the Algyő High can be portrayed by a *single tectonic framework*.

The Dorozsma fault zone, dipping to the NE, joins to a major shear zone which extends from the eastern margin of the Algyő High, to the NE, beneath

the Hódmezővásárhely–Makó Graben. This major shear zone is delineated by a complex reflection pattern. It is several km thick and may have played a dominant role in the formation of the graben. This *extraordinary zone of weakness* can be followed laterally to the east of profile kilometer 40 and to a depth of about 24 km, where it is interrupted by a number of arcuate short sets of reflectivity. These localized, vertically arranged reflections are attributed to a magmatic intrusion developed in the lower crust at a point of reduced strength and viscosity [STREHLAU and MEISSNER 1987]. The reduction in strength of the lower crust and the uppermost domain of the mantle is a result of the thermal effects due to an intrusion ascending from a considerable depth [FOUNTAIN 1989]. This process is probably responsible for a number of intrusions of magmatic bodies into the uppermost mantle of the region [POSGAY 1993]. Beyond the intrusive body at 59 and 75 km and depth of 26–27 km, the strong and slightly dipping reflections are (Encls. 1 and 2) interpreted as a depthward continuation of the fracture zone.

From 70 to 80 km and below a depth of 35 km the reflection energy of the seismic section decreases significantly and the dip becomes more gentle. Beyond 80 to 85 km the predominant pattern of reflectivity turns subhorizontal. The high conductivity layer (crosses in Encls. 2 and 4) rises steeply to a depth of about 35 km beyond 70 km. This highly conductive domal body and zone of seismic transparency is interpreted as a major *uplift of the asthenosphere*. Comparable geophysical signatures were recognized along the relevant intersecting portion of PGT-1 [POSGAY et al. 1995]. It appears that the apex of this domal uplift is further to the east beyond the survey line. It is probable that the fracture zone originating at the margin of the Algyő High terminates adjacent to this structure. The synrift phase of the lithospheric extension contributed to the generation of the Hódmezővásárhely–Makó Graben, the metamorphic core complex associated with the Algyő High and a consequent development of the Dorozsma Graben at a later stage of tectonic progression. An extraordinary thinning of the lithosphere around the NE part of the profile led to an anomalously high rise of the asthenosphere. The rapid cooling of this uplifted segment of the asthenosphere led to fracturing and additional subsidence within the Hódmezővásárhely–Makó Graben and the Dorozsma Graben. Most of the seismically recognizable NE dipping faults, which may have played a substantial role in the formation of the grabens, may have formed in the synrift phase of the tectonic development of the region. To make the phenomenon physically more perceptible several

additional possible fracture zones have been interpreted on the seismic sections (Encls. 2 and 4).

Under the Békés Basin, at a variety of depths of the lithosphere, a composite set of arcuate reflectivity patterns can be identified consisting of characteristically upward convex reflecting surfaces. These localized patterns of arrivals are thought to be images of sequences of *magmatic intrusions*. Evidently the magmatism was reactivated several times and its latest stages penetrated the lower sedimentary deposits of the basins. As a local phenomenon, towards the NE end of the profile (as far as 60 km) the crust-mantle boundary appears — that from 0 to about 60 km can be characterized by a strikingly robust reflecting surface — only occasionally. It is assumed that the magmatism did not permit the complete formation of a solid boundary. Along PGT-1 the crust-mantle boundary can be identified fairly unambiguously [POSGAY et al. 1995]. Thus the location of the crust-mantle boundary, beneath the basin is marked according to the indication of the PGT-1 cross profile. We infer that beneath the Békés Basin the crust suffered extensive attenuation. Apart from the thick, young sedimentary series, and the significant rise of the crust-mantle boundary, it is difficult to account for the excess of magmatic material in the crust [SCLATER et al. 1980, PINET and COLLETTA 1990].

The profile of deep penetration permits one to draw conclusions also on the complexity of the nappe system formed during the Alpine orogeny. The Mesozoic formations forming the basement of the Pusztaföldvár–Battonya Ridge are identified on the seismic section by characteristic parallel reflections of high amplitudes, indicative of layered strata. The deep well marked with 2 allowed us to infer the lower-Codru nappe thrust over upper-Codru beds [GYÖRFI 1994]. The section leads us to assume that the overthrust plane can be encountered at the bottom of Neogene formations around 36 and 64 km of PGT-4. The seismic pattern reveals partial folding and fracturing of these rocks. The locally highly correlatable units are abruptly disrupted by visually evident displacements. Contacts between blocks of depositionally unrelated rock masses can be realized by abrupt changes of reflectivity characteristics. Any geological identification of these allochtonous nappes is highly contradictory [GYÖRFI 1994, GROW et al. 1994]. A number of crossing profiles or 3-D surveys (with specially designed low-frequency survey methods) are required to image these complex rock units with sufficient distinctness.

7. Schematic model of basin evolution

When the formation of the basin was initiated (about *20-25 Ma ago*, *Fig. 20a*) the original *crust of 30 km thickness* was perceived to be a consequence of the last great metamorphic event [MEISSNER 1986] of the terrane, the Hercynian-Variscan orogeny [FÜLÖP et al. 1987].

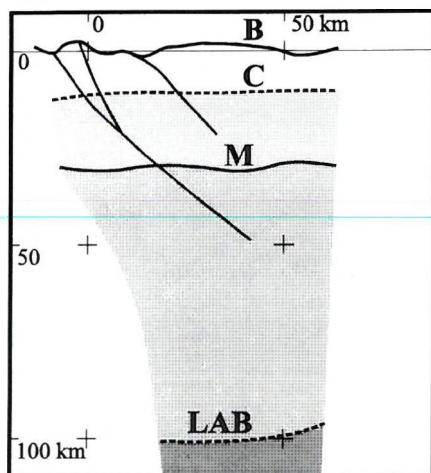In assuming the lithospheric thickness of the initial model the key points of consideration had to be as follows:

— the thickness of the lithosphere should show an empirical inverse relationship to the superficial density of heat flow [ÁDÁM 1980],

— attention should also be given to the relationship between the heat flow and the tectono-thermal age [ČERMÁK 1979].

Taking into account the above factors, the *thickness of the entire lithosphere* of the initial model was estimated to be *100 km* (this corresponds to about 300 Ma and 50 mW/m^2) of which 70 km was contributed by the lithospheric mantle .

The ratio of the estimated initial thickness of the crust to the crustal thickness of segments of the interpreted seismic profile varies between 1.2 and 2.1. The same (i.e. calculated vs. actual) ratio for the mantle lithosphere is between 1.8 and 5.4. It can be assumed that at the beginning of basin formation the zones of the upper and lower lithosphere were heterogeneous locally [COWARD 1986] and this may also have interfered with the deformation of individual structural entities of the region. It is also probable that the mechanical strength of certain zones underwent modification as a result of variation in temperature, and the development of fracture zones during the course of basin formation. For example retrograde phase changes (amphibolitization, serpentinization of dry rocks) may have led to a local weakening of basic and ultrabasic rocks.
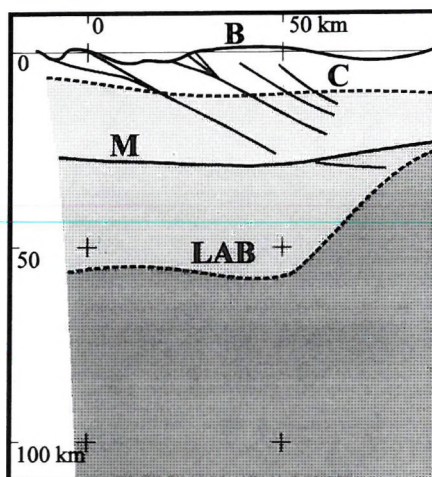
Relating the *mean extension* to the whole profile section, values of *1.5 and 2.5* were obtained for the *crust and the mantle lithosphere,* respectively. Consequently the extension of the mantle lithosphere appears to be areally smaller than that of the crust [COWARD 1986]. A number of symmetrically aligned echelons of basins is known along the direction of the PGT-4 survey (*Fig. 21*). The outer basins developed as half-grabens and their main faults dip towards the Békés Basin. The basin and their ridges of separation, from W to E are as follows: Dorozsma Graben, Algyő High, Hódmezővásárhely–Makó Graben, Pusztaföldvár–Battonya Ridge, Békés Basin, Zarand
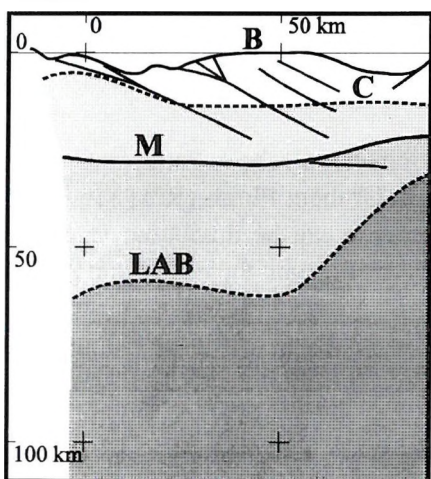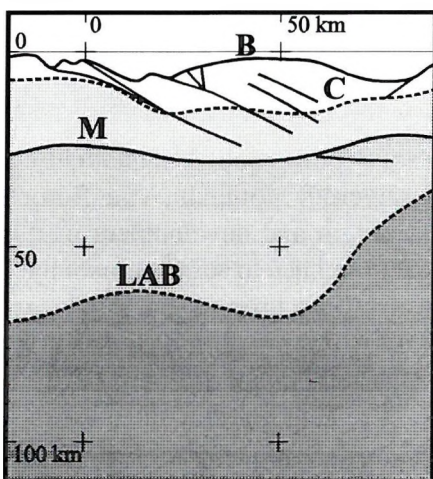
Fig. 20. Basin formation models of the Dorozsma Graben, the Hódmezővásárhely–Makó Graben and the Békén Basin assumed for 20–25, 15, 6 Ma and for the present date

20. ábra. A Dorozsmai árok, a Hódmezővásárhely–Makói árok és a Békési medence 20–25, 15, 6 millió évvel ezelőttre és a mai időpontra feltételezett kifejlődési modellje
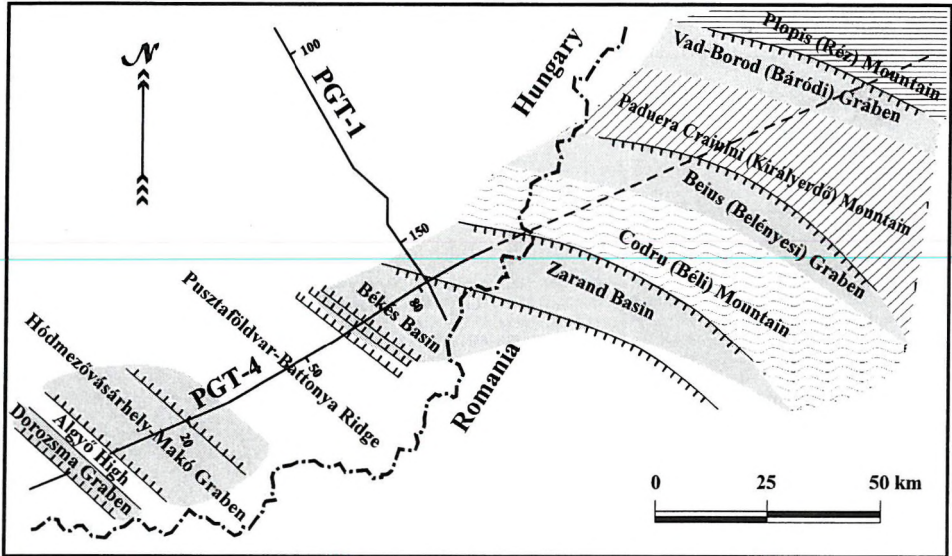
Fig. 21. Sketch of symmetrically aligned echelon of basins along the direction of the PGT-4 survey, modified after GYÖRFI [1994]. The outer basins developed as half-grabens and their main faults dip towards the Békés Basin and the neighbouring Zarand Basin

21. ábra. A PGT-4 szelvény irányában elhelyezkedő medencesor helyszín vázlata módosítva GYÖRFI [1994] után. A külső medencék félárokként fejlődtek ki és fő töréseik a Békési és a szomszédos Zarándi medence felé lejtenek

Basin, Codru (Béli) Mountain, Beius (Belényesi) Graben, Paduera Craiului (Királyerdő) Mountain, Vad–Borod (Báródi) Graben, Plopis (Réz) Mountain. The origin and development of this basin row can be attributed to a fault system, related to attenuation of the lithosphere beneath the Békés and Zarand Basins. This process led to the extension of a crustal portion *about 100 to about 150 km long,* which was identical (by and large) with the extension of a substantially shorter portion of the mantle lithosphere.

The length of the initial model crust along profile PGT-4 study is 60 km and, with its comparable upper mantle depth, is indicated in Fig. 20a. The depths of the fault-zones denoted on the model suggest that at this stage the maximum stress regime reached the maximum load-bearing capacity stress guide zones of the crust and mantle lithosphere [LISTER and DAVIS 1989, CHEN and MOLNÁR 1983]. In estimating the thickness of the stress guide in the mantle lithosphere, an additional eclogitic zone [MORGAN et al. 1994] was also assumed. Compared to theoretical models [WERNICKE 1981 and

1985, COWARD 1986] the assumed dip of the fault zones of the initial model appears to be relatively steeper.

For the model, about *15 Ma ago* (Fig. 20b) a major catastrophic event has been assumed to have taken place during the time interval which elapsed from the time of faulting of the initial model and the stress guides. Beneath the Békés and Zarand Basins the crust and lithospheric mantle were already subjected to fracturing and thinning, and a considerable mass of magma intruded, accompanied by an intensive warming period. The *mantle lithosphere* must have been heavily involved in this event so that its structure and physicochemical properties were changed significantly. As a consequence (beneath the Békés and Zarand Basins almost in its whole thickness) it probably *became similar to the asthenosphere*.

Through reduction of strength in depth the upper crust slipped along the fault zone which separates the Algyő High from the Hódmezővásárhely–Makó Graben. *The extent of separation may have reached about 15 km.* The movement was greater adjacent to the weakened fault zone and led to the formation of a half-graben. Mesozoic beds — as implied by borehole data along the profile and result of a grid of exploration seismic surveys [GROW et al. 1989 and 1994] — may have slipped down from the Algyő high at the same time. Due to the *slip of the upper crust the load on the lower crust was reduced* [WERNICKE 1985] and the Algyő area rose isostatically. Such a rise manifest itself by the metamorphic pre-Neogene basement in the area, by the domal uplift of the lower crust suggested by the seismic section, and by the characteristic gravity and magnetic anomalies of the region [POSGAY 1963, 1967, and KOVÁCSVÖLGYI 1995]. The domal uplift of 7–8 km on the boundary between the upper and lower crust allows us to infer that due to isostatic emergence of the Algyő area a part of the metamorphic basement was subjected to denudation, too.

In the Hódmezővásárhely–Makó Graben and the Békés Basin, 1–2 km thickness of synrift sediments were deposited (Encls. 2 and 4, see also in Figs. 4 and 6). At the beginning of this process the Hódmezővásárhely–Makó Graben may have been a double (or triple) graben. The dividing ridge(s) developed in submarine environment during the continuing extension of the lithosphere.

Structural attitudes of the postrift sediments suggest the early complex evolutionary phase of the graben. A factor which appeared earlier in the studied area and which is believed to be more significant was the faster cooling and contraction of the asthenosphere at a smaller depth beneath the Békés

and Zarand Basins. Contraction of the asthenosphere at an anomalous depth (on a regional scale) beneath the Carpathian Basin must have appeared later and to a lower extent. The first effect resulted in the unusually thick accumulation of Neogene sediments in the Hódmezővásárhely–Makó Graben and the Békés Basin. It is understood that *the fractured zones* played a major role in the development of the Hódmezővásárhely–Makó Graben. They *formed a weakened portion of the lithosphere that transmitted the contraction of the asthenosphere beneath the Békés and Zaránd Basins towards the graben even during the thermal phase*. This explains the formation of anomalously thick Tertiary sedimentary deposits in the Hódmezővásárhely–Makó Graben although the asthenosphere there lies at the average depth characteristic of the Carpathian Basin. This view also seems to be supported by the observation that the maximum thickness of sediments is found in the southwestern part of the graben, which allows one to assume the preservation of its origin of formation as a half-graben.

The magmatic activity continued in the postrift phase. Seismic evidence (Encls.2 and 4) dates the last phase of the magmatism as Upper Miocene. The seismic section beneath the Békés Basin suggests that a great amount of magma intruded into the lithosphere from the asthenosphere and accumulated in a shallow depth, contrary to the postulation of constant volume of the lithosphere [PINET and COLLETTA 1990].

The subsidence and inundation of the Algyő Ridge and of the Pusztaföld-vár–Battonya Ridge *5–7 million years ago* is attributed to regional contraction of the asthenosphere in the Carpathian Basin (Fig. 20c). The delta fronts reached the region of PGT-4 in this period too [VAKARCS et al.1994] blanketing the ridges with the bulk of delta sediments. Earlier these ridges were above the water level of the inland lake.

The contraction of the higher portion of the asthenosphere beneath the Békés and Zarand Basins continued to contribute to the relief depression caused by contraction of the asthenosphere on a regional scale. Thus the Hódmezővárásrhely–Makó Graben and the Békés Basin subsided at a faster pace than the ridges which were in an elevated position earlier (Figs. 3, 4 and Fig. 20d). Geodetic surveys reveal that the subsidence of the Hódmezővásárhely–Makó Graben is still an ongoing process in recent times [JOÓ et al. 1991].

8. Application in prospecting for oil and gas

One of the mandates of the lithosphere–asthenosphere research programme is to establish a method that images the subsurface from young sedimentary strata down to the asthenospheric depth. Such a method aims at
— identifying structures in the young Neogene sedimentary complex and mapping the pre-Neogene basement. (Roll-over structures connected to the listric fault in the Békés Basin. Seismic amplitude anomalies related to Mesozoic structures in the pre-Neogene basement);
— detecting fractures penetrating deeply into the lithosphere thereby helping the understanding of both tectonic patterns and local structures,
— inferring an attenuation of the crust and the lithosphere under young basins that furnishes a fundamental clue to theories on the origin of basins,
— providing information concerning the shape of the asthenospheric updoming and of its magmatic activity which may contribute to the improvement of our understanding of basin subsidence and hydrocarbon maturation models.

The pre-Neogene basement has recently played an important role in hydrocarbon exploration. Results of deep seismic surveys can therefore act as initial guide lines in this process. There is a high probability that the pre-Neogene basement may contain a significant amount of oil and gas. The vertically exaggerated section of PGT-4 (Fig. 4) reveals intriguing sedimentological and genetic features. Units I-II are the main hydrocarbon-generating formations. Geochemical investigations point to the fact that calcareous marl members of unit IV generated young immature/moderately mature oil at a shallow depth (about 2 km). Another oil generation process at greater depth took place when units I-II were at a depth of 3–4 km. During the short distance of migration the immature oil was trapped in the fractured weathered top zone of the uplifted basement or in the basal conglomerate — silty calcareous marl formation, which overlay it.

The mature oil with a longer migration path may have moved in two different ways: it could have migrated in the turbidite unit (III) along faults and became trapped in wedging out sandstones or moved along the pre-Neogene unconformities and accumulated in tectonic traps of the basment slope.

The amplitude of a dim spot anomaly indicates a very probable presence of Mesozoic reservoir at that particular depth.

Prediction of migration of gas is more difficult. Mature gas of high CO_2 content discovered in the basement may originate from different Mesozoic sequences. CO_2 may have been generated in metamorphic carbonates and migrated along overthrusts within the basement. The gas found in the Lower Pannonian (Upper Miocene) sandstones may have migrated in the turbidite unit III from the Hódmezővásárhely–Makó Graben. Alternatively, it may have followed listric faults, from the deeper zone of the basement into unit IV, where it was trapped in sandstone wedges of domal uplift.

9. Summary

Interpretation of the 1992 international deep seismic reflection profiling furnished interesting results from the young sediments to the asthenosphere. This cooperative study supplemented a series of experiments that had been conducted very successfully by the Eötvös Loránd Geophysical Institute of Hungary (ELGI) for the past quarter of this century, aiming to extend the depth penetration of seismic reflection surveys to study the *upper mantle*. The purpose of all of the programmes was to develop field procedures and data processing methods to utilize frequencies several octaves lower than the frequency range traditionally applied by seismic prospecting. An additional aim of the 1992 international survey was the testing of the Canadian equipment (PRS model), originally designed for refraction surveys, for its suitability in seismic reflection mode. This experiment was concluded with success. The exploitable seismic frequency limit was reduced to *1–2 Hz* in a survey which imaged the entire lithosphere.

The reflection depth section of the PRS recorded data with ELGI processing is displayed in a part of *Fig. 22*. Prominent features of the section were extrapolated into an interpretive model which outlines the tectonic framework of a series of basins in the region of investigation. Profile PGT-4 is a part of the Hungarian Geotraverse Project. It crosses the Hódmezővásárhely–Makó Graben, the Békés Basin (both of which are filled with thick sequences of Neogene sediments), and the Pusztaföldvár–Battonya pre-Neogene domal uplift. On the seismic depth section the depth of the asthenosphere determined by magnetotelluric survey is marked with crosses.

It is evident that due to extensive horizontal stresses that arose in the synrift phase stage, the load-bearing stress guide zones of the lithosphere were ruptured. A great amount of magma intruded into the lithosphere and transformed the lithospheric mantle to such an extent that its physicochemical properties became comparable (beneath the Békés and Zarand Basins almost throughout its whole thickness) to the asthenosphere. The extension of a relatively short (about 60 km) portion of the lithospheric mantle induced the extension of a significantly longer (about 100 km) segment of the upper crust (to about 150 km). We infer that this tectonic process led to the formation of an inward dipping *fault system*. The individual fault zones dip towards the *domal uplift of the asthenosphere*. In the early synrift phase the upper crust downthrusted along a set of faults. Along some fault zones the movement was more extensive forming half-grabens: Dorozsma Graben, Hód-mezővásárhely–Makó Graben, Beius (Belényesi) Graben and Vad–Borod (Báródi) Graben. Beneath the central (Békés and Zarand) basins the crust weakened to a level that magma intruded and replaced a major portion of the lithospheric mantle.

During the phase of cooling and contraction of the magma infested region (in the postrift phase) the fault zones acted as zones of mechanical weakness. The asthenosphere rose to its highest position beneath the central basins and the cooling there was extremely intensive. Contraction of the domal structure caused not only the subsidence of the central basins but, through a number of *fault zones, generated the half-graben-like basins along its margins*. Within the Carpathian Basin the lithosphere was also subjected to regional extension, because of which the asthenosphere reached an anomalously shallow depth. Subsidence of the tectonic high in between the basin sequences below the level of the interior lake and the beginning of sedimentation in the area is attributed to the *regional* cooling of the asthenosphere.

The results and methodologies of this successful experiment present an excellent guide for mineral exploration of the pre-Neogene basement. A number of local seismic amplitude anomalies have been recognized which could be possible future targets for *oil and gas exploration*. New data could also be added to the *nappe structure* system formed at the time of the Alpine orogeny.

The very thick (7–8 km) Neogene basin sediments were also presented with new perspectives. Underlying the already known sedimentary strata, limestone (or quartz-cemented sandstone) beds of *Lower Badenian and Lower Miocene* (perhaps Paleogene) age are assumed. The *magma* intruded into the
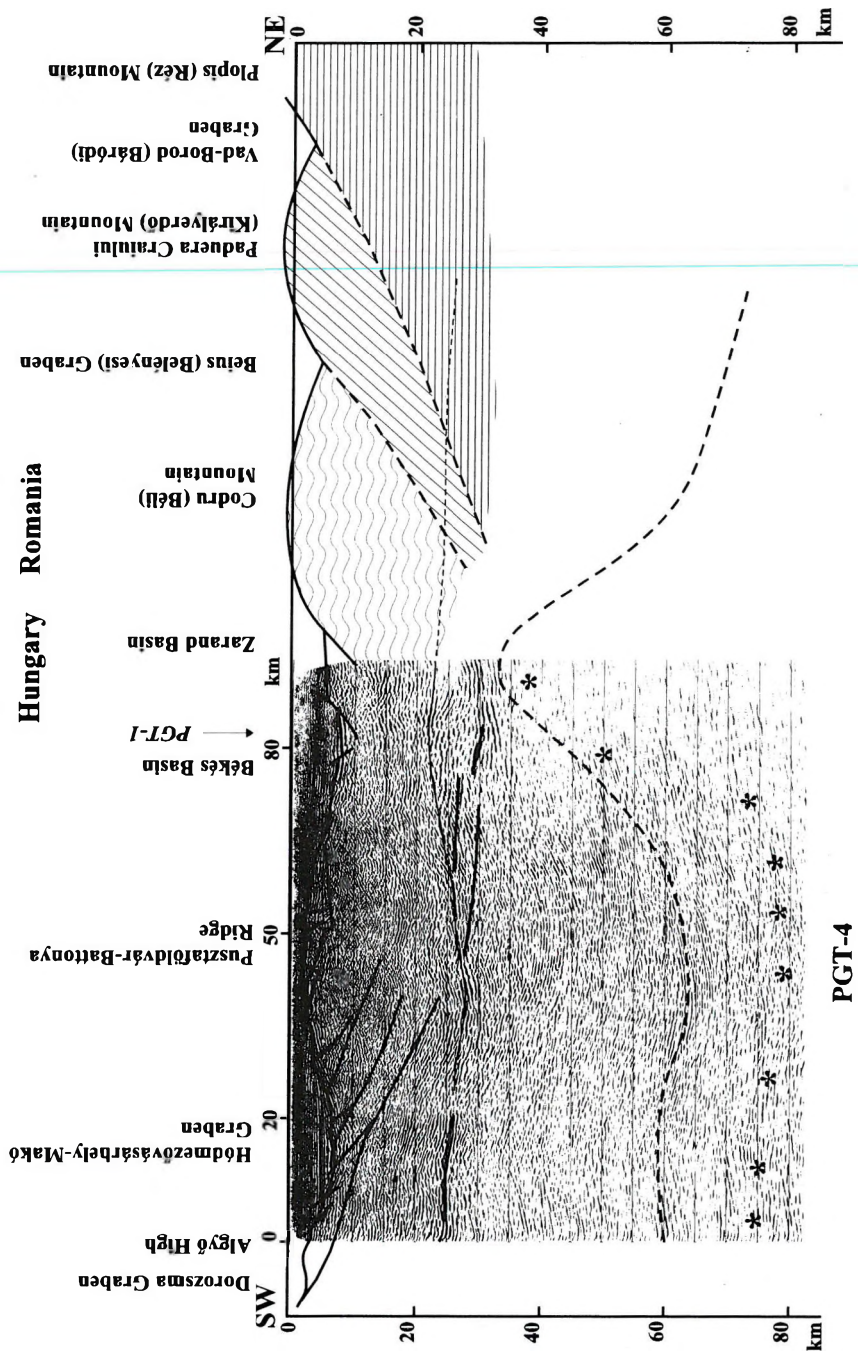
Neogene complex and the roll-over structure along a *listric fault* is also a new revelation.

Low-frequency deep penetrating seismic surveys combined with magnetotelluric studies offer a powerful tool for oil and gas exploration. Seismic amplitude analysis may also be utilized to detect deep seated oil and gas accumulations. Within the present data set the combined seismic amplitudes and magnetotelluric investigations led to the inference of target areas with possible hydrocarbon saturation. At greater depths, *stratigraphic traps* on the flanks of the uplifted structure and the *roll-over structures* formed on the NE side of the listric fault may present new exploration targets as well.

Acknowledgements

Fig. 22. Extension of the results of the Hungarian Geotraverse for the basin echelon known along the direction of the PGT-4 survey [modified after GYÖRFI 1994]. On the seismic depth section, crosses are drawn to indicate the depth of the asthenosphere as determined by magnetotelluric survey. The basin system is attributed to a deep fault system, related to attenuation of the lithosphere beneath the Békés and the Zarand Basin

22. ábra. A Magyar geotraverz eredményeinek kiterjesztése a szelvény irányába eső medencesorra [módosítva GYÖRFI 1994 után]. A PGT-4 szeizmikus mélységszelvényen keresztekkel jelöltük az asztenoszféra magnetotellurikus mérésekkel meghatározott mélységét. Értelmezésünk szerint a medencerendszert az asztenoszféra magaslat felé irányuló mélytörés rendszer alakította ki

—Ministry of Energy, Mines and Resources,
—University of Saskatchewan,
in Switzerland:
—Eidgenössische Technische Hochschule.

REFERENCES

ALBU I., PÁPA A. 1992: Application of high-resolution seismics in studying reservoir characteristics of hydrocarbon deposits in Hungary. Geophysics **57**, pp. 1068–1088

ÁDÁM A. 1980: Relation of mantle conductivity to physical conditions in the asthenosphere. Geophysical Surveys 4. D. Reidel Publishing Company, pp. 43–55

ÁDÁM A., SZARKA L., STEINER T. 1993: Magnetotelluric approximations for the asthenospheric depth beneath the Békés Graben, Hungary. J. Geomag. Geoelectr. **45**, pp. 761–773

BALLA Z. 1984: The Carpathian loop and the Pannonian basin: a kinematic analysis. Geophys. Trans. **30**, pp. 313–353

BALOGH K., JÁMBOR Á. 1987: Determining the geochronological position of the Kunság (Pannonian s.str) stage formations in Hungary. (In Hungarian.) MÁFI Annual Report, **69**, pp. 27–36

ČERMÁK V. 1979: Heat flow map of Europe. *In:* Terrestrial fleat flow in Europe. Eds.: ČERMÁK V., RYBACH L. Springer. Berlin, pp. 3–40

CHEN W. P., MOLNÁR P. 1983: Focal depths of intracontinental and intraplate earthquakes and their implications for the thermal and mechanical properties of the lithosphere. J. Geoph. Res. **88/B5.**, pp. 4183–4214

CHRISTENSEN N. I. 1989: Pore pressure, seismic velocities, and crustal structure. Geol. Soc. Am. Memoir **172**, pp. 783–798

COWARD M. P. 1986: Heterogeneous stretching, simple shear and basin development. Earth and Plan. Sci. Lett. **80**, pp. 325–336

CSONTOS L., TARI G., BERGERAT F., FODOR L. 1991.: Evolution of the stress fields in the Carpatho Pannonian area during the Neogene. Tectonophysics **199**, pp. 73–91

CSONTOS L., NAGYMAROSY A., HORVÁTH F., KOVÁC M. 1992: Tertiary evolution of the Intra-Carpathian area: a model. Tectonophysics **208**, pp. 221–241

DZWINEL J. 1983: Fundamental concept and practical aspects of cybernetic system for direct exploration of mineral deposits. Acta Geoph. Polnica., **31**, pp. 297–315

DZWINEL J., NAGY Z. 1985: New achievements of field application of the WEGA-D system. 47th EAEG Meeting, Budapest

FÜLÖP J., BREZSNYÁNSZKY K., HAAS J. 1987: The new map of basin basement of Hungary. Acta Geol. Hung. **30** (1–2), pp. 3–20

FOUNTAIN D. M. 1989: Growth and modification of lower continental crust in extended terrains: the role of extension and magmatic underplating. *In*: Properties and Processes of Earth's Lower Crust. Eds.: MEREU R. F., MUELLER S., FOUNTAIN D. M., Am. Geophys. Union — Int. Union Geod. and Geophys. Geophysical Monographs **51**, pp. 287–299

GROW J. A., POGÁCSÁS Gy., BÉRCZI-MAKK A., VÁRNAI P., HAJDÚ D., VARGA E., PÉRÓ Cs. 1989.: The tectonic and structural framework of the Békés Basin. (In Hungarian with English summary) Magyar Geofizika **30** (2–3), pp. 63–97

GROW J. A., MATTICK R. E., BÉRCZI-MAKK A., PÉRÓ Cs., HAJDÚ D., POGÁCSÁS Gy., VÁRNAI P., VARGA E. 1994: Structure of the Békés basin inferred from seismic reflection, well and gravity data. *In*: Basin analysis in petroleum exploration. Eds.: TELEKI P. G., MATTICK R. E. and KÓKAI J., Kluwer Dordrecht / Boston / London, pp. 1–8

GYÖRFI I. 1994 : Structural development of Neogene basins in SE Hungary and the Transylvanian Central Range. (In Hungarian.) Thesis Eötvös Loránd University, Univ'. Library Geological Department, Budapest

HAJNAL Z., REILKOFF B., POSGAY K., HEGEDŰS E., TAKÁCS E., ASUDEH I., MUELLER St., ANSORGE J., DeIACO R. 1996: Crustal scale extension in the Central Pannonian Basin. Tectonophysics, (in print)

HARVEY P. J. 1993: Porosity identification using amplitude variations with offset in Jurassic carbonate, offsore Nova Scotia. The Leading Edge, **12/3**, pp. 180–184

HORVÁTH F. 1986: Geophysical model of the formation of the Pannonian basin. (In Hungarian.) Ph.D. thesis, Eötvös Loránd University, Budapest pp. 1–148

HORVÁTH F. 1993: Towards a mechanical model of the formation of the Pannonian basin. Tectonophysics **226**, pp. 333–357

HORVÁTH F., ROYDEN L. 1981: Mechanism for the formation of the Intra-Carpathian basins: a review. Earth Evol. Sci., Vieweg, Wiesbaden, **1**, pp. 307–316

HORVÁTH F., DÖVÉNYI P., SZALAY Á., ROYDEN L. H. 1988: Subsidence, thermal, and maturation history of the Great Hungarian Plain. *In*: The Pannonian Basin, a study in basin evolution. Eds.: ROYDEN L. H., HORVÁTH F., AAPG Memoir **45**, pp. 355–372

HORVÁTH F., POGÁCSÁS Gy. 1988: Contribution of seismic reflection data to chrono-stratigraphy of the Pannonian Basin. *In*: The Pannonian Basin, a study in basin evolution. Eds: ROYDEN L. H., HORVÁTH F., AAPG Memoir **45**, pp. 97–105

HUGHES L. J., ZONGE K. L., CARLSON N. R. 1985: The application of electrical techniques in mapping hydrocarbon related alteration. *In*: Unconventional methods in exploration for petroleum and natural gas. Ed.: DAVIDSON M. J., DALLAS, Southern Methodist Univ. Press., IV, 5–2

JOÓ I., DRAGOESCU I., KUZNETSOV Y.G., MLADENOVSKI M. M., NÉMETH Zs., VANKO J., WYRZYKOWSKI T. 1991: Explanatory description to the map of the horizontal

velocity gradients of the recent vertical movements in the Carpatho–Balkan region. Multilateral Technical-Scientific Cooperation of Geodetic Services of Bulgaria, Czech and Slovak Republic, Hungary, Poland, Rumania and Soviet Union, Manuscript

KARUS E. W., KUZNETSOV O. L., KIRICHEK M. A., PETUKHOV A.V. 1985: Direct prospecting of oil-gas deposits including complex of geophysical and geochemical techniques. 30 Int. Geoph. Symp. Moscow

KILÉNYI É., KRÖLL A., OBERNAUER D., ŠEFARA J., STEINHAUSER P., SZABÓ Z., WESSELY G. 1991: Pre-Tertiary basement contour map of the Carpathian Basin beneath Austria, Czechoslovakia and Hungary. Geophys. Trans. **36**, pp. 15–36

KÓKAI J., POGÁCSÁS Gy. 1991: Hydrocarbon plays in Mesozoic nappes, Tertiary wrench basins and interior sags in the Pannonian Basin. First Break **9/7**, pp. 315–334

KOVÁCS S. 1982: Problems of the 'Pannonian Median Massif' and the plate tectonic concept. Contributions based on the distribution of Late Paleozoic — Early Mesozoic isopic zones. Geol. Rundsch. **71**, pp. 617–639

KOVÁCSVÖLGYI S. 1995: Interpretation of gravity and magnetic anomalies of SE Hungary (In Hungarian.) Magyar Geofizika **36**, pp. 198–202

KŐRÖSSY L. 1992: Hydrocarbon geology of the Duna–Tisza Interfluve, Hungary. (In Hungarian.) Általános Földtani Szemle **26**, pp. 3–162

LISTER G. S., DAVIS G. A. 1989: The origin of metamorphic core complexes and detachment faults formed during Tertiary continental extension in the northern Colorado River region, U.S.A. J. of Structural Geology. **11**, (1–2), pp. 65–94

MÁRTON E. 1981: Tectonic implication of paleomagnetic data for the Carpatho-Pannonian region. Earth Evol. Sci., Vieweg, Wiesbaden, **1**, pp. 257–264

MATTICK R. E., PHILIPS R. L., RUMPLER J. 1988: Seismic stratigraphy and depositional framework of sedimentary rocks in the Pannonian Basin in Southeastern Hungary. *In*: The Pannonian Basin, a study in basin evolution. Eds: ROYDEN L. H., HORVÁTH F., AAPG Memoir **45**, pp. 117–145

MATTICK R. E, RUMPLER J., UJFALUSY A., SZANYI B., NAGY I. 1994: Sequence stratigraphy of the Békés Basin. *In*: Basin analysis in petroleum exploration. Eds.: TELEKI P. G., MATTICK R. E., KÓKAI J., Kluwer Dordrecht / Boston / London, pp. 39–65

MEISSNER R. 1986: The Continental Crust. Academic Press. Harcourt Brace Jovanovich. London, 393 p.

MORGAN J. V., HADWIN M., WARNER M. R., BARTON P. J., MORGAN R. P. Ll. 1994: The polarity of deep seismic reflections from the lithospheric mantle: evidence for a relict subduction zone. *In*: Seismic reflection probing of the continents and their margins. Eds.: CLOWES R. M., GREEN A. G., Tectonophysics **232**, pp. 319–328

NAGY Z. 1992: Advances in integrated interpretation of seismics with magnetotellurics. 54th EAEG Meeting, Paris

OSTRANDER W. J. 1984: Plane-wave reflection coefficients for gas sands at nonnormal angles of incidence. Geophysics **49**, pp. 1637–1648

PINET B., COLLETTA B. 1990: Probing into extensional sedimentary basins: comparison of recent data and derivation of tentative models. *In*: Seismic Probing of Continents and their Margins. Eds.: LEVEN J. H., FINLAYSON D. M., WRIGHT C., DOOLEY J. C., KENNETT B. L. N., Tectonophysics **173**, pp. 185–197

POGÁCSÁS Gy., JÁMBOR L., MATTICK R. E., ELSTON D. P., HÁMOR T., LAKATOS L., LANTOS M., SIMON E., VAKARCS G., VÁRKONYI L., VÁRNAI P. 1989.: Chronostratigraphic framework of Neogene formation in the Great-Hungarian Plain as revealed by combination of seismo- and magnetostratigraphy. (In Hungarian with English summary). Magyar Geofizika **30**, (2-3), pp. 41–62

POGÁCSÁS Gy., MATTICK R. E., ELSTON D. P., HÁMOR T., JÁMBOR Á., LAKATOS L., LANTOS M., SIMON E., VAKARCS G., VÁRKONYI L., VÁRNAI P. 1994: Correlation of seismo- and magnetostratigraphy in Southeastern Hungary. *In*: Basin analysis in petroleum exploration. Eds.: TELEKI P. G., MATTICK R. E., KÓKAI J., Kluwer Dordrecht / Boston / London, pp. 143–160

PÓKA T. 1988: Neogene and Quartenary volcanism of the Carpathian-Pannonian region: changes in chemical composition and its relationship to basin formation. *In*: The Pannonian Basin, a study in basin evolution. Eds: ROYDEN L. H., HORVÁTH F., AAPG Memoir **45**, pp. 257–277

POSGAY K.1963: A comprehensive map of the magnetic masses in Hungary and its interpretation. Acta Techn. Acad. Sci. Hung. **43**, (3-4), pp. 271–287

POSGAY K.1967: A comprehensive study of geomagnetic bodies in Hungary. (In Hungarian with English summary), Geophys.Trans. **16**, (4), pp. 1–118

POSGAY K. 1975: Mit Reflexionsmessungen bestimmte Horizonte und Geschwindigkeitsverteilung in der Erdkruste und im Erdmantel. Geophys. Trans. **23**, pp. 13–17

POSGAY K. 1993: Formation of the crust-mantle boundary in the previous upper mantle. Geophys. Trans. **37**, (4), pp. 243–251

POSGAY K., ALBU I., PETROVICS I., RÁNER G. 1981: Character of the Earth's crust and upper mantle on the basis of seismic reflection measurements in Hungary. Earth Evol. Sci., Vieweg, Wiesbaden, **1**, pp. 272–279

POSGAY K., ALBU I., RÁNER G., VARGA G. 1986: Characteristics of the reflecting layers in the Earth's crust and upper mantle in Hungary. *In*: Reflection Seismology: A Global Perspective. Eds.: BARAZANGI M., BROWN L. Am. Geophys. Union, Geodyn. Ser., **13**, Washington, pp. 55–65

POSGAY K., HEGEDŰS E., TÍMÁR Z. 1990: The identification of mantle reflections below Hungary from deep seismic profiling. *In*: Seismic Probing of Continents and their Margins. Eds.: LEVEN J. H., FINLAYSON D. M., WRIGHT C., DOOLEY J. C., KENNETT B. L. N., Tectonophysics **173**, pp. 379–385

POSGAY K., SZENTGYÖRGYI K. 1991: Strike-slip fault system crossing the lithosphere at the Eastern part of the Pannonian basin. (In Hungarian with English summary.) Magyar Geofizika **32**, pp. 1–15

POSGAY K., BODOKY T., HEGEDŰS E., KOVÁCSVÖLGYI S., LENKEY L., SZAFIÁN P., TAKÁCS E., TIMÁR Z., VARGA G. 1995: Asthenospheric structure beneath a Neogene basin in southeast Hungary. *In*: Interplay of extension and compression

in basin formation. Eds.: CLOETINGH S., D'ARGENIO B., CATALANO R., HORVÁTH F., SASSI W. , Tectonophysics **252**, (1-4), pp. 467-484

SCLATER J. G., ROYDEN L., HORVÁTH F., BURCHFIEL B. C., SEMKEN S., STEGENA L. 1980: The formation of the Intra-Carpathian basins as determined from subsidence data. Earth and Planet. Sci. Let., **51**, pp. 139-162

SPENCER Ch. W., SZALAY Á., TATÁR É. 1994: Abnormal pressure and hydrocarbon migration in the Békés Basin. *In*: Basin analysis in petroleum exploration. Eds.: TELEKI P. G., MATTICK R. E., KÓKAI J., Kluwer Dordrecht / Boston / London, pp. 201-219

STEGENA L., GÉCZY B., HORVÁTH F. 1975: Late Cenozoic evolution of the Pannonian basin. Tectonophysics **26**, pp. 71-90

STREHLAU J., MEISSNER R. 1987: Estimation of crustal viscosities and shear stresses from an extrapolation of experimental steady state flow data. *In*: Composition, Structure and Dynamics of the Lithosphere – Asthenosphere System. Eds.: FUCHS K., FROIDEVAUX C., Geodynamics Series, AGU, 16, pp. 69-87

SZEDERKÉNYI T., ÁRKAI P., LELKES-FELVÁRI Gy. 1991: Crystalline groundfloor of the Great Hungarian Plain and South Transdanubia, Hungary. Geodynamic Evolution of the Pannonian Basin. Ed.: KARMATA St., Acad Conf. **LXII**/4. Beograd

SZEIDOVITZ Zs. 1990: Report on seismic reflection measurement around Tisza-gyenda—Fegyvernek in 1988–89. (In Hungarian.) MOL Rt. and ELGI Archives

TAKÁCS E. 1996: Study of possible geological causes of amplitude anomalies within the pre-Tertiary basin's bottom. (In Hungarian.) Submitted, Magyar Geofizika

TARI G., HORVÁTH F., RUMPLER J. 1992: Styles of extension in the Pannonian Basin. Tectonophysics **208**, pp. 203-219

VAKARCS G., VAIL P. R., TARI G., POGÁCSÁS Gy., MATTICK R. E., SZABÓ A. 1994: Third-order Middle Miocene—Early Pliocene depositional sequences in the prograding delta complex of the Pannonian Basin. Tectonophysics **240**, pp. 81-106

VARGA G. 1992: Analysis of the investigation of geothermal reservoirs of high enthalpy by magnetotelluric measurements. (In Hungarian.) ELGI Archives

VARGA G., NEMESI L. 1994: Deep structure of the Békés Basin and Makó Graben on the basis of new magnetotelluric measurements and 2D inversion. (In Hungarian.) ELGI Archives

WERNICKE B. 1981: Low-angle normal faults in the Basin and Range Province: nappe tectonics in an extending orogen. Nature **291**, pp. 645-648

WERNICKE B. 1985: Uniform-sense normal simple shear of the continental lithosphere. Can. J. Earth Sci. **22**, pp. 108-125

Nemzetközi együttműködésben végzett mélyreflexiós kutatás a "Magyar geotraverz" mentén

POSGAY K., TAKÁCS E., SZALAY I., BODOKY T., HEGEDŰS E., JÁNVÁRINÉ K. I., TÍMÁR Z., VARGA G. — BÉRCZI I., SZALAY Á., NAGY Z., PÁPA A. — HAJNAL Z., REILKOFF B. — MUELLER ST., ANSORGE J., DE IACO R. — ASUDEH I.

Magyar, kanadai és svájci együttműködésben DK Magyarországon kis-frekvenciás, reflexiós, szeizmikus litoszférakutatásokat végeztünk 1992-ben. A nemzetközi mérések jól illeszkedtek az ELGI negyed évszázados kísérletsorozatába, mellyel a szeizmikus reflexiós mérések mélységi behatolását kívánta kiterjeszteni a *felső köpeny* kutatására. A kísérletek célja olyan terepi és feldolgozási metodika kialakítása volt, mellyel a nyersanyagkutató szeizmikus méréseknél használt frekvenciatartománynál több oktávval kisebb frekvenciák is felhasználhatók. A nemzetközi mérés kulcsproblémája a refrakciós mérésekhez tervezett kanadai (PRS típusú) berendezések mélyreflexiós alkalmazása volt. A kísérlet sikerrel zárult. Az átviteli frekvenciatartományt sikerült *1–2 Hz* - ig csökkenteni és a teljes litoszféra szerkezetét megismerni.

A PGT-4 jelű szeizmikus szelvény az algyői kiemelt szerkezet oldaláról indult, a Hódmezővásárhely–Makói árkot, a Pusztaföldvár–Battonya-i medencealjzat felboltozódást és a Békési medencét harántolta (*1. ábra*).

A kanadai berendezéssel párhuzamosan (kisebb fedésszámmal) az előző mélyreflexiós kutatásoknál használt (MDS-18 típusú) felszerelést is üzemeltettük tájékoztató összehasonlítás, továbbá a neogén üledékek és a preneogén medencealjzat jobb felbontású vizsgálata végett. A méréseket kiegészítettük a szelvény végekre telepített, a mérés egész ideje alatt helyben maradó (svájci, magyar és kanadai) állomásokkal (*2. ábra*).

A terepi mérések megtervezésében és kivitelezésében a három ország kutatói együttműködtek. A feldolgozás és értelmezés feladatmegosztással folyik. Ebben a cikkben az ELGI-ben végzett feldolgozás első eredményeit ismertetjük.

A neogén összlet az MDS-18 berendezéssel felvett, kinagyított függőleges léptékű szelvényen (*3. és 4. ábrák*) jól tanulmányozható. A közelítőleg 6 millió évnél fiatalabb rétegsor a szelvény teljes hosszában megtalálható. A rétegsor alján jelentős amplitúdóval és jellegzetes elvégződésekkel jelentkező, sárga színnel jelölt, reflektáló szintek delta üledékekkel azonosíthatók. Előzőleg a Pusztaföldvár–Battonyai hegyhát magasabb része a beltó szintje fölött volt. A neogén rétegsor alsóbb szintjei a hegyhát oldalában kiékelődnek.

A szeizmosztratigráfiai, szekvenciasztratigráfiai, magnetosztratigráfiai vizsgálatok és a radiometriai kormeghatározások eredménye szerint [VAKARCS et al. 1994] a sekély tenger a szarmata és pannon emeletek határán (11,5 Ma) izolálódott a világtengerektől és tóvá alakult. A szarmata végén és a pannon emelet elején a Békési medence és a Hódmezővásárhely–Makói árok elmélyülése gyorsabb volt mint az üledék felhalmozódása, viszonylag éhező medencék voltak [POGÁCSÁS et al. 1989].

A Békési medencében, a 70. szelvénykilométer táján a neogén üledékek mélyebb szintjébe történt *magmás benyomulásra* következtethetünk, amely megemelte a felette levő üledékeket (*5. és 6. ábrák*). A magmás benyomulást *felső miocén (alsó pannon) bazalt*ként értelmeztük. Felette egy *lisztrikus vető* figyelhető meg, amelynek ÉK- i, azaz a medence felőli oldalán átforduló (roll-over) szerkezet látható. Valószínű, hogy a szerkezet kialakulása a magmatikus benyomulás és az üledékes rétegsor eltérő kompakciójával magyarázható. A magmatikus tevékenység a konszolidált kéreg teljes mélységében nyomozható (*1–4. mell.*).

Feltételezésünk szerint mindkét medence mély részén a bádeni rétegek alatt *alsó miocén* (esetleg paleogén) üledékek is keletkeztek. Ez a *szinrift formáció* enyhén tört szerkezetű és jelentős, kb. 1500 m vastagságú. Nagy amplitúdóval és kis frekvenciával jelentkezik. A 2. és 4. mellékleten és a 4. és 6. ábrán ezt a rétegsort zöld színnel jelöltük. A magnetotellurikus mérések szerint az összlet ellenállása több mint 200 Ωm [VARGA és NEMESI 1994]. A szeizmikus és magnetotellurikus eredmények együttes értelmezése alapján *vastag pados mészkövet, vagy kvarcos kötésű homokkövet* tételezünk fel.

A Hódmezővásárhely-Makói árok az alsó miocén idején két (2. és 4. mell.) vagy három (*7. ábra*) részre választódott el. Az elválasztó gerinc(ek) magassága többszáz méterre becsülhető. Az árokrészek kialakításában a DNy-i oldalukon található mélytörészónák és az ezekhez csatlakozó kisebb törések játszhattak jelentős szerepet. A felső bádeni idején a tenger a gerinc(ek) fölé emelkedett és közös üledékgyüjtő alakult ki.

A Békési medencében a szinrift időszakban a medence belseje felé lejtő törések alakultak ki. A 85.-87. szelvénykilométer táján látható, sokszáz méter elvetési magasságú törészóna az alsó miocén rétegeket is elvetette. A jelentős elvetésre mind a szeizmikus képből, mind a magnetotellurikus mérésekkel meghatározott nagyellenállású réteg mélységváltozásából következtethetünk (2. és 4. melléklet).

A PGT-4 szelvényen, **a preneogén medencealjzatban**, 29-32, továbbá 57-60 szelvénykilométer között a környezetéből kiemelkedő, közel vízszintes **amplitúdó anomáliát** észleltünk. A *8. és 9. ábrán* látható szelvényrészletet 2-40 Hz szűréssel készítettük.

Részletesebben az 57-60 szelvénykilométer között észlelt amplitúdó anomáliát vizsgáltuk meg. A kis-frekvenciás metodika használhatóságára következtettünk abból, hogy ugyanezen a szelvényszakaszon 10 Hz-es alulvágás esetén a kérdéses amplitúdó anomália már nem figyelhető meg (*10. ábra*), azaz csak *a litoszféra-asztenoszféra kutatáshoz kifejlesztett kisfrekvenciás metodikával határozható meg*. Értelmezéséhez longitudinális hullámsebesség, sűrűség és Poisson szám becslés történt [TAKÁCS 1996], különös figyelmet fordítva a reflexiós tényező előjelére. A kőzetfizikai paraméterek becslése a vizsgálati helyen mért szeizmikus csatorna, illetve az amplitudó-észlelési távolság (AVO) modellezésével történt (*11. és 13. ábra*). A vizsgálatok alapján valószínű, hogy az anomális amplitúdójú reflexiót mezozoós karbonátos kőzetek törés- és repedésrendszerében lévő *széndioxid és víz*, vagy *szénhidrogén gáz és olaj*, vagy ezeknek más kombinációja okozhatta (*12. ábra*).

Az elképzelés kiegészítésére ismertetjük a PGT-1 és PGT-2 kereszteződésénél (1., *15. és 16. ábrák*) észlelt amplitúdó anomália vizsgálatát, amelynél a szeizmikus modellvizsgálatnál akusztikus karottázs adatokból indulhattunk ki (*17., 18. és 19. ábrák*) és az értelmezést területi magnetotellurikus eredmények is segítették (*14. ábra*). A szeizmikus modellvizsgálat és az ismertetett WEGA-D felismerő rendszerrel végzett vizsgálat azt mutatja, hogy az amplitúdó anomália *potenciális kőolaj és földgáz előfordulás*ként értelmezhető [NAGY 1992].

A **konszolidált litoszféra** szerkezetét tanulmányozva a nagy behatolású szelvényből az alpi orogén alatt kialakult takarórendszer bonyolultságára is következtethetünk. A Pusztaföldvár-Battonyai gerincen furásokból ismert és a szeizmikus szelvényen azonosított mezozoikumot nagy amplitúdójú, rétegzettségre utaló reflexiók jellemzik. Ezek a *Kodru takarók* mezozoikumához tartoznak [GYÖRFI 1994].

Az alattuk látható képből töréses, gyűrődéses szerkezetre következtethetünk. A szeizmikus kép arra utal, hogy a Hódmezővásárhely-Makói árok és az Algyői medencealjzat magaslat között törés tételezhető fel, amelyik az Algyői szerkezet alatti, a Dorozsmai árok felé irányuló töréssel egyesülve a szelvény ÉK-i vége felé lejt (2. és 4. mell.). A vázolt zónától ÉK felé, a Hódmezővásárhely-Makói árok alól kiinduló további törések is feltételezhetők, azaz egy több km vastag, kis sziládságú zónára lehet következtetni, amely értelmezésünk szerint döntő szerepet játszhatott az árok kialakulásában. Ez a nyírási zóna — enyhébb dőléssel — az alsó litoszférában is nyomozható.

A 70. és a 80. szelvénykilométer között, 35 km alatt a reflexiós energia jelentősen lecsökken, a reflektáló felületek dőlése enyhül és 80-85. szelvénykilométertől kezdve uralkodóan közel vízszintes lesz (1-4 mell.). A jólvezető réteg a 70. szelvénykilométer után meredek emelkedővel 35 km fölé magaslik. A csökkent szeizmikus energiájú és jól vezető MT tartományt az *asztenoszféra felboltozódásá*ként értelmezzük. (A magnetotellurikus adatokat 2D felépítés feltételezésével dolgoztuk fel. Elképzelhető, hogy a 2D feltételezéssel a valóságosnál kisebb mélységet határoztunk meg [ÁDÁM et al. 1993]). A Pannon geotraverzen a szeizmikus (PGT-1), a magnetotellurikus és a geotermikus eredmények integrált interpretációja alapján a Békési medence alatt az asztenoszféra megemelt helyzetére következtettünk [POSGAY et al. 1996]. A Magyar geotraverzen a mélyreflexiós (PGT-4) és a magnetotellurikus adatok szerint a litoszféra-asztenoszféra határ emelkedése a Békési medencén túl is valószínűnek látszik, azaz a Békési medence mély részéhez viszonyítva az asztenoszféra felboltozódása ÉK felé helyezkedik el és elképzelhető, hogy az Algyői szerkezet felől lejtő, töréses zóna ennek közelében végződik. A Makói árok alatt a kéreg-köpeny határ és a litoszféra-asztenoszféra határ is csak enyhe domborulatot képez (2. és 4. mell.).

Az eredmények értelmezéséhez vázolt **medencefejlődési modell**ünk szerint a szinrift fázisban a köpenylitoszférának a szelvényvég tájára eső része jobban megnyúlt mint a köpeny-litoszféra többi része. Ennek következménye volt, hogy az Algyő felől lejtő törészóna mentén litoszféraméretű megcsúszás következett be, létrehozva a Hódmezővásárhely-Makói árkot, a metamorf kőzetekből álló medencealjzatú, viszonylag vékony felső kéreggel jellemezhető Algyői magaslatot és valószínűleg a Dorozsmai árkot is. A köpenylitoszféra rendkívüli elvékonyodása a szelvény ÉK-i részén az asztenoszférának az átlagosnál nagyobb megemelkedéséhez is vezetett. A viszonylag magasabbra került asztenoszférarésznek az átlagosnál korábbi és gyorsabb kihűlése a *meggyengült (töréses) zóna közvetítésével* a Hódmezővásárhely-Makói árok (és a Dorozsmai árok) további besüllyedéséhez vezetett (*20. ábra*). Nézetünk szerint ezzel magyarázható, hogy a Hódmezővásárhely-Makói árokban anomális vastagságú üledék keletkezett annak ellenére, hogy az asztenoszféra a Kárpát medencére jellemző átlagos mélységben valószínűsíthető. Az asztenoszférának a Kárpát medencében történt regionális összehúzódása hatásaként értelmezzük az Algyői medencealjzat domborulatnak és a Pusztaföldvár-Battonyai hegyhátnak 5-7 millió évvel ezelőtti megsüllyedését és elöntését (20c ábra).

A PGT-4 szelvényszakasz *átlagos megnyúlásá*ra a *kéregre 1,5* és a *köpeny-litoszférára 2,5* értéket kaptunk, azaz egy *kb. 100 kilométeres kéregszakasz kb.150 km-re* történt megnyúlása volt (nagyjából) azonos egy lényegesen rövidebb (kb. 60 km-es) köpeny-litoszféra szakasz megnyúlásával. (Ezt alátámasztja például, hogy az algyői törészóna menti felső kéreg megcsúszásból kb. 15 km-es térmeghosszabbodásra következtethetünk.) A szelvény irányában egy — nagy vonalaiban szimmetrikus — medencesor ismert (*21. ábra*). A külső medencék félárokként fejlődtek ki és fő töréseik a Békési és a szomszédos Zarándi medence felé lejtenek [GYÖRFI 1994]. A medencesor és az azokat elválasztó hegyhátak Ny-ról K felé a következők: Dorozsmai árok, Algyői szerkezet, Hódmezővásárhely-Makói árok, Pusztaföldvár-Battonyai medencealjzat domborulat, Békési medence, Zarándi (Zarand) medence, Béli hegység (Codru-Moma), Belényesi (Beius) árok, Királyerdő (Paduera Craiului), Báródi (Vad-Borod) árok, Réz (Plopis) hegység. Feltételezhető, hogy a medencesor keletkezése a litoszférának a Békési és a Zarándi medence alatti felszakadásával kapcsolatos törésrendszerre vezethető vissza (*22. ábra*). Ezekben a medencékben és az alattuk elhelyezkedő litoszférarészben következtethetünk a legjelentősebb magmabenyomulásra is.

Tudomásunk szerint a Kárpát medencében végzett kisfrekvenciás reflexiós mérések az *elsők*, ahol az eredményekből a *teljes litoszféra* szerkezete vázolható [POSGAY et al. 1981, 1995., HAJNAL et al. 1996]. Érdekesnek látszott, hogy a Magyar geotraverzen kapott eredményeket összevessük olyan medencefejlődési modellel, amely a mérések értelmezését elősegítheti. A kapott eredmények emlékeztetnek WERNICKE [1981 és 1985] medence kialakulási modelljére. A felszíntől az alsó litoszféráig tartó nyírási zóna felszínközeli részén keletkezett a Hódmezővásárhely-Makói árok és

feltételezésünk szerint a Dorozsmai árok. „Core Complex range"-ének helyén a PGT-4 szelvény elején is feldomborodik az alsó kéreg (a Dorozsmai árok és a Hódmezővásárhely–Makói árok között), és a litoszféra-asztenoszféra határnak a mélytörészóna mélyrésze (a szelvényben ÉK) felé történő emelkedése valószinűsíthető.

Eltérést jelent WERNICKE modelljéhez viszonyítva a Hódmezővásárhely–Makói árok nagy mélysége és annak magyarázata.

A mélylitoszférára vonatkozó új ismereteken kívül a medencealjzat és a fiatal üledékek mélységéből is érdekes szerkezetekre lehetett a mérési adatokból következtetni, amelyek a nyersanyagkutatás, a nagyszerkezet megismerése és módszertani szempontokból is figyelemre méltók lehetnek.

Új kutatási perspektivákat a kiemelt szerkezet lejtőin kialakult csapdák, illetve a lisztrikus vető oldalán létrejött átforduló (roll-over) szerkezetek jelentik.

Mantle plumes or EM distortions in the Pannonian Basin? (Inversion of the deep magnetotelluric (MT) soundings along the Pannonian Geotraverse)

Antal ÁDÁM[*],
László SZARKA[*], Ernő PRÁCSER[**], Géza VARGA[**]

Results are given here of magnetotelluric investigations of 19 long-period magnetotelluric soundings along the NW-SE oriented Pannonian Geotraverse during the past eight years. After a brief description of the data acquisition systems and data processing methods used the measured and interpreted data, giving information about both the deep structure of the lithosphere/asthenosphere and the basinal structure of the region, are presented.

Based on 1-D inversions of sounding curves and also on different (Occam- and RRI) 2-D inversions along the Geotraverse the main conclusions are as follows.

— The average asthenospheric depth — based on the relationship between the asthenospheric depth and the regional heat flow and on other related information — was found to be in the range of 50–70 km, depending on the type of curve and number of sites taken into consideration.

— Although the near-surface electric inhomogeneities distort the MT sounding curves, it can be realized that below narrow, deep extensional 3-D subbasins, like the Békés graben, conducting asthenospheric plumes come up to a depth of about 40 km in accordance with the upwelling of the highly dense mantle material, indicated by gravity anomalies and the recent seismic results in the region.

— The stable magnetotelluric anisotropy (which can be found everywhere in the Pannonian Basin) is due to structural inhomogeneities.

1. Introduction — MT results in the past

The Pannonian Geotraverse (PGT1) — according to the definition of the International Lithosphere Programme (ILP) — is an interdisciplinary research profile (or zone), which crosses Hungary in the NW-SE direction in the eastern part of the Pannonian Basin including the following main tectonic units or geological formations from north towards south:

— the Paleozoic Gemericum
— the Miocene andesites of the Mátra Mts
— Szolnok flysch belt (supposed by some authors to be the contact zone of the two microplates of the Pannonian Basin)
— typical 3-D subbasins of the Great Hungarian Plain, e.g. narrow, extensional Békés graben (*Figs. 1 and 2*).
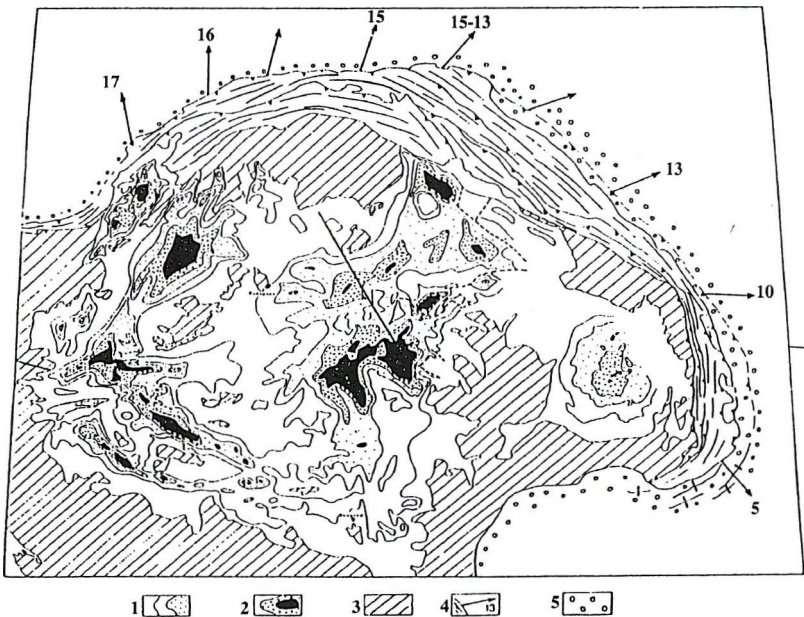
Fig. 1. Simplified isopach map of the Neogene–Quarternary formations [after JIRICEK 1979 from HORVÁTH and ROYDEN 1981]. Key: 1—1 km and 2 km depth isolines; 2—3 km and 4 km depth isolines; 3—Pre-Neogene outcrops; 4—Flysch Carpathians and timing of their major deformations [after JIRICEK 1979]; 5—Foredeep molasse

1. ábra. Egyszerűsített izopach térkép a neogén-kvarter formációkról (JIRICEK [1979] után HORVÁTH és ROYDEN [1981] tanulmányából): 1—1 és 2 km-es mélység izovonalak; 2—3 és 4 km-es mélység izonovalak; 3—Preneogén kibúvások; 4—Flis Kárpátok és a nagyobb deformációk ideje millió évben [JIRICEK 1979 után]; 5—Molasz az elősüllyedékben
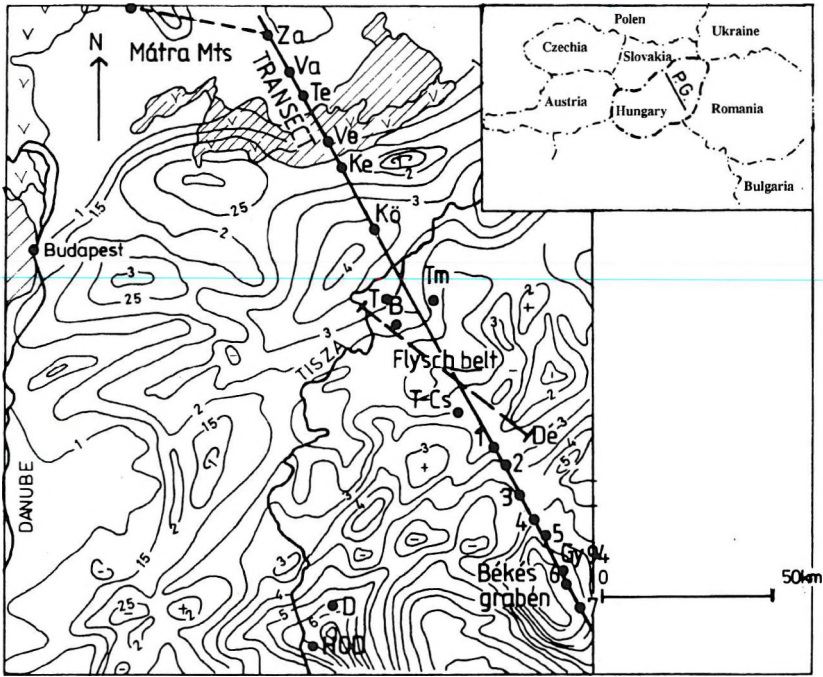
Fig. 2. Isopach map of the eastern part of the Pannonian Basin [HORVÁTH and ROYDEN 1981] with the MT sites along the Pannonian Geotraverse (PGT1) [ÁDÁM et al. 1993]

2. ábra. A Pannon-medence keleti felének izopach térképe (HORVÁTH és ROYDEN [1981] után) a Pannon Geotraverz (PGT1) mentén mért MT helyekkel [ÁDÁM et al. 1993]

(See these structures and the PGT1 profile on the isopach map of the Pannonian Basin in Figs. 1 and 2.)

The length of the PGT1 is about 200 km.

This paper reports on the acquisition, processing and interpretation of the 19 (in some cases only 17) magnetotelluric (MT) deep soundings measured along the PGT1.

Telluric and magnetotelluric research already has a long (more than 40 years) tradition in Hungary and at the very beginning of the sixties it led to some fundamental statements concerning the physics and structure of deep Earth in the Pannonian Basin, viz.

— the regional structure of the highly resistive basement of the basin and its inhomogeneities (basin and range) [ÁDÁM and VERŐ 1964, 1967]

— upwelling of the asthenosphere under the hot basin [mantle diapir, ÁDÁM 1963, 1965]

— regional anisotropy of the resistivity distribution in connection with tectonics [ÁDÁM 1969]

— conducting Paleozoic graphitic formations and their role in tectonics and seismicity of the area [ÁDÁM 1971, 1992, ÁDÁM and VERŐ 1964, TAKÁCS 1968]

— relation of the depth of the crustal and mantle conductivity anomalies to the regional heat flow [ÁDÁM 1976, 1978], etc.

In consequence of the improvement of MT instruments by the introduction of the digital technique both the quantity and quality of the MT measurements have been increased in Hungary, and the basic statements of the resistivity distribution in the underground have been proved. The MT method itself went through a significant development. So far mostly the EM distortions caused by resistivity inhomogeneities have been clarified by using mainly numerical methods (modelling, inversion, decomposition). (One of the first classical papers of this kind was published by BERDICHEVSKY and DMITRIEV in 1976.) If we wish to refine the above mentioned statements concerning the physics of the deep Earth in the Pannonian Basin, distortion theories should be taken into consideration.

The present paper first of all aimed at determining the relationship between the apparent depth of the electric asthenosphere — obtained by formal 1-D or 2-D MT inversions — and the real depth derived by taking into account the possible EM distortions.

As conclusions, the connection of the regional asthenospheric depth with the heat flow and the link between the conductive mantle plume and the seismic horizons as well as gravity and magnetic anomalies below the Békés graben will be discussed.

2. MT data acquisition along the Pannonian Geotraverse

As the sedimentary basin in the Great Hungarian Plain is covered by thick sediment (more than 2 km) of low resistivity (Figs. 1 and 2), investigation of the Earth's crust and mantle needs very long period EM variations. Therefore, instead of induction coil highly sensive ($\varepsilon \leq 0.01$ nT) and very stable static magnetic variometers have been used to record geomagnetic field variations [ÁDÁM and MAJOR 1967]. With these variometers, geomagnetic variations of any long period can be recorded. Generally periods longer than

$T = 1$ hour (in some cases longer than half a day) have been used for soundings. They are especially needed to indicate the asthenosphere by the Rho_{max} curves (of quasi B-polarization?) as strong galvanic distortion (S-effect) can shift the indication of the asthenosphere towards the longer periods. The lower period limit of these instruments is some seconds due to the eigenperiod of about 2 s of the recording system, therefore the sediment cover cannot be resolved into individual layers. (The short period observation is first of all the task of the Hungarian Oil Company (MOL) in Hungary, since this organization is interested in near-surface exploration.) In the Great Hungarian Plain we succeeded in selecting undisturbed measuring sites for deep investigation, hence the application of the remote reference station could be omitted. Two of the deep soundings (Litke, Gyula 94) were measured by digital MT instrumentation by the Geophysical Institute of the Polish Academy of Sciences. The upper period-limit of these soundings is more than 10^4 s.

3. MT data processing

The MT data processing at GGKI is based on the program by VERÓ [1972] which has been supplemented during the last two decades by new parts. Nowadays many authors, first of all LARSEN[1977], BAHR [1988] and GROOM and BAILEY [1989, 1991] elaborated theories and numerical techniques for determining a galvanic electric scattering or distortion operator in the regional 2-D co-ordinate frame. Among the studies of these techniques both on models and field data GROOM et al.'s [1993] and JONESet al.'s [1993] papers are to be mentioned. The description of the impedance tensor in these cases is given by the following formula:

$$Z(\omega) = R(\Theta)C(\Theta)\begin{bmatrix} 0 & Z_{\parallel}(\omega) \\ -Z_{\perp}(\omega) & 0 \end{bmatrix} R^T(\Theta) \tag{1}$$

where — $C(\Theta)$ according to the supposition — is the frequency independent 'distortion operator', $R(\Theta)$ the rotation operator, $Z_{\parallel}$ the impedance associated with the Transverse Electric (TE) mode (i.e. E-polarization), and $Z_{\perp}$ is the impedance of the Transverse Magnetic (TM) (i.e. B-polarization) model.

It is questionable whether BAHR's or GROOM and BAILEY's decomposition can be carried out along the Pannonian Geotraverse as their precondition is a '2-D resistivity distribution'. According to Figs. 1 and 2, this condition

is generally not fulfilled as will later be shown by the typical 3-D Békés graben which belongs to 'Class 7: a regional 3-D anomaly' in BAHR's [1991] classification. The 3-D/3-D scattering model (i.e. 3-D regional structure distorted by 3-D near-surface inhomogeneity) cannot be treated. Our special study [ÁDÁM 1969] discusses a kind of regional conductivity anomaly appearing in other parts of the Pannonian Basin, especially in the Transdanubian Central Range. We shall try to apply the decomposition for these data sets.

4. MT sounding curves (Rho,φ), static shift (site gain) and directional characteristics

a) Rho sounding curves

As a part of VERŐ's MT data processing program [VERŐ 1972], the measuring coordinate system is to be rotated to determine the $Z_{xy}(\Theta)$ and $Z_{xx}(\Theta)$ polar diagrams. The $Z_{xy}(\Theta)$ extreme values serve for computing Rho_{max} and Rho_{min} and their phases.

The Rho_{max} sounding curves (*Fig. 3*) — not taking into account the strongly different curves of station Terpes (Te) galvanically distorted by local 3-D inhomogeneity — form two groups: one is characteristic of the Great Hungarian Plain, the other one of the North Hungarian Central Range, i.e. they express regional peculiarities. Their drawing together on the basis of their geometric mean for static shift correction would result in the elimination of the real regional difference. At $T = 25$ s the computed average resistivity values are:

Great Hungarian Plain: 5.87 ±1.56 Ωm   (n = 13)

North Hungarian Central Range: 27.2 ±7.4 Ωm (n = 5)

n = data number. The scatter in both cases is about 27 per cent.

The Rho_{max} curves in the 'S-interval' indicating the resistive basement are steeper than the Rho_{min} curves, i.e. they are less influenced by the side (induction) effect. The inverted resistivity of the basement is generally more than 100 Ωm and so it is nearer to the borehole logging data than that derived from Rho_{min} curves (see 1-D inversion profiles in Figs. 15 and 16). On the basis of these peculiarities of the Rho_{max} curves and of their directional
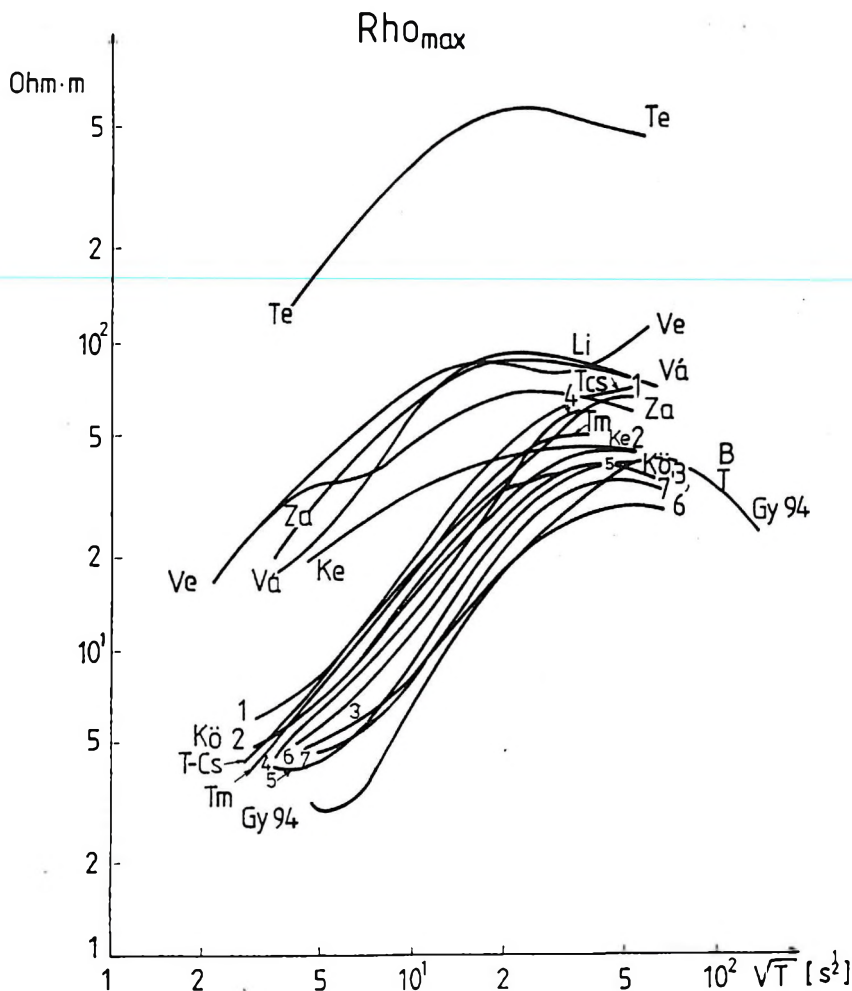
Fig. 3. Rho_max curves (See abbreviations in Table I)

3. ábra. Rho_max görbék (L. a rövidítéseket az I. táblázatban)

characteristics as well as of the relation of the latter ones to the tectonic lines, one can suppose that the Rho_{max} curves better approximate the character of B-polarization (TM mode). The weak indication of the conductive asthenosphere below a thick resistive lithosphere also hints at this character.

In the case of the Rho_{min} sounding curves (*Fig. 4*) the above-mentioned two groups — measured in the Great Hungarian Plain and in the North Hungarian Central Range — do not separate from each other so clearly as in
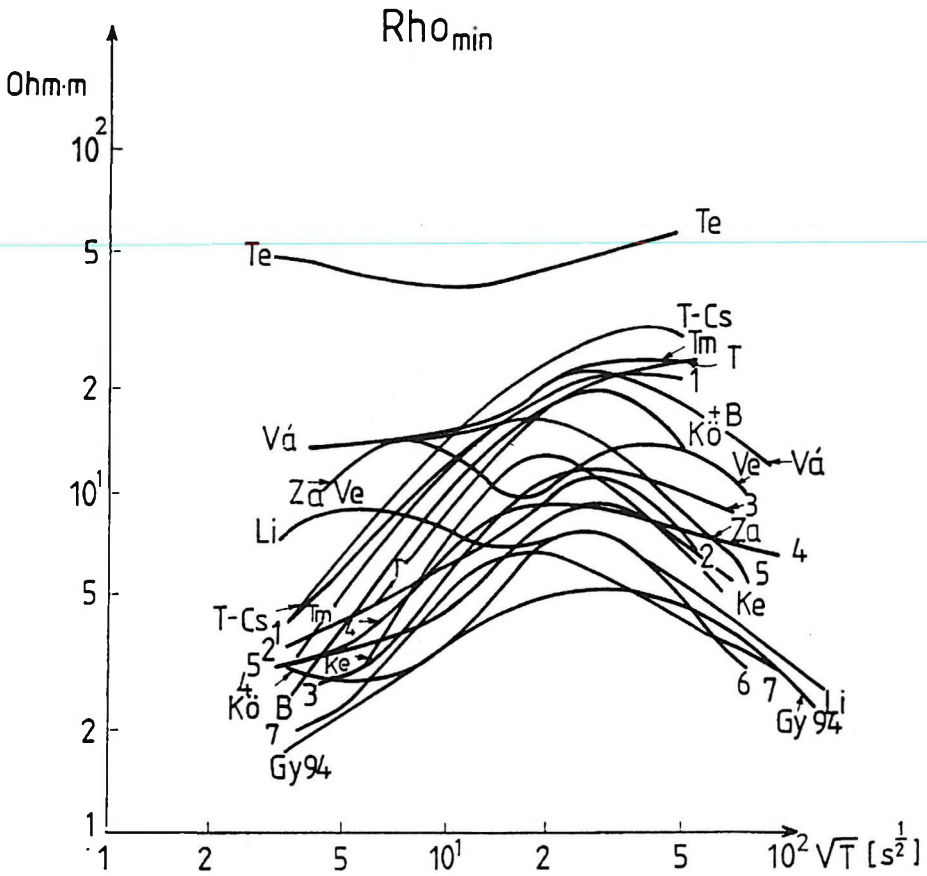
Fig. 4. Rho$_{min}$ curves (See abbreviations in Table I)

4. ábra. Rho$_{min}$ görbék (L. a rövidítéseket az I. táblázatban)

the case of Rho$_{max}$ curves. This phenomenon also hints at the induction (side) effect appearing more strongly in the Rho$_{min}$ curves, and so giving them *E*-polarization (TE mode) character. The resistivity values at 25 s are:

Great Hungarian Plain: 3.83 ± 1.36 Ωm (35 per cent) (n = 14)

North Hungarian Central Range: 11.4 ± 1.68 Ωm (15 per cent) (n = 4)

The basement resistivity obtained by 1-D inversion from Rho$_{min}$ curves is generally less than 100 Ωm, in some cases even less than 10 Ωm due to

very strong EM distortion (side effect) or partly because of the anisotropy of the basement rock (?).

The phase curves (φ) (*Figs. 5 and 6*) — except for their short period parts characterizing the near-surface structures — can hardly be separated
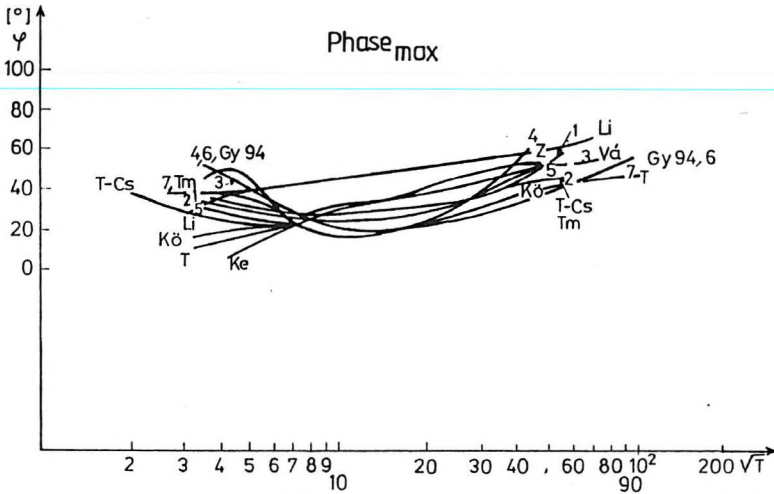
Fig. 5. Phase curves corresponding to Rho$_{max}$ (φ_{max}) (See abbreviations in Table I)

5. ábra. Rho$_{max}$-nak megfelelő fázisgörbék (φ_{max}) görbék (L. a rövidítéseket az I. táblázatban)
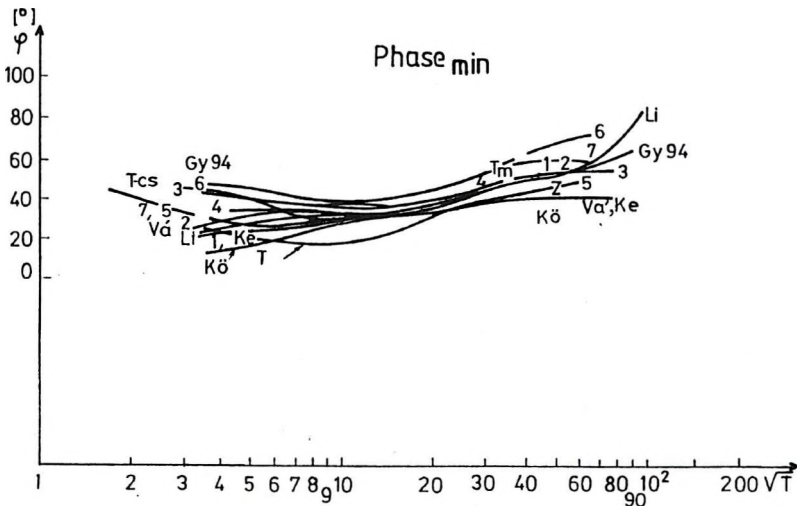
Fig. 6. Phase curves corresponding to Rho$_{min}$ (φ_{min}) (See abbreviations in Table I)

6. ábra. Rho$_{min}$-nek megfelelő fázisgörbék (φ_{min}) görbék (L. a rövidítéseket az I. táblázatban)

from each other. The maximum phase curve of Litke (φ_{max}) is an outlier rising out from the group with its higher values in the whole period range due to the crustal conductor of the Paleozoic basement of the Gemericum. In the southern part of the Geotraverse, in the foreground of the Békés graben, the phase curves of measuring sites 1 and 4 start to increase at shorter periods than the other curves doubtless under the influence of distortion. (These phase curves gave the very low resistivity values of the asthenosphere when using 1-D inversion.)

The values of the φ_{min} curves belonging to the Rho$_{min}$ direction are greater than those of φ_{max} curves indicating the lower resistivities in the layer section (sediment, basement rock) in this direction.

b) The direction of $Z_{xy\ max}$ (or Rho$_{max}$): αRho_{max}

Figure 7a, b, c shows the α_{Rhomax} directions at periods 9, 100 and 900 s. Their general tendencies are summarized in rose diagrams (*Fig. 8*). At $T=9$ s the α_{Rhomax} directions almost equally cover the whole quarter between north and east. This character dominates the whole profile. As the average resistivity of the sediment is about 4.9 Ωm, this directionality characterizes the upper ~3 km of the sedimentary cover. The deeper structures modify this effect therefore there is a strong change in the directionality from 100 s first of all in the southern part of the Geotraverse in the Békés graben and in its northern foreground where the northern direction becomes dominant (see the rose diagrams at 100 and 900 s in Fig. 8). When comparing this directionality with that observed in the area of the Transdanubian conductivity anomaly, some regionality in the MT anisotropy in the Pannonian Basin [ÁDÁM 1969] can be concluded doubtless in connection with E.NE —W.SW tectonic lines (mainly strike slips) as is shown by HORVÁTH's [1993] 'Neogene tectonic map' (*Fig. 9*). There is no change in the direction in the central part of the Geotraverse. It remains stable in the whole period range (about NE—SW).

Figure 50 in DÖVÉNYI's [1994] dissertation shows the major stress directions measured around the Pannonian Geotraverse (*Fig. 10*). In the southern part of the Great Hungarian Plain the major stress is directed to N.NE—S.SW, but in its central part there is a rotation towards the east. Similar tendencies can be observed in the Rho$_{max}$ directions (see Fig. 7c for $T=900$ s). As the Rho$_{max}$ directions are determined by the structural inhomogeneities of the basin, one may suppose that they have been generated
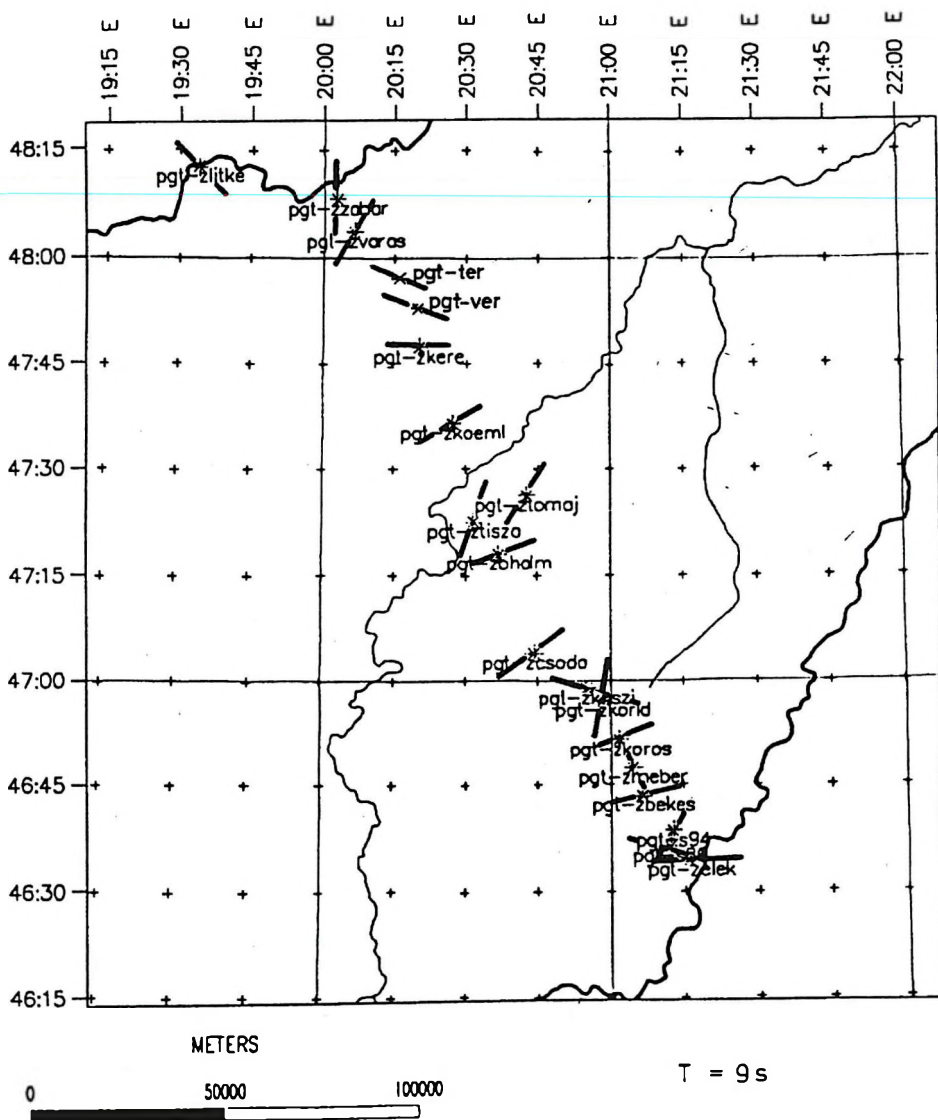
a)

Fig. 7. Direction of the Rho$_{max}$ values (αRhomax) at a) 9 s, b) 100 s, c) 900 s

7. ábra. Rho$_{max}$ értékek iránya (αRhomax) a) 9 s, b) 100 s, c) 900 s

b)

Fig. 7. Direction of the Rho$_{max}$ values (α_{Rhomax}) at a) 9 s, b) 100 s, c) 900 s

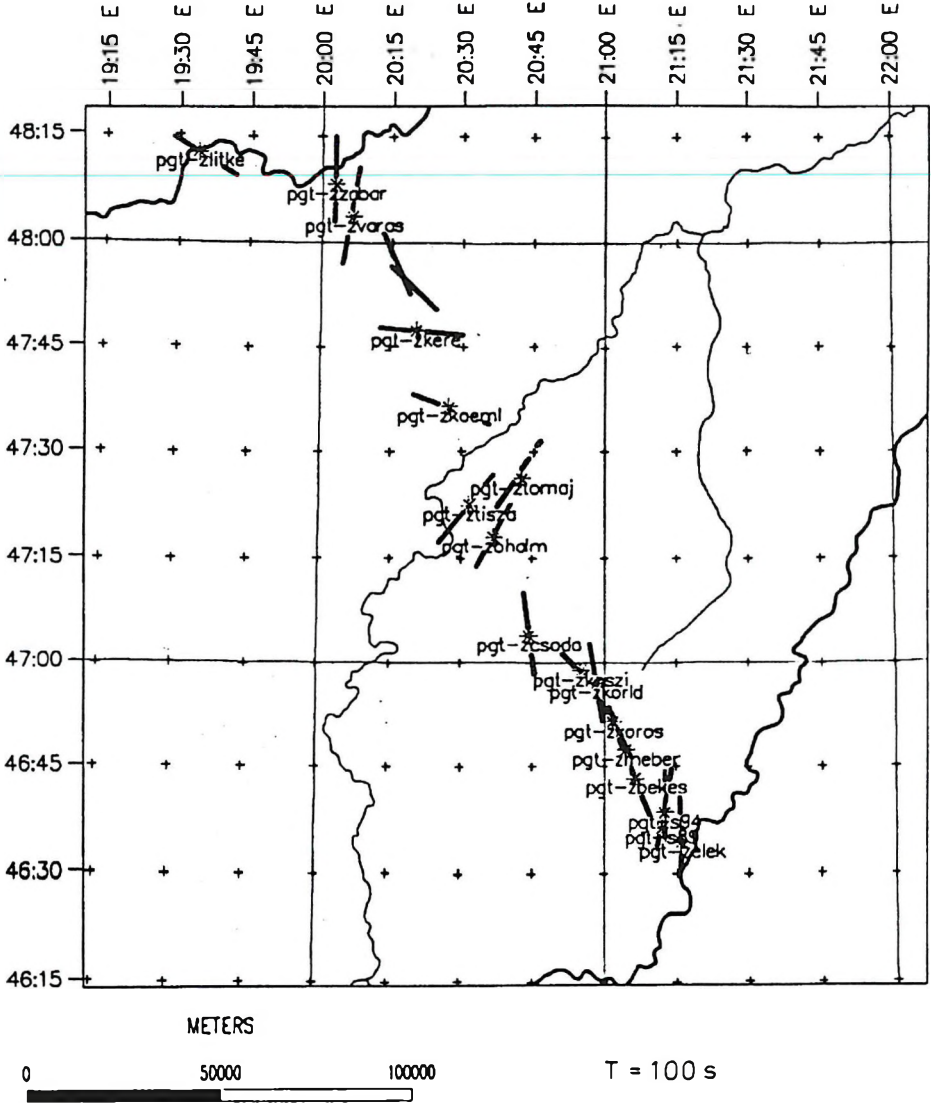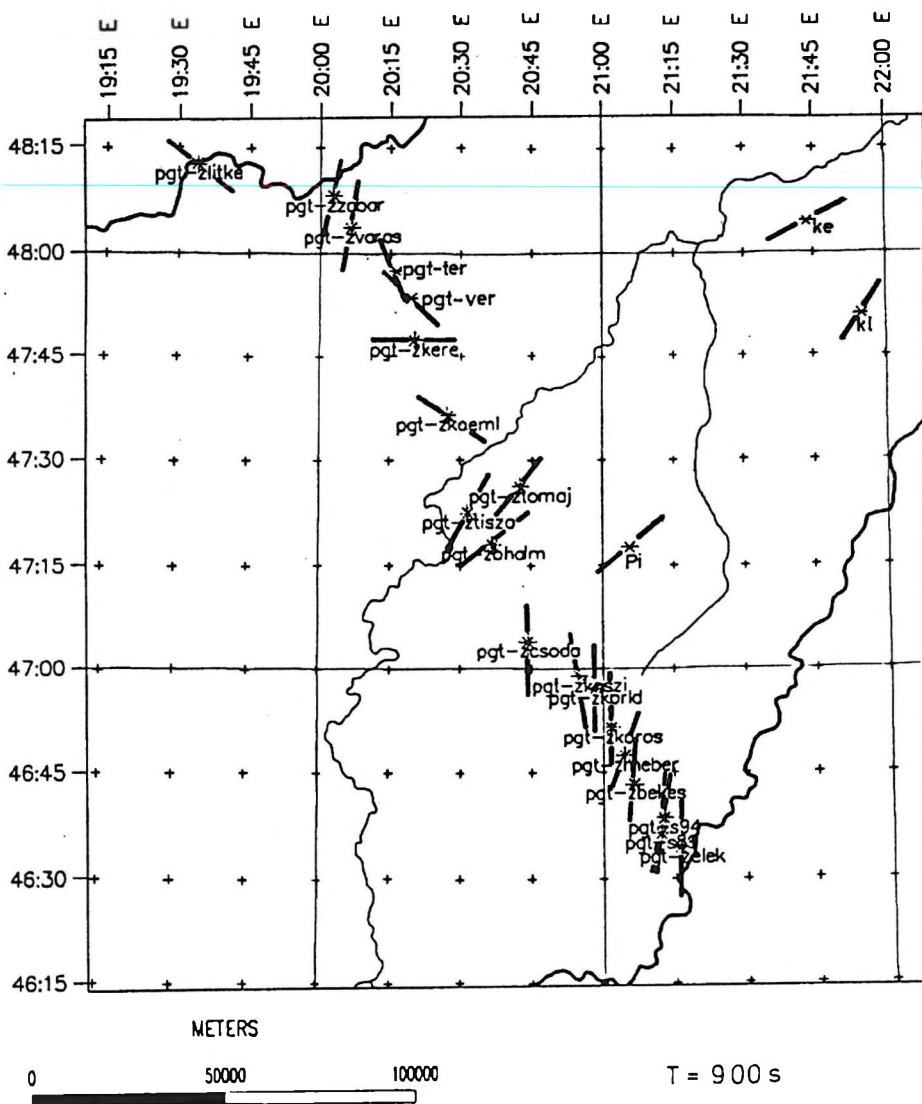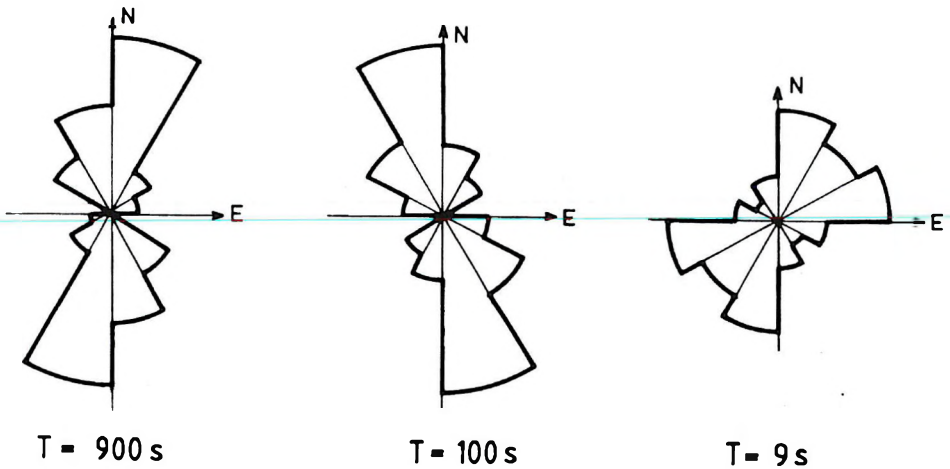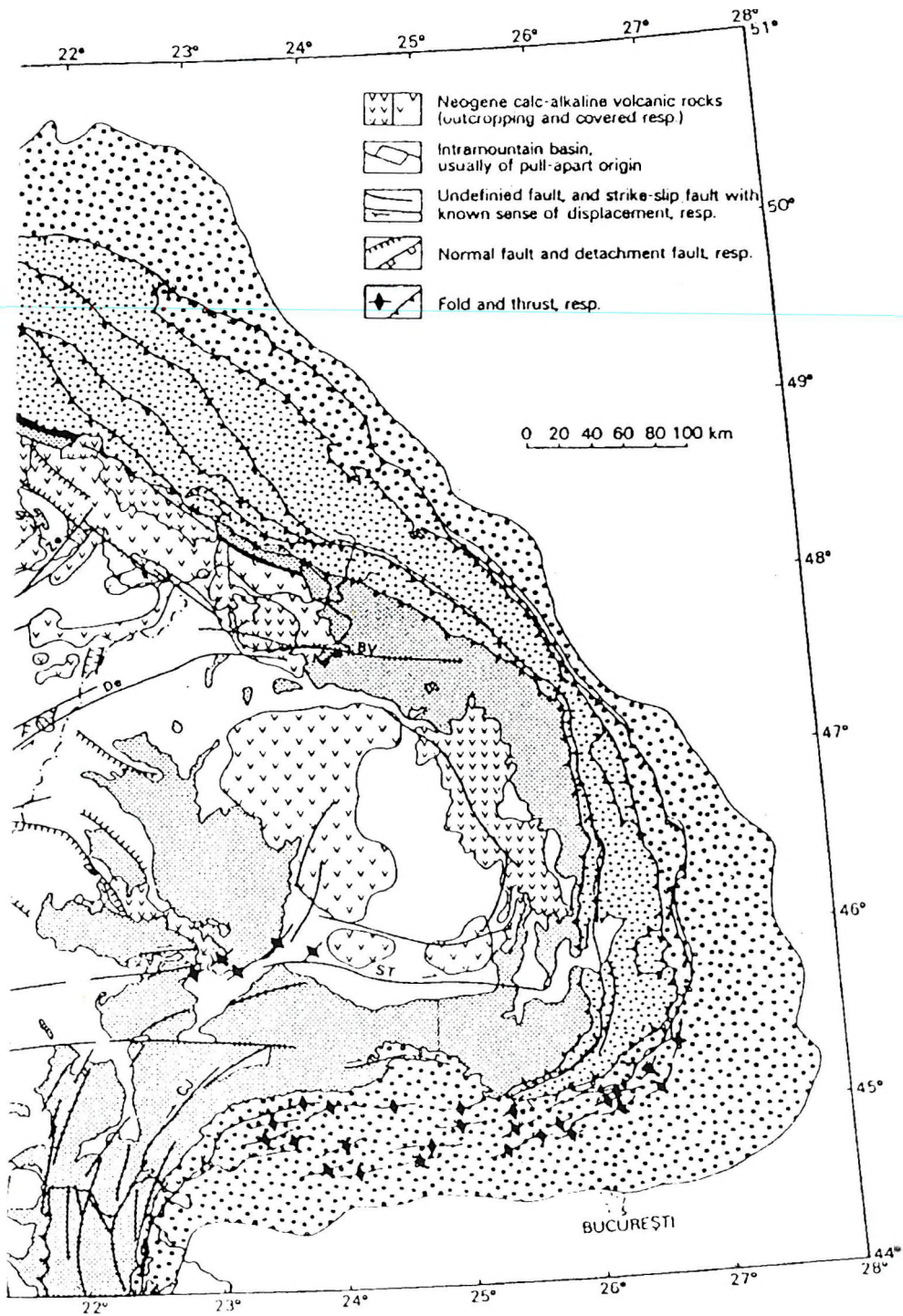*7. ábra.* Rho$_{max}$ értékek iránya (α_{Rhomax}) a) 9 s, b) 100 s, c) 900 s

c)

Fig. 7. Direction of the Rho$_{max}$ values (αRhomax) at a) 9 s, b) 100 s, c) 900 s

7. ábra. Rho$_{max}$ értékek iránya (αRhomax) a) 9 s, b) 100 s, c) 900 s

Fig. 8. Directions of the α_{Rhomax} at 900, 100 and 9 s shown by rose diagrams

8. ábra. α_{Rhomax} iránya 900, 100 és 9 s-nál

by the same stresses as those observed by DÖVÉNYI It is emphasized once more that while in the southern part of the country the Rho_{max} directions (α_{Rhomax}) change with period (see Figs 7a, b, c and the rose diagrams in Fig. 8), in PGT's central part the directions are stable about NE—SW independently of the periods. As the penetration depth of MT fields depends on the period, in PGT's central part the surface structure has a deep root determining thus a stable current direction (canalization) and MT anisotropy. It is questionable whether this phenomenon is in any way linked with the collision of the two microplate of the middle of the Pannonian Basin.

5. Pseudosections

The pseudosections were constructed by using the GEOTOOLS MT program system with an input of the impedance values '*xy*' corresponding to Rho_{max}, and its phase; '*yx*' to Rho_{min} and its phase.

a) The phase (PH) pseudosections are shown in *Figs. 11* and *12* as a function of the logarithm of the frequency. The minimum values of the PHXY

Symbol	Description
Neogene calc-alkaline volcanic rocks (outcropping and covered resp.)
Intramountain basin, usually of pull-apart origin
Undefined fault, and strike-slip fault with known sense of displacement, resp.
Normal fault and detachment fault, resp.
Fold and thrust, resp.

0 20 40 60 80 100 km

BV

D

ST

CJ

BUCUREŞTI

nonian Basin and the surrounding Alpine-Carpathian-Di-
some of the main faults are as follows: B = Balaton line;
ne; D = Dráva line; Da = Darnó line; De = Derecske line;
iósjenő line; He = Hernád line; I = Idrija line; K = Kapos
= Muráň line; Ma = Mecsekalja line; MD = Mölltal-Drau-
riadriatic (Insubric) line; Po = Pottendorf line; S = Sava
inberg line; ST = South Transylvanian line; TR = Telegdi-
n line [HORVÁTH 1993]

ző Alpi-Kárpáti és Dinári hegységek miocén tektonikai
s(vető)vonalakat jelölik:B = Balaton vonal; BV = Bogdan
Dráva vonal; Da = Darnó vonal; De = Derecske vonal;
-Diósjenő vonal; He = Hernád vonal; I = Idrija vonal;
= Lab vonal; M = Muráň vonal; Ma = Mecsekalja vonal;
Mürz vonal; PA = Periadriatic (Insubric) vonal; Po = Pot-
achtal-Ennstal vonal; St = Steinberg vonal; ST = South
onal; Za = Zagreb vonal; Ze = Zemplén vonal [HORVÁTH
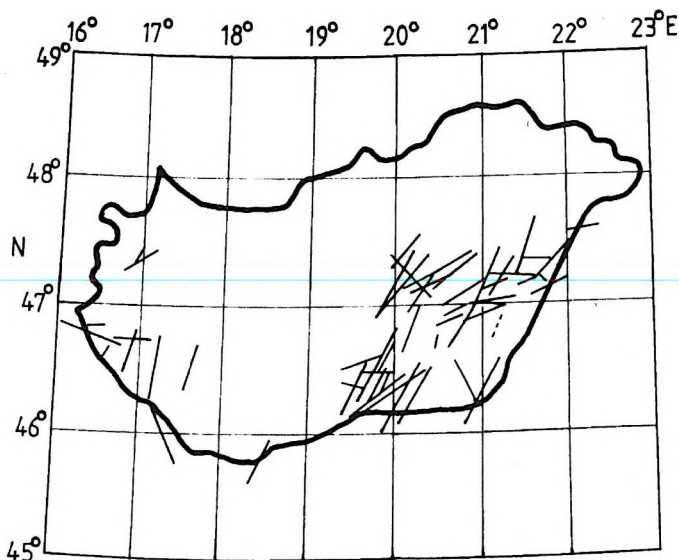
Fig. 10. Major stress direction in Hungary after Dövényi [1994]. The small lines show the direction of maximum horizontal major stress determined by different techniques

10. ábra. A fő feszültségi irányok Magyarországon Dövényi szerint [1994]. A kis vonalak a különböző technikával meghatározott maximális vízszintes főfeszültségeket jelzik

pseudosection shift to the lower frequencies (longer periods) from north (on the left side) towards south (on the right side), i.e. the greatest sediment thickness of the Békés graben. The phase values greater than 45° appear at about $T=1000$ s indicating the conducting asthenosphere. In the foreground of the Békés graben a double synclinal structure with high phase values at about $T = 10$ s hints at the roughness of the 3-D basement structure. This phenomenon is an indication that EM distortion is to be expected in the structure of the asthenosphere.

In the PHYX phase pseudosection the high frequency, i.e. near-surface, 'image' is more varied than in the case of the PHXY section. The minimum phase values corresponding to the sedimentary basin are greater, especially in the Békés graben (see sites 6 and Gy 94) than in PHXY. The high phase values indicating the asthenosphere around 60° in Fig. 12 appear at shorter periods hence the PHYX curves give a shallower asthenosphere depth than the PHXY ones.

b) The Rho pseudosections show the upper sedimentary cover by low resistivity values at the highest frequencies. The Rhoxy (Rho$_{max}$)

pseudosection — *(Fig. 13)* approximating the quasi *B*-polarization — better expresses the basin structure (see in Figs. 1 and 2). The Earth's crust is represented by high resistivities. The low resistivity of the asthenosphere begins to appear at $T = 10^4$ s first of all at the northern part of the Geotraverse. The role of different distortions (especially the *S* effect) will be treated later. At the southern end of the PGT in the Békés graben and its foreground the mentioned double deep synclinal structure is represented by low resistivities. This rugged basement structure is illustrated by the quasi *E*- polarized Rhoyx pseudosection, too *(Fig. 14)*, but more distorted than in the case of Rhoxy. The induction (side) effect can be observed, for example in the area of the Northern Hungarian Central Range. In the Békés graben the resistivity values do not increase above 10 Ωm at long periods. On the Rhoyx section the low resistivity asthenosphere is indicated at about $T = 3.10^3$ s. As in the case of 2-D structures the *E*-polarized sounding curves give more reliable or less distorted depth values to the top of conductivity formations, the Rhoyx pseudosection approximating this polarization may inform about the position of the asthenosphere in the Pannonian Basin, if the EM distortion of the 3-D structure did not disturb it. In the latter case, both extreme sounding curves are distorted. As a typical example for this effect the 3-D modelling of the Békés graben will be shown [ÁDÁM et al. 1993].

6. 1-D layer sequences, their profile and MT distortions

First the 1-D layer sequence was determined from the extreme MT curves by STEINER's [1989] 1-D inversion program using the L1 or L2 norm. At the northern end of the Geotraverse, at the sites Litke (Li) and Zabar (Za) above the Paleozoic basement of the Gemericum, graphitic formations cause conductivity anomalies in the upper crust with decreasing conductance towards the south. The conducting layer in the middle and lower crust can only be supposed beneath the thick sediment cover of the Great Hungarian Plain. A weak indication on the conductor could be obtained by the Bostick transformation along the additional profile to the PGT [ÁDÁM et al. 1989].

Apart from these crustal conductors, the lithosphere along the PGT can be simplified to a 3 layer case with sediment on the surface, conducting asthenosphere at its bottom, and resistive lithosphere in the middle.
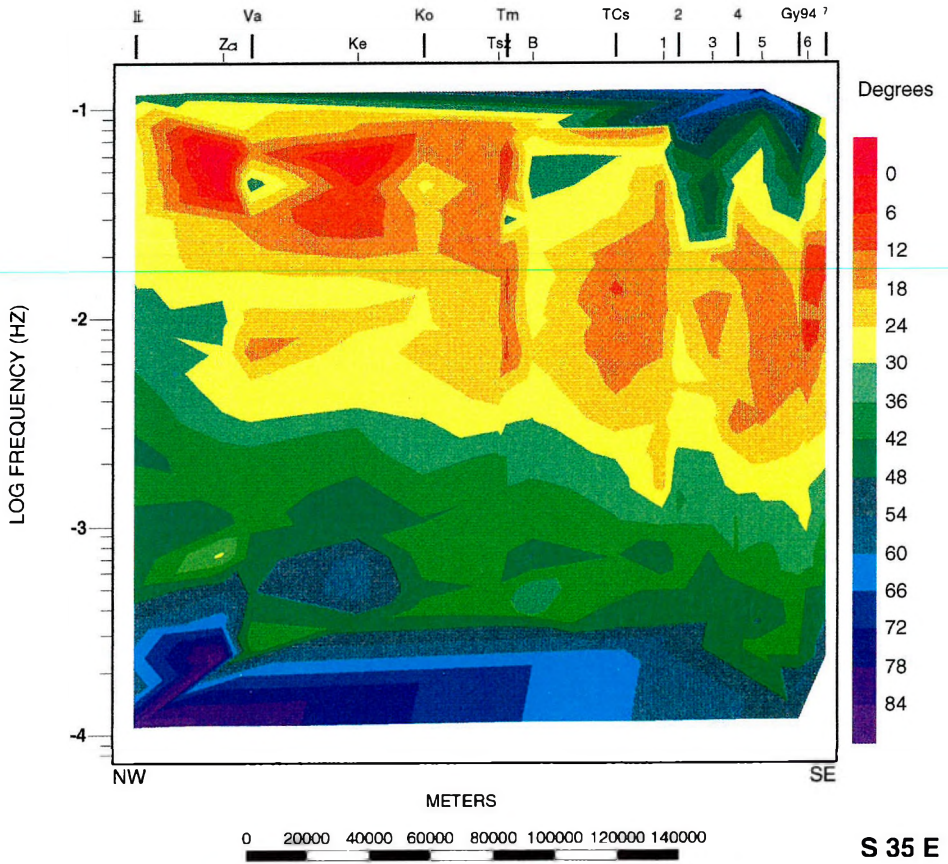
Fig. 11. Phase pseudosections of Rho$_{max}$(xy) along the Pannonian Geotraverse (PGT1)

11. ábra. A Rho$_{max}$ (xy)-hoz tartozó fázis pszeudoszelvény a Pannon Geotraverz (PGT1) mentén
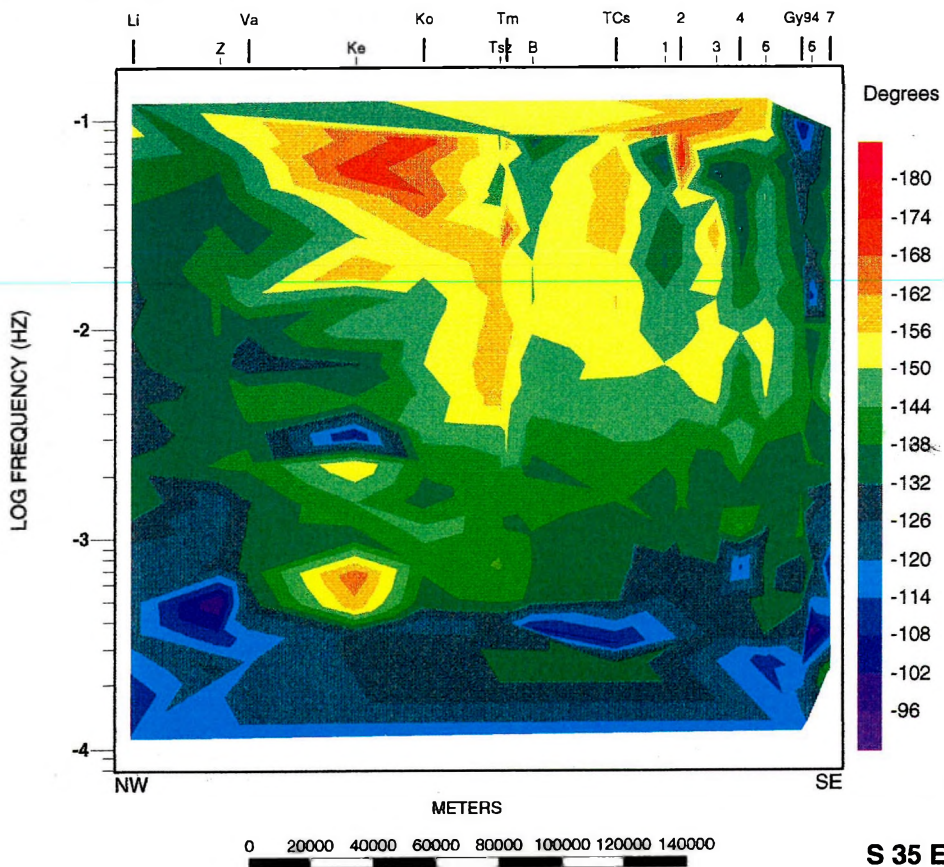
Fig. 12. Phase pseudosections of Rho$_{min}$(*yx*) along the Pannonian Geotraverse (PGT1)

12. ábra. A Rho$_{min}$ (*yx*)-hoz tartozó fázis pszeudoszelvény a Pannon Geotraverz (PGT1) mentén
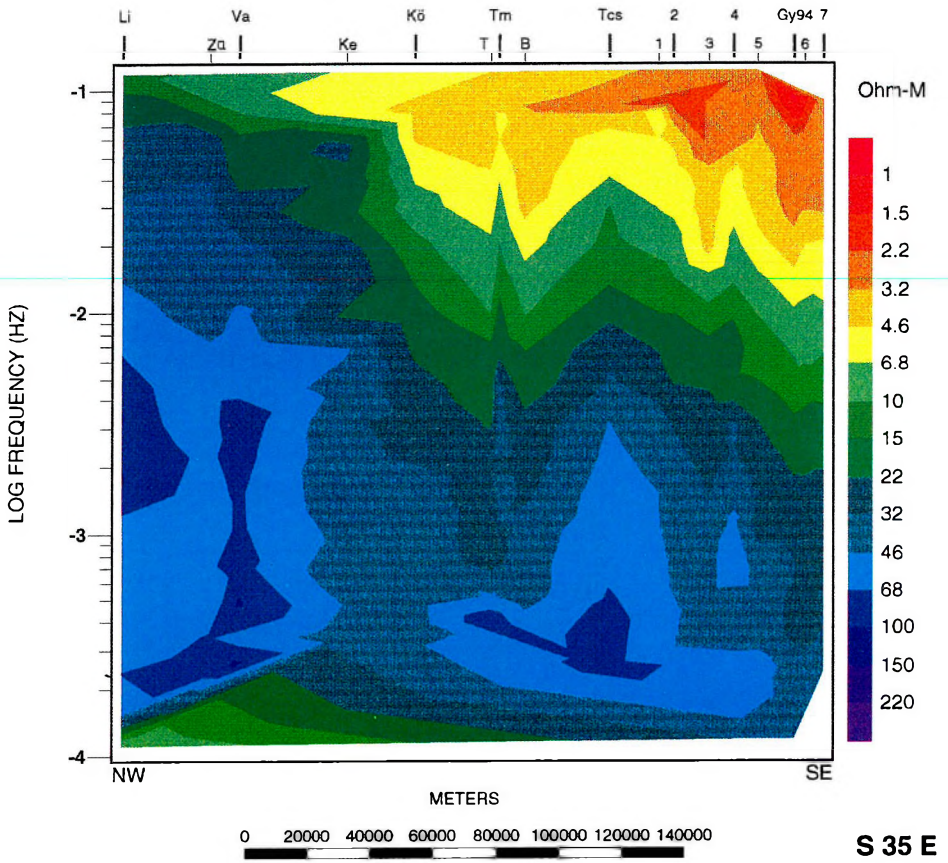
Fig. 13. Rho$_{max}$(Rhoxy) pseudosection along the Pannonian Geotraverse (PGT1)

13. ábra. A Rho$_{max}$ (Rhoxy) pszeudoszelvény a Pannon Geotraverz (PGT1) mentén
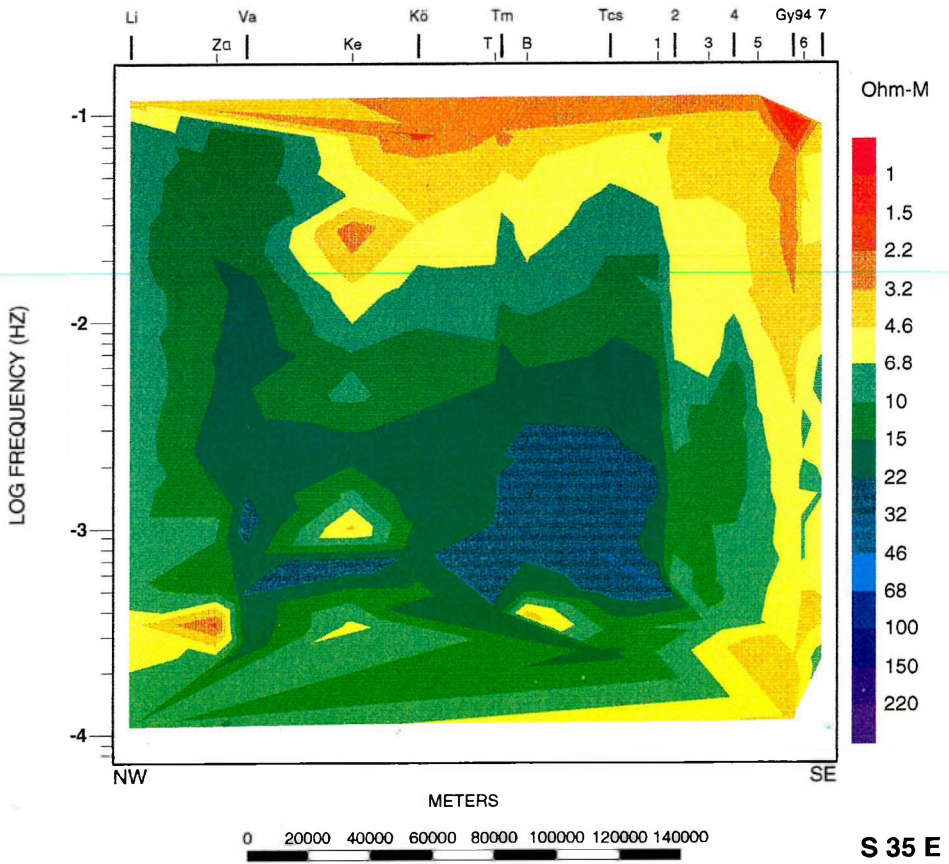
Fig. 14. Rho$_{min}$(Rhoyx) pseudosection along the Pannonian Geotraverse (PGT1)

14. ábra. A Rho$_{min}$(Rhoyx) pszeudoszelvény a Pannon Geotraverz (PGT1) mentén

As the sounding curves start only after some seconds, there is no possibility as mentioned to divide the sediment cover into individual layers. The conductance (*S*-value) of the sediment, or — from other geological/geoelectrical information, — the average resistivity and the thickness of the sediment can be determined. The detailed study of the basin structure in Hungary is the task of the ELGI and MOL, hence our investigation aimed first of all at determining the lithosphere–asthenosphere structure taking into account the EM distortion caused by the geological noise.

Table I includes the depth values of the crustal and mantle (asthenosphere) conductors obtained from 1-D formal inversion. *Fig. 15* connects the 1-D layer sequences obtained from Rho_{min} (quasi TE mode, *E*-polarized) curves; *Fig. 16* is the same for Rho_{max} (quasi TM model, *B*- polarized) curves.

The average depth of the asthenosphere determined by Rho_{min} curves (Fig. 15) is 48.5±13.3 km calculated from 15 data. The asthenosphere beneath two local deep 3-D subbasins is apparently updoming (mantle plume?). Towards the Békés graben from the Túrkeve-Csodaballa (T—Cs) MT site to MT site 3, the depth of the asthenosphere gradually decreases then at site 4 it apparently crosses the crust-mantle boundary similarly to site 7 due to EM distortions. At these points the apparent depth is less than 20 km. A similar phenomenon can be observed below the other deep subbasin around Kerecsend (Ke) (see the sedimentary basin of low resistivity on the Rhoxy pseudosection). There is no essential difference in the resistivity of the asthenosphere in the northern and southern parts of the Geotraverse, where it does not reach 10 Ωm. The greater values around 10 Ωm appear in the middle section of the PGT. The average resistivity is 5.4±4.7 Ωm (without the values of those sites where the apparent depth of the conductive basement is shallower than 30 km). The apparent upwelling of the conducting basement (asthenosphere) beneath the 3-D subbasin is known as a consequence of EM distortion (geological noise). This effect has been studied in connection with the 3-D Békés graben by Price thin sheet modelling [ÁDÁM et al. 1993] as already mentioned here, based on BERDICHEVSKY and DMITRIEV's [1976] earlier theoretical results (*Fig. 17*). This apparent updoming of the asthenosphere appears on the quasi *B*-polarized (TM mode) Rho_{max} profile, too (Fig. 16).

If one omits the Rho_{min} depth values less than 40 km which are assumed to be distorted, then for the average depth of the asthenosphere one gets 58.2±8.8 km.

Site	Rho$_{min}$		Rho$_{max}$		Year
(with abbreviation)	crust	mantle	crust	mantle	
Litke (Li)	7.9 (2913 S)	34.1		64.2	1994
Zabar (Za)	16.5 (1000 S)	40.5	16.0 (250 S)	68.5	1987
Váraszó (Va)		60.0	20.8 (50 S)	66.3	1987
Terpes (Te)	10.1 (500 S)			200.0	1987
Verpelét (Ve)	12.2	34.6		125.6	1988
Kerecsend (Ke)	19	?	26.1	?	1988
Kömlő (Kö)		65.5	23.5	?	1988
Tomajmonostora (Tm)	17.5 (200 S)	63.5	17.5 (180 S)	65.3	1987
Tiszagyenda (T)		65.3		135.3	1988
Bánhalma (B)		58.2		85.5	1989
T-Csodaballa (T-Cs)	17.5 (200 S)	68.5	17.5 (200 S)	64.5	1987
Kősziget (1)		56.2		176.1	1989
Körösladány (2)		46.3		106.1	1989
Köröstarcsa (3)		30.9		89.0	1989
Mezőberény (4)	19.6	?		136.0	1989
Békés (5)		36.6		76.0	1988
Gyula 94 (Gy 94)		35.4		59.6 (216)	1994
Gyula 89 (6)		31.1		58.0	1989
Elek (7)	18.5	?		78.2	1988

Table I. Apparent depth to the top of CA's (1-D inversion) (with crustal conductance in [*S*])

I. táblázat. A jólvezető formációk mélysége (1-D inverzió alapján) (a kéregbeli jólvezető horizontális vezetőképességével [S]-ben)
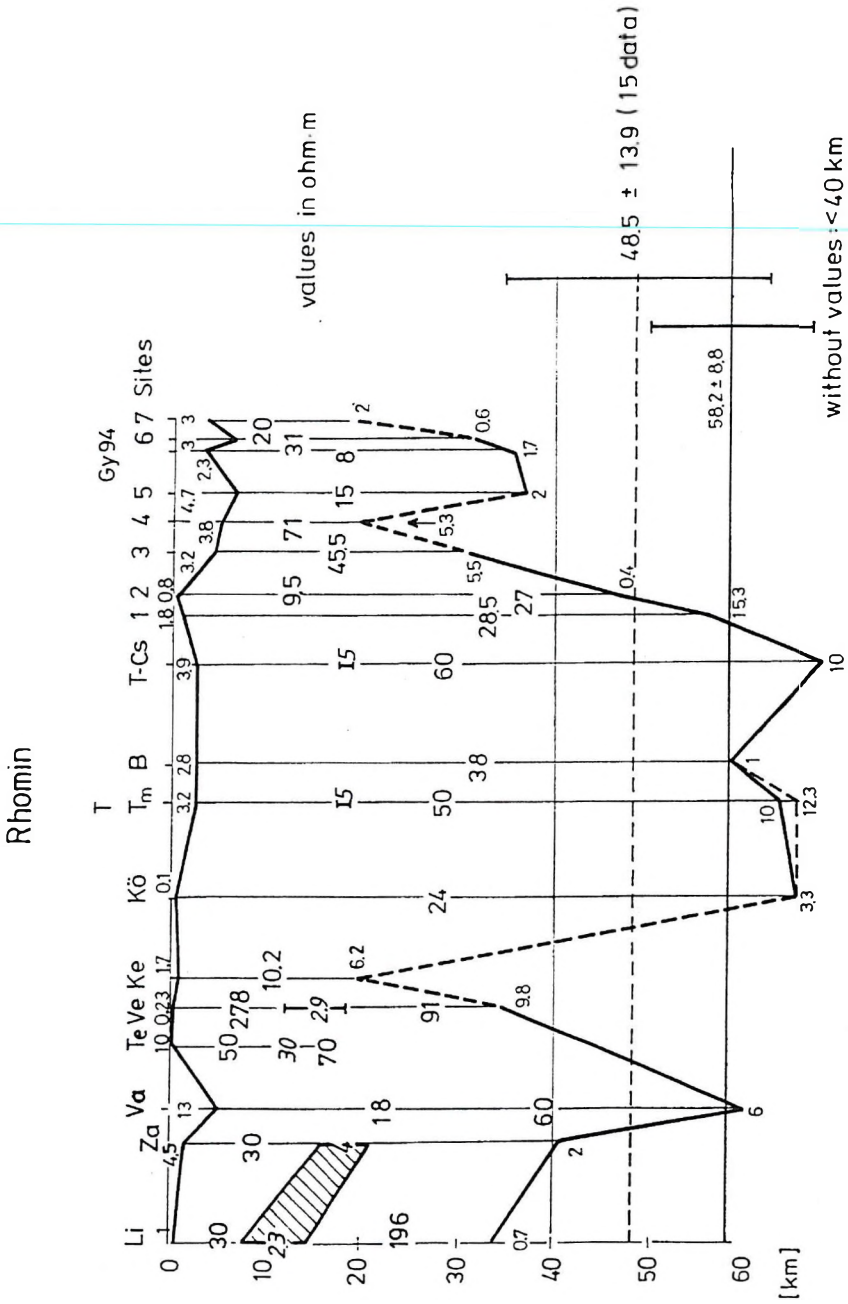
Fig. 15. Results of 1-D inversions as a layer profile derived from Rho$_{min}$ curves

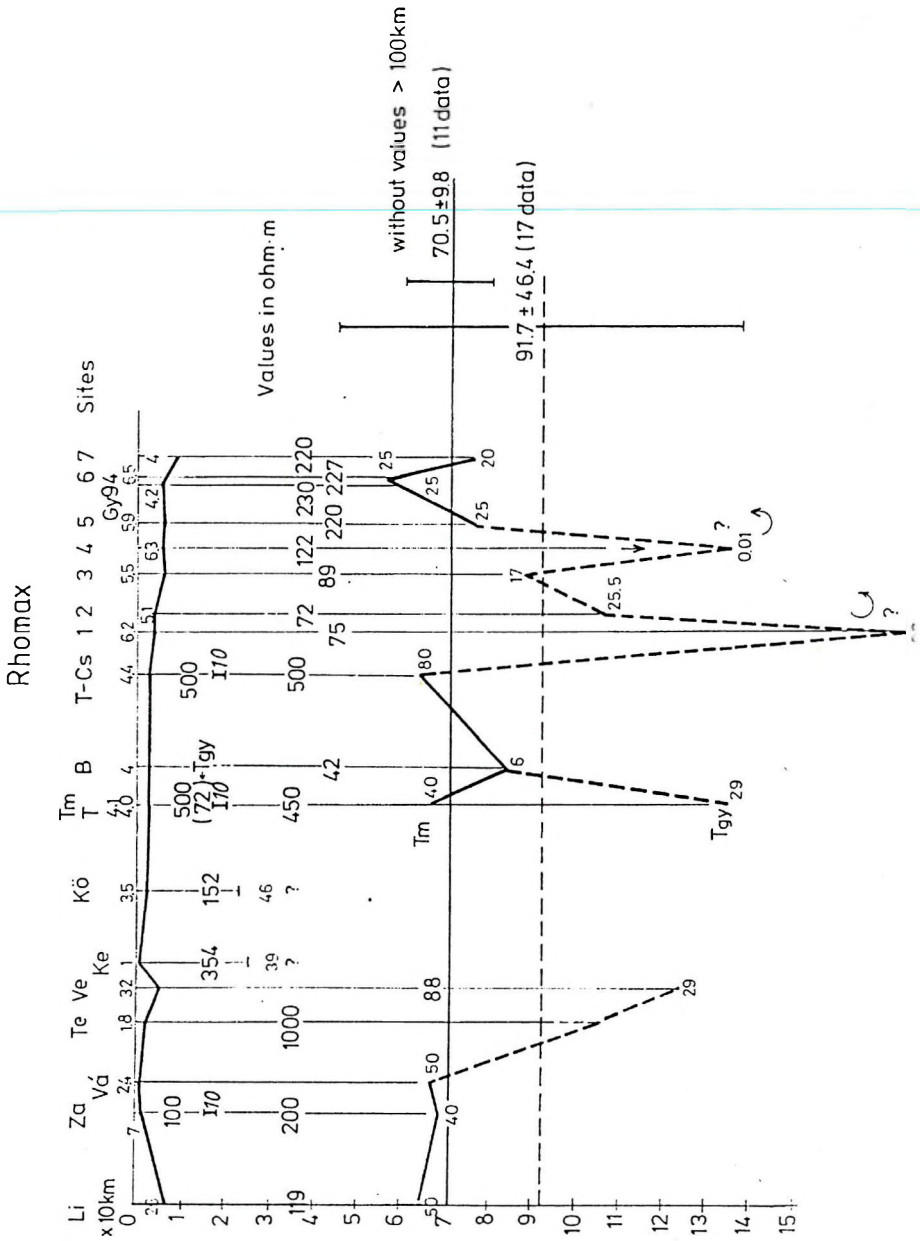15. ábra. A Rho$_{min}$ görbék 1-D inverziójával nyert rétegszelvény

Fig. 16. Results of 1-D inversions as a layer profile derived from Rho$_{max}$ curves

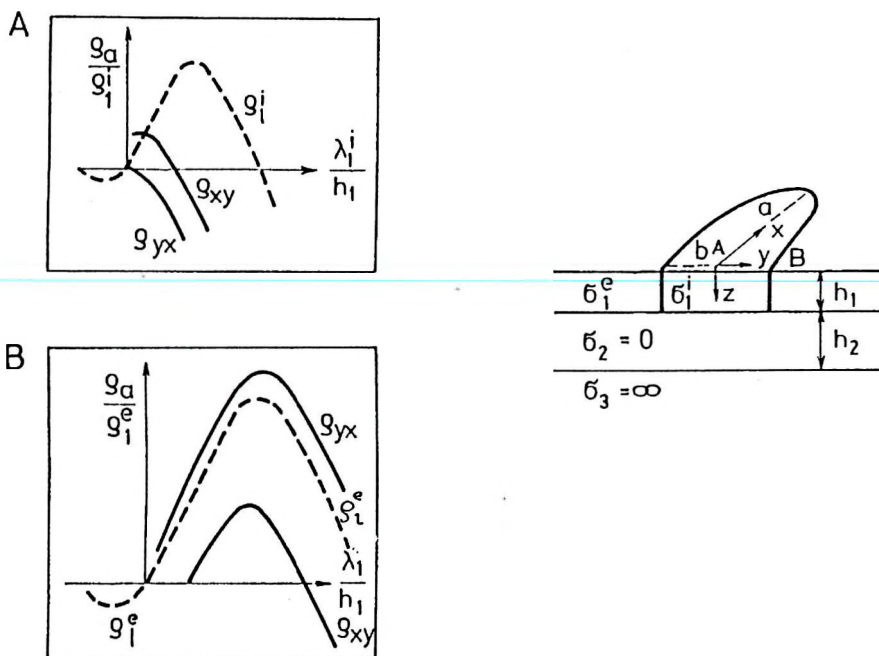16. ábra. A Rho$_{max}$ görbék 1-D inverziójával nyert rétegszelvény

Fig. 17. BERDICHEVSKY and DMITRIEV's (1976) 3-D model (conducting embedding) and its effect on the quasi E (ρ_{xy}) and B-polarized ρ_{yx}) MTS curves. $a/b=2$, $\sigma_1^i/\sigma_1^e = 16$, $h_2/h_1 = 20$. ρ_l^i and ρ_l^e are sounding curves belonging to 1-D layer sequences inside (i) and at the border (e) of the embedding

17. ábra. BERDICHEVSKY és DMITRIEV [1976] 3-D modellje (jólvezető beágyazás) és σ_l^i és σ_l^e szondázási görbék, amelyek az 1-D rétegsorhoz tartoznak a beágyazódáson belül (i) és annak határán (e)

The 1-D layer model based on quasi B-polarized (TM mode) Rho_{max} curves (Fig. 16) generally gives greater asthenospheric depths than those derived from Rho_{min} curves (Fig. 15). The indication of the crustal and mantle conductor is in this case — corresponding to the B-polarization — weaker. Using all 17 data the average apparent depth calculated is 91.7±46.4 km; the resistivity of the mantle condutor is 30.4±19.1 Ωm. The higher resistivity values (~40–50 Ωm) appear on the northern part of the PGT, the lower ones (~25 Ωm) in the southern part in connection with the earlier mentioned regionality.

Figure 16 shows a more rugged surface of the conducting basement (asthenosphere) in the mantle than Fig. 15. Beneath the deep 3-D subbasins

(Békés graben and area of Kerecsend (Ke) and Kömlő (Kö)) there is an apparent updoming similarly to Fig. 15. The depths greater than 100 km appear at the rims of the local deepening of the basin (subbasins), i.e. in the 'horsts' — for example at sites 1 and 4, where the Rho_{max} direction rotates with period and the resistivities of the asthenosphere derived by 1-D inversion are extremely low values (0.7 and 0.01 Ωm). Both sites lie at the elevation between two subbasins as can well be seen on the pseudosections. According to *Fig. 18* after BERDICHEVSKY and DMITRIEV [1976], the conducting basement has an apparent deepening on the *B* polarized sounding curves due to the galvanic distortion (*S*–effect) of these horsts. If the depth values greater than 100 km are omitted, the average of 11 data is 70.5±9.8 km for Rho_{max} curves. In this case the difference in the asthenospheric depth between the two quasi undistorted data sets is only about 10 km.

It is questionable wether the origin of the local apparent updoming of the conducting basement beneath the 3-D subbasins can be fully explained by galvanic distortion (*S*-effect). This apparent updoming asthenosphere may include a real elevation component, too, as a weakened remnant of the Miocene mantle plume — as was first shown by POSGAY et al. [1992] on the basis of a study of the deep reflexion seismic results in this area. The density increase in the crust corresponding to the mantle plume has been traced by the gravity (and magnetic anomaly) map by NEMESI and STOMFAI [1992] and KOVÁCSVÖLGYI [1995]. POSGAY et al. [1995] confirmed later their fundamental statement, i.e. the mantle plume below the Békés graben probably includes the updoming of the asthenosphere, too, with new curved reflection seismic horizons. Nevertheless, the asthenosphere being a thermal horizon (representing ~1200°C) certainly was at a higher position than at present and deepened after its updoming in the Miocene due to cooling and without further heat impulses, while the dense mantle peridotite of the plume remains as a wedge in the crust causing a gravity/magnetic anomaly.

In an attempt to ascertain the real situation 3-D forward modelling was carried out by WANNAMAKER et al.'s [1984] programme taking the conducting asthenosphere to be at a depth of 60 km (average depth in the Pannonian Basin). The depth isolines of the Békés graben are shown in *Fig. 19*; the geoelectric 3-D model — derived from VARGA and RÁNER [1990] 2-D layer section in the Békés graben — with the meshes for computation is illustrated in *Fig. 20*. *Figure 21* gives the apparent depth values of the asthenosphere calculated from the model sounding curves by 1-D inversion, along a profile corresponding to the PGT. According to this latter figure, the apparent depth
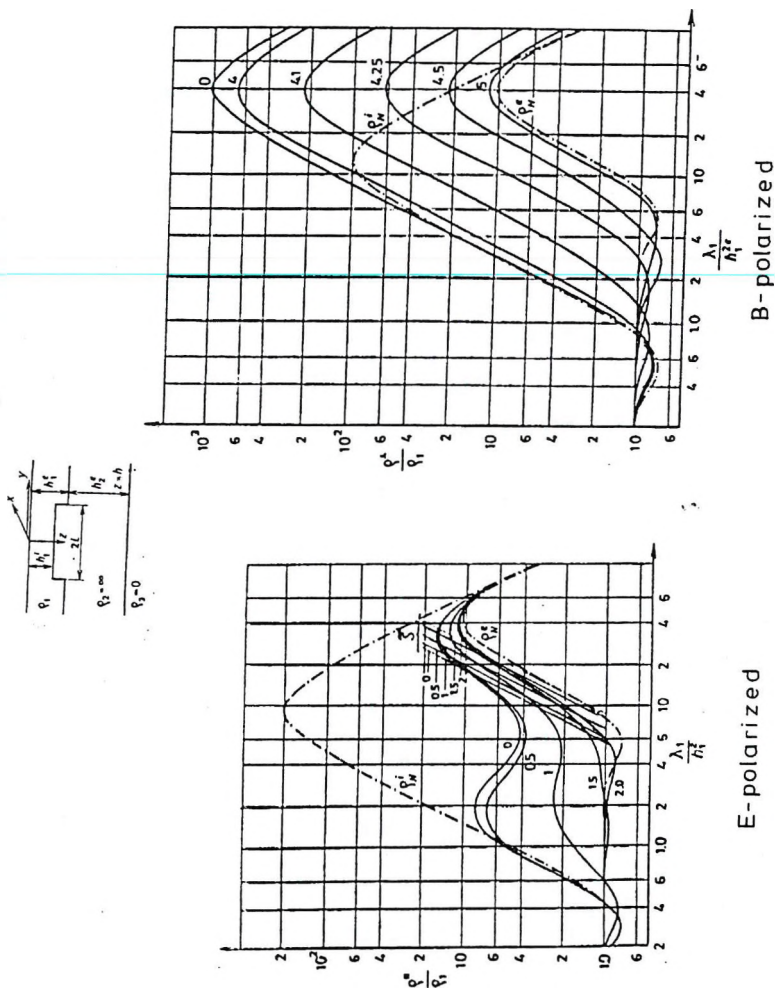
Fig. 18. *E*- and *B*-polarized curves above a horst model as a function of relative distance from the centre of the horst. Parameters for *B*-polarized (Transversal) MTS curves: $\rho_2/\rho_1 = \infty$; $\rho_3/\rho_1 = 0$; $h_1^i/h_1^e = 0.1$; $h_2^e/h_1^e = 20$; $L/h_1^e = 4$; curves are digitized by $|y|/h_1^e$. Parameters for *E*-polarized (Longitudinal) MTS curves: $\rho_2/\rho_1 = \infty$; $\rho_3/\rho_1 = 0$; $h_1^i/h_1^e = 0.05$; $h_2^e/h_1^e = 20$; $L/h_1^e = 1$; curves are digitized by $|y|/h_1^e$ [BERDICHEVSKY and DMITRIEV 1976]

18. ábra. *E* és *B* polarizációs görbék egy kiemelkedés felett a kiemelkedés közepétől való távolság függvényében. A *B* polarizációs (transzverzális) MTSz görbe paraméterei: $\rho_2/\rho_1 = \infty$; $\rho_3/\rho_1 = 0$; $h_1^i/h_1^e = 0.1$; $h_2^e/h_1^e = 20$; $L/h_1^e = 4$; a görbék $|y|/h_1^e$ -vel vannak digitalizálva. Az *E* polarizációs görbék paraméterei: $L/h_1^e = 1$; digitalizálási köz: $|y|/h_1^e$ [BERDICHEVSKY és DMITRIEV 1976]
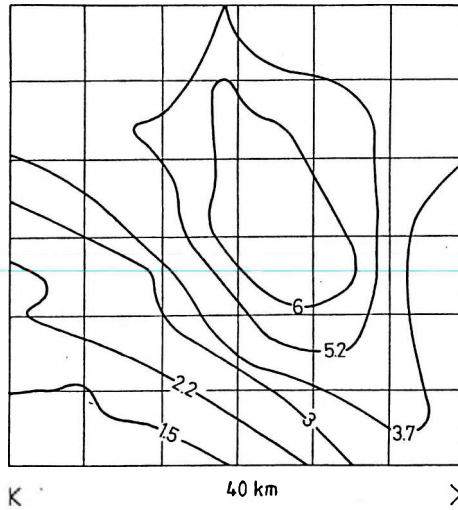
Fig. 19. Depth isolines in kilometers from the basement of the Békés graben simplified from the isopach map

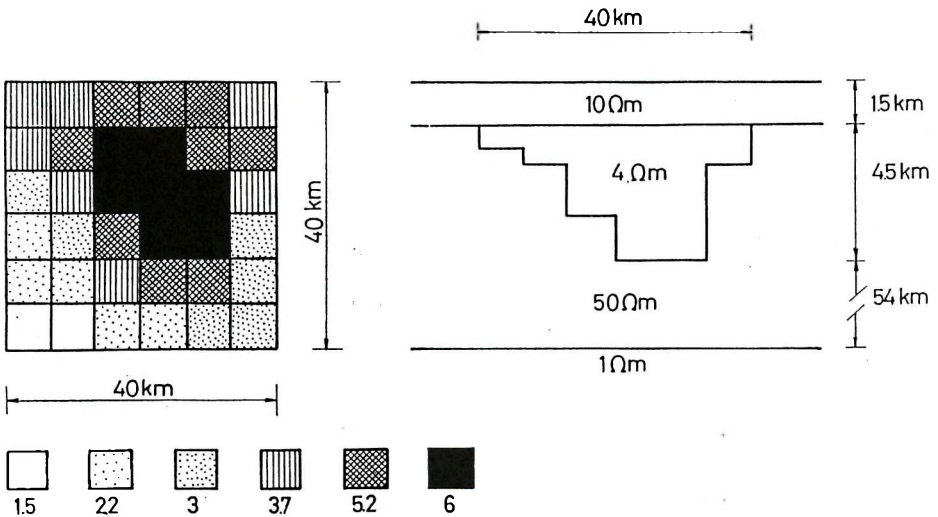*19. ábra.* A Békési árok medencealjzatának mélység izovonalai km-ben (egyszerűsítve izopach térkép alapján)

Fig. 20. Conductance meshes of the 3-D forward modelling representing the Békés graben

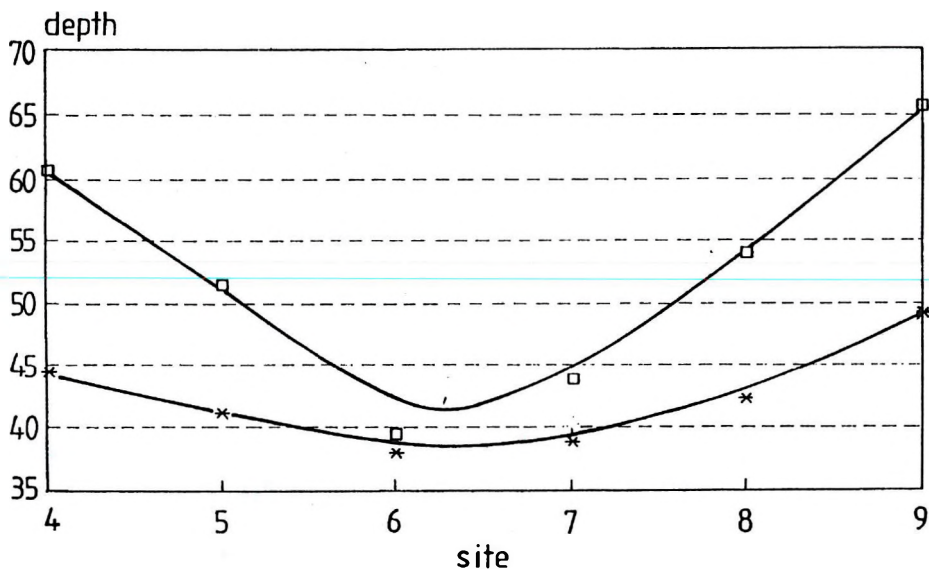*20. ábra.* 3-D modellezés horizontális vezetőképesség hálója a Békési árokra

Fig. 21. Apparent depth to the conducting asthenosphere along a profile corresponding to the PGT derived by 1-D inversion from the results of 3-D Békés forward modelling (oriented by the magnetic strike (□) and its perpendicular direction (*))

21. ábra. A jólvezető asztenoszféra látszólagos mélysége a PGT1-nek megfelelő szelvény men-tén 3-D modellezés ereménygörbéiből 1-D inverzióval meghatározva (□ a mágneses csapás irányában, * rá merőlegesen)

decrease of the asthenosphere in the centre of the 3-D graben is about 20 km (from 60 km to 40 km) due to galvanic distortion supposing that the geoelectric model of the 3-D sedimentary basin (graben) is correct and the error of the calculation can be neglected. If these latter conditions are fulfilled, and the apparent asthenospheric depth is less than 40 km in the Békés graben, — as indeed it is (31.1–36.6 km and site 7 18.5 km!) — the statement can be allowed that beneath the 3-D subbasins of the Great Hungarian Plain along the PGT the asthenosphere even nowadays is in an elevated position based on gravity, magnetic and seismic data and the corrected heat flow [SZAFIÁN et al. 1994]. Further support for this statement would doubtlessly be provided by further 3-D modelling with more accurate surface geoelectric structure.

7. Results of the 2-D inversions

The 2-D inversion of the MT data of PGT was carried out by two programs: by the RRI code of SMITH and BOOKER [1991] and by GEO-TOOLS 2-D Occam inversion [CONSTABLE et al. 1987].

The RRI code is characterized by JIRACEK [1995] in the following way: 'The method is very fast because it is iterative and approximates the horizontal derivatives of the electric and magnetic fields with their values from the previous iteration. The inverse problem at each site becomes essentially uncoupled 1-D ones followed by interpolation between sites prior to 2-D forward calculations for the next iteration. The number of floating point multiplications can be reduced by a factor of 100 compared to standard 2-D inversion. Inverse models derived by the RRI method are smooth, minimum structure ones that minimize the mean square of a function involving the 2-D Laplacian of the logarithm of the conductivity.' A comparison of this RRI method with the Occam one is given in the Appendix.

Both inversions with Rho_{max} and Rho_{min} curves — i.e. those of SMITH and BOOKER [1991] (*Figs. 22* and *23*), and the Occam ones (*Figs. 24* and *25*) — show practically similar features in the resistivity distribution for crust and mantle as do the resistivity sections obtained by 1-D inversion for the same extreme sounding curves (Figs. 15 and 16). Beneath the deep 3-D subbasins the asthenosphere is shown in an elevated position by these inversions, too. Only with the help of 3-D modelling (or 3-D inversion?) can it be estimated how much is the real elevation from this apparent one, as has been attempted for the Békés graben.

The 2-D models calculated from Rho_{max} and Rho_{min} curves are essentially different concerning the depth of the asthenosphere (conducting basement). In the case of the Rho_{max} curve the Occam inversion — which identified the asthenosphere with a resistivity less than 32 Ωm — gives about 100–110 km for the depth apart from the deep subbasins. The inversion of Rho_{min} curves resulted in a shallower asthenosphere, which is identified in this case by a resistivity less than 15.8 Ωm.

As might well have been expected, the 2-D inversion did not eliminate the distortion effect of the 3-D subbasins (grabens), therefore 2-D models may include a false layer structure due to the galvanic distortions. The correct and detailed deep geoelectric structure of the Pannonian Basin could only be determined by using the 3-D inversion technique if this latter were to be elaborated by the EM induction community. Nevertheless, at present the
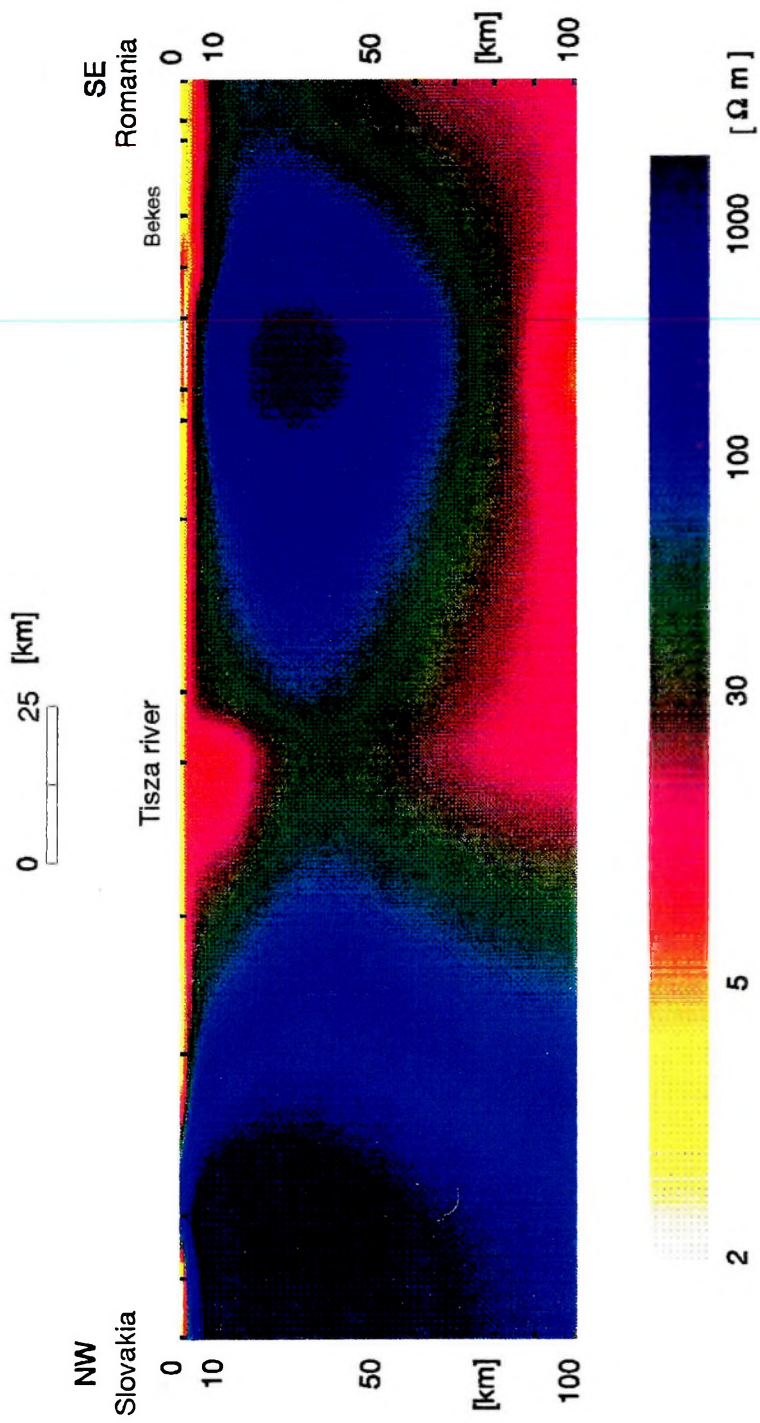
Fig. 22. 2-D inversion results of the Rho_max curves along PGT1 using SMITH and BOOKER's [1991] RRI inversion

22. ábra. A PGT1 mentén mért Rho_max görbék SMITH és BOOKER [1992] RRI 2-D inverziójával nyert eredménye
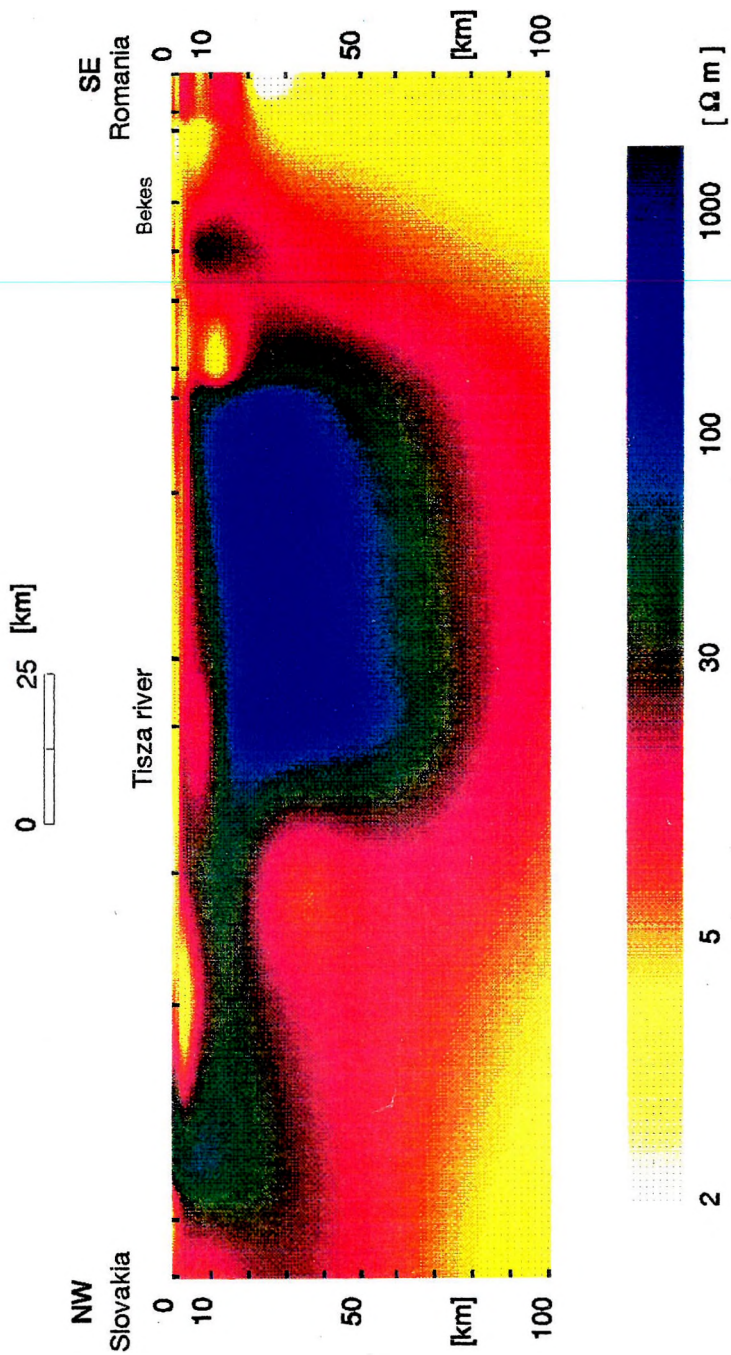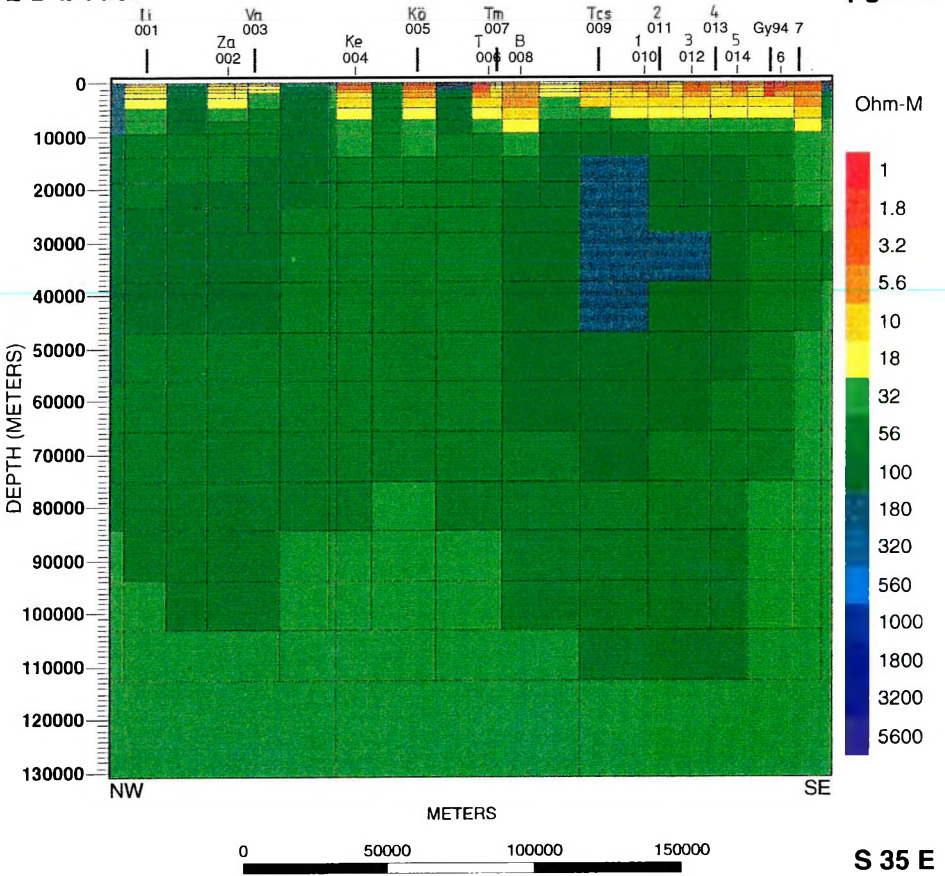
Fig. 23. 2-D inversion results of the Rho_min curves along PGT1 using SMITH and BOOKER's [1991] RRI inversion

23. ábra. A PGT1 mentén mért Rho_min görbék SMITH és BOOKER [1992] RRI 2-D inverziójával nyert eredménye

Fig. 24. 2-D Occam inversion results of the Rho_{max} curves

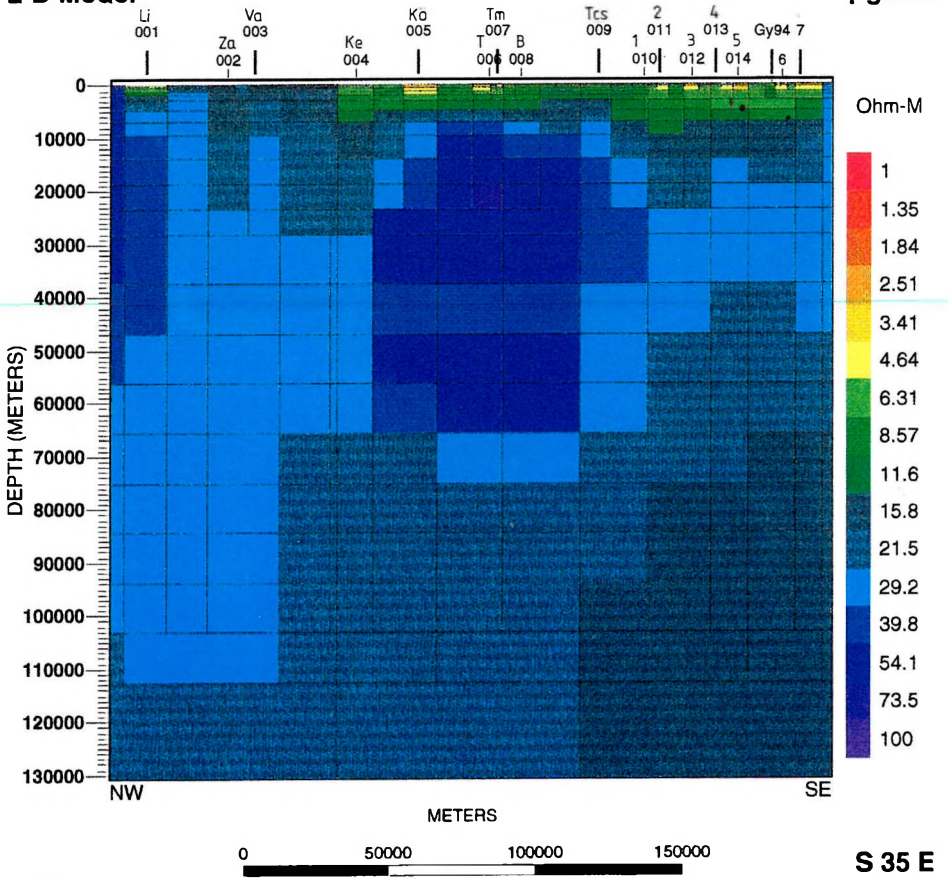*24. ábra.* 2-D Occam inverzióval a Rho_{max} görbék alapján nyert ellenállásszelvény

Fig. 25. 2-D Occam inversion results of the Rho$_{min}$ curves

25. ábra. 2-D Occam inverzióval a Rho$_{min}$ görbék alapján nyert ellenállásszelvény

average asthenospheric depth and the anisotropy deduced from the extreme sounding curves carry fundamental physical information for the crust and mantle of the Pannonian Basin.

8. Conclusions: physical relationships

a) Geothermal relationships

Since the interpretation of the first deep MT soundings in the Pannonian Basin in the early sixties it has been known [ÁDÁM 1963, 1965] that the asthenosphere in the Pannonian Basin — which corresponds to the partial melting of the mantle peridotite — is in an elevated position (updoming) relative to that of the surrounding old tectonic units (e.g. East European Platform, Variscan belts) and is closely linked with their heat flow, i.e. with the Earth's inner temperature. This statement is supported nowadays by 2-D magnetotelluric sections crossing the young and old tectonic belts [HJELT and KORJA 1993].

The average 'undisturbed' asthenospheric depth determined for the Pannonian Basin — i.e. 58.2 and 70.5 km — can be described by ÁDÁM's [1976, 1978] empirical relationship between the asthenospheric depth and the regional heat flow (*Fig. 26*). The average depth, i.e. 58.2 km, deduced from the quasi *E*-polarized Rho_{min} curves better corresponds to the regional heat flow in the Pannonian Basin.

b) Are there conductive asthenospheric (mantle) plumes below the 3-D deep subbasins?

As mentioned, the crustal/mantle anomaly i.e. the mantle plume below the Békés graben, was first detected by the deep seismic reflection measurements of POSGAY et al. [1992] and later confirmed using a more sophisticated technique. Their curved seismic horizons hint at the possible upwelling of the asthenosphere, too. The nearsurface position of the remains of the Miocene dense mantle peridotite (?) is modelled by gravity and magnetic computations by NEMESI and STOMFAI [1992] and KOVÁCSVÖLGYI [1995]. Concerning the position of the asthenosphere representing the temperature
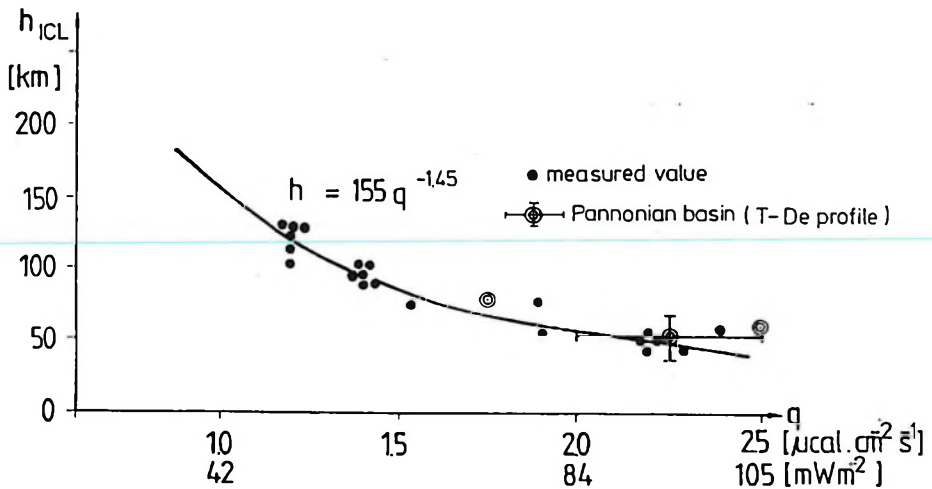
Fig. 26. Empirical relation between the asthenospheric depth and regional heat flow
[ÁDÁM 1978]
26. ábra. Tapasztalati összefüggés az asztenoszféra mélysége és a regionális hőáram között
[ÁDÁM 1978]

of the solidus of the peridotite and hence partially molten material, the magnetotelluric method has a decisive role. Nevertheless, the question in the title can only be answered by taking into account the EM distortion theory and the 2-D and 3-D modelling results.

As concluded, the apparent asthenospheric depths less than the distorted 40 km (see Fig. 21) (18–35 km by 1-D inversion) may prove the present elevation of the remains of the electric asthenosphere, too, not only below the Békés graben but the other 3-D subbasin — the so called Jászság subsidence in the region of Kerecsend (Ke) and Kömlő (Kö). Hence the regional mantle diapir of the Pannonian Basin may have some smaller shallower parts (plumes) beneath the strong local deepening of the basin due certainly to the uneven extension of the Pannonian Basin. In view of this investigation of the other deep subbasins of the Pannonian Basin could be of interest, among them, for example, the Rába graben in the Little Hungarian Plain (Danube Basin) where the dense peridotite is also in an elevated position. In this respect one should mention BIELIK's [1991] gravity studies which generalize the crustal upwelling dense material for almost all extensional deep subbasins of the Pannonian Basin.

Acknowledgements

REFERENCES

ÁDÁM A. 1963: Study of the electrical conductivity of the Earth's crust and upper mantle (in Hungarian). Methodology and Results. Dissertation, Sopron, 106 p.

ÁDÁM A. 1965: Einige Hypothesen über den Aufbau des oberen Erdmantels in Ungarn. Gerlands Beiträge zur Geophysik, **74**, pp. 20–40

ÁDÁM A. 1969: Appearance of the electrical inhomogeneity and anisotropy in the results of the complex electrical exploration of the Carpathian basin. Acta Geod. Geoph. Mont. Hung., **4**, pp. 87–197

ÁDÁM A. 1971: Determination of graphitic formations by magnetotellurics beneath electrically shading layers in the Hungarian basin and some genetical consequences (in Hungarian). Geonómia és Bányászat, **4**, pp. 297–308

ÁDÁM A. 1976: Quantitative connection between regional heat flow and depth of conductive layers in the Earth's crust and upper mantle. Acta Geod. Geoph. Mont. Hung., **11**, pp. 503–509

ÁDÁM A. 1978: Geothermal effects in the formation of electrically conducting zones and temperature distribution in the Earth. Phys. Earth Planet. Int., **17**, pp. P21–P28

ÁDÁM A. 1992: Crustal conductors as tectonic indicators. *In*: Proceedings for the Jubilee Symposium of the 10 years Finnish-Soviet co-work in geoelectrics. KAIKKONEN, P. (ed.), University of Oulu, Report No. **18**, pp. 1–17

ÁDÁM A., MAJOR L. 1967: Stabilized high-sensitivity immersion magnetic variometer for magnetotelluric investigations (Type MTV-2). Acta Geod. Geoph. Mont. Hung., **2**, pp. 211–215

ÁDÁM A., LANDY K., NAGY Z. 1989: New evidence for the distribution of the electric conductivity in the Earth's crust and upper mantle in the Pannonian Basin as a 'hotspot'. Tectonophysics, **164**, pp. 361–368

ÁDÁM A., SZARKA L., STEINER T. 1993: Magnetotelluric approximations for the asthenospheric depth beneath the Békés graben, Hungary. J. Geomag. Geoelectr., **45**, pp. 761–773

ÁDÁM A., VERŐ J. 1964: Ergebnisse der regionalen tellurischen Messungen in Ungarn. Acta Technica, **47**, pp. 63–77

ÁDÁM A., VERŐ J. 1967: Newer results of electromagnetic measurements in Hungary (in Hungarian). Geofizikai Közlemények, **16**, pp. 25–52

BAHR K. 1988: Interpretation of magnetotelluric impedance tensor: regional induction and local telluric distortion. J. Geophys., **62**, pp. 119–127

BAHR K. 1991: Geological noise in magnetotelluric data: a classification of distortion types. Phys. Earth Planet. Int., **66**, pp. 24–38

BERDICHEVSKY M. N., DMITRIEV V. I. 1976: Distortion of magnetic and electric fiels by near-surface lateral inhomogeneities. Acta Geod. Geoph. Mont. Hung., **11**, pp. 447–483

BIELIK M. 1991: Density modelling of the Earth's crust in the intra-Carpathian basins. Serbian Academy of Sciences and Arts, Academic Conferences Volume LXII. Beograd, pp. 123–132

CONSTABLE S. C., PARKER R. L., CONSTABLE C. G. 1987: Occam's inversion: A practical algorithm for generating smooth models from electromagnetic sounding data. Geophysics, **52**, pp. 289–300

DEGROOT-HEDLIN, CONSTABLE S. C. 1990: Occam's inversion to generate smooth, two-dimensional models from magnetotelluric data. Geophysics, **55**, pp. 1613–1624

DÖVÉNYI P. 1994: Geophysical studies related to an understanding of the lithospheric evolution of the Pannonian Basin (in Hungarian). Thesis, Eötvös University Budapest 119 p.

GROOM R. W., BAILEY R. C. 1989: Decomposition of magnetotelluric impedance tensors in the presence of local three dimensional galvanic distortion. J. Geophys. Res., B, **93**, pp. 1913–1925

GROOM R. W., BAILEY R. C. 1991: Analytic investigations of the effects of near-surface three dimensional galvanic scatterers on MT tensor decompositions. Geophysics, **56**, pp. 496–518

GROOM R. W., KURTZ R. D., JONES A. G., BOERNER D. E. 1993: A quantitative methodology to extract regional magnetotelluric impedances and determine the dimension of the conductivity structure. Geophys. J. Int., **115**, pp. 1095–1118

HJELT S. E., KORJA T. 1993: Lithospheric and upper-mantle structures, results of electromagnetic soundings in Europe. Phys. Earth Planet. Int., **79**, pp. 137–179

HORVÁTH F. 1993: Towards a mechanical model for the formation of the Pannonian Basin. Tectonophysics, **226**, pp. 333–357

HORVÁTH F., ROYDEN K. 1981: Mechanism for the formation of the intra-Carpathian basins: A review. Earth Evol. Sci., 2(3–4), pp. 307–316

JIRICEK R. 1979: Tectonogenetic development of the Carpathian area in the Oligocene and Neogene (in Slovakian with English summary). In: Tectonic Profiles through the West Carpathians, M. MAHEL (ed.), Publ. Geol. Int. D. Stur, Bratislava, pp. 203–214

JIRACEK G. R. 1995: Geoelectromagnetics charges on Reviews of Geophysics. Supplement, pp. 169–176

JONES A. G., GROOM R. W., KURTZ R. D. 1993: Decomposition and modelling of the BS87 dataset. J. Geomag. Geoelectr., **45**, pp. 1127–1150

KOVÁCSVÖLGYI S. 1995: Interpretation of gravity and magnetic anomalies in SE Hungary. (in Hungarian with English summary) Magyar Geofizika, **36**, (3), pp. 198–202

LARSEN J. C. 1977: Removal of local surface conductivity effects from low frequency mantle response curves. Acta Geod. Geoph. Mont. Hung., **12**, pp. 183–186

NEMESI L., STOMFAI R. 1992: Some supplements to the exploration of the basement of Békés-basin. (in Hungarian with English summary) Magyar Geofizika, **33**, (2–3), pp. 70–79

POSGAY K., HEGEDŰS E., TÍMÁR Z., BODOKY T. 1992: Asthenospheric structures: encouraging results of a deep seismic experiment. 5th International Symposium on Seismic reflection probing of the continents and their margins. Abstract. Banff, Alberta, Canada, 6–12 September, 1992

POSGAY K., BODOKY T., HEGEDŰS E., KOVÁCSVÖLGYI S., LENKEY K., SZAFIÁN P., TAKÁCS E., TÍMÁR Z., VARGA G. 1995: Asthenospheric structure beneath a Neogene basin in SE Hungary. Tectonophysics, **252**, pp. 467–484

SMITH J. T., BOOKER J. R. 1991: Rapid inversion of two- and three-dimensional magnetotelluric data. J. Geophys. Res., **96**, pp. 3905–3922

STEINER F. 1989: MT inversion using least-absolute-values and least-squares. 34th Internat. Geophys. Symposium, Sept. 4–8, 1989, Budapest. Abstracts and Papers of the Technical Program, pp. 639–650

SZAFIÁN P., LENKEY L., DÖVÉNYI P., HORVÁTH F. 1994: Geothermal numerical model analysis along the Pannonian Geotraverse. Magyar Geofizika (in Hungarian with English summary). (Submitted for publication)

TAKÁCS E. 1968: Anomalous conductivity of the upper crust in the NW foreground of the Bakony Mountains. Acta Geod. Geoph. Mont. Hung., **3**, pp. 155–160

VARGA G., RÁNER G. 1990: Geophysical investigations along basic geological profiles: magnetotelluric measurements along the line EK-2 and the Pannonian Geotraverse. Report of the Eötvös Loránd Geophysical Institute, Budapest. Manuscript

VERŐ J. 1972: On the determination of magnetotelluric impedance tensor. Acta Geod. Geoph. Mont. Hung., **7**, pp. 333–351

WANNAMAKER P. E., HOHMAN G. W., WARD S. H. 1984: Magnetotelluric responses of three-dimensional bodies in layered earths. Geophysics, **49**, pp. 1517–1533

Appendix

Both applied inversion algorithms are based on the linearization of the direct problem and in both cases the smooth models are preferred. For the inversion a good initial model is needed. As a result of the iteration steps the model is modified in such a way that the difference between the measured and theoretical data belonging to the approximative model will continually

decrease. In other words: the theoretical data will more and more approximate the measured data.

In the case of the RRI technique [SMITH and BOOKER 1991] the solution of the direct problem is given by using the method of finite differences. Here the inversion needs measuring results in the horizontal direction at each point of the grid. This can be achieved with iteration. The iteration step or each measuring point can be described by a one-dimensional problem:

$$\Delta \vec{d} \approx \mathbf{F} \Delta \vec{m}, \tag{a1}$$

where d is a vector of size n_d. It contains the measured data at the given measuring site, m is a vector of dimension l. It contains the conductance values below the given site, $\mathbf{F}$ is a matrix of size $n_d \times l$, n_d is the number of data, l is the horizontal size of the grid.

At first glance the RRI technique appears to be nothing more than a series of one-dimensional inversions but in fact this is not the case since matrix $\mathbf{F}$ describing the relationship between the change of model parameters (i.e. the conductivities) and the change of measured data at the given site depends on the whole two-dimensional model. For this reason the inversion results at different sites cannot evolve independently of each other. The main aim with the RRI technique is not the minimization of the norm

$$\left\| \Delta \vec{d} - \mathbf{F} \Delta \vec{m} \right\|, \tag{a2}$$

but, rather, it is the solution of the equation

$$\Delta \vec{d} - \vec{e} = \mathbf{F} \Delta \vec{m}. \tag{a3}$$

It means that instead of striving to obtain the best adjustment, the algorithm selects the smoothest version from several theoretical models, having the same difference between the measured and theoretical data.

e is a prefixed vector of errors, decreasing continually with the iteration process. Better adjustments and smoother models in the case of a given β are given automatically by minimization of function W:

$$W = \left(\mathbf{R}\vec{m} - \vec{c} \right)^T \left(\mathbf{R}\vec{m} - \vec{c} \right) + \beta \vec{e}^T \vec{e}, \tag{a4}$$

where $\mathbf{R}$ is a smoothing matrix of $n_d \times l$, $\vec{c}$ is a vector of size n_d.

The other inversion technique, the so called Occam inversion [DEGROOT-HEDLIN and CONSTABLE 1990], is a true 2-D inversion based on the minimization of function U as follows:

$$U(\vec{m}) = R(\vec{m}) + \mu^{-1}\left(\left\|\mathbf{D}\left(\Delta\vec{d} - \mathbf{F}\Delta\vec{m}\right)\right\| - X_*^2\right) \tag{a5}$$

where R is the smoothing function, μ^{-1} is the Lagrange multiplier, $\mathbf{D}$ is a diagonal tensor for weighting the measured data, X_* is the expected value of the measuring errors, $\mathbf{F}$ is a Jacobian matrix of size $M \times N$, $M = n_d p$, $N = pl$, p is the number of gridpoints in direction y.

Vector $\vec{m}$ contains the whole set of model parameters, while all the measured data are contained in vector d. In the case of the Occam inversion [CONSTABLE et al. 1987] the direct problem is solved by using the finite element technique. One iteration step at a SUN10 workstation can be as long as several hours whereas the RRI method needs only several minutes.

The origin of this difference comes partly from the fact that with the RRI the direct problem should be solved only once, while the Occam inversion computes it several times. The other reason is the difference between the sizes of the matrices. For the RRI case a significantly smaller problem is solved at p times, where the size of the matrix is

$$M = n$$
$$N = l.$$

In order to have not too big a number of model parameters, the Occam inversion makes it possible to reduce the number of cells belonging to certain sites of the grid in the direct problem. The contracted cells have the same model parameter. For this reason the Occam inversion models consist of larger blocks than the RRI ones.

Köpenyfeláramlás vagy EM torzulás a Pannon medencében?
(A Pannon Geotraverz mentén mért mély magnetotellurikus (MT) szondázások inverziója)

ÁDÁM Antal, SZAKRA László, PRÁCSER Ernő, VARGA Géza

Az ÉNy-DK-i irányú Pannon Geotraverz mentén az elmúlt 8 év során mért 19 hosszú periódusú magnetotellurikus szondázás eredményeit ismerteti a tanulmány.

Az adatgyűjtő rendszer és feldolgozó módszer rövid ismertetése után a mért és értelmezett adatokat mutatja be, amelyek tájékoztatnak mind a litoszféra–asztenoszféra mélyszerkezetéről, mint a terület medence-szerkezetéről.

A szondázási görbék 1-D és különböző 2-D inverziója (Occam és RRI) alapján az alábbi következtetések vonhatók le:

1. Az asztenoszférát átlagosan — az asztenoszféra mélysége és a regionális hőáram közötti összefüggésnek és egyéb kapcsolatos információknak megfelelően — 50-70 km mélységben jelzik a szondázási görbék típusuktól és a számításba vett mérési helyüktől függően.

2. Bár a felszínközeli elektromos inhomogenitások eltorzítják az MT görbéket, kikövetkeztethető, hogy a keskeny, mély extenziós 3-D medencerészeken, mint amilyen a Békési árok is, a jólvezető asztenoszféra felemelkedik mintegy 40 km mélységig. Ezt valószínűsíti a gravitációs és az újabb szeizmikus mérések által észlelt nagy sűrűségű köpenyanyag-megemelkedés is.

3. A Pannon medencében szinte mindenütt jelentkező és eléggé állandó jellegű magnetotellurikus anizotrópia szerkezeti inhomogenitásoknak tulajdonítható.

Results of deep reflection seismic measurement south of Rechnitz/Burgenland/Austria

Franz WEBER[*], Rupert SCHMÖLLER[*,**],
Rudolf K. FRUHWIRTH[**]

Deep reflection seismic measurements were carried out in 1992 on a profile south of Rechnitz, Burgenland. 30 kg explosives were blasted in 6 shotholes over a fixed geophone spread of 4800 m with 96 channels, with distances of 700 m between shotholes. This field procedure leads to a 2- to 3-fold coverage. Band limited deconvolution gave the best signal enhancement results. Dynamic corrections for the shallow depth range are based on refraction analysis; a stacking velocity of 6000 m/s was estimated for the deeper section.

Below the base of Tertiary at a depth of about 280 m there is a reflection-free zone down to 5 seconds two-way traveltime. Below this zone sporadic reflection elements appear down to 7 seconds, a band of fair reflections in the range between 7 and 8 seconds indicating a transitional zone. The Moho is attributed to the deepest reflection at 10 seconds. The Moho and the reflections above dip slightly to the west.

1. Introduction

The transition zone between the Alps and the Pannonian area offers favourable conditions for seismic energy propagation and interpretation. It

* Department for Geophysics, Mining University Leoben, Franz-Josef Straße 18, A-8700 Leoben/Austria
** Department for Applied Geophysics, JOANNEUM RESEARCH Forschungsgesellschaft mbH, Roseggerstraße 17, A-8700 Leoben/Austria

is known from regional investigations in the Transdanubian area of Hungary between Lake Balaton and the Hungarian-Austrian border that reflections from great depths can be recorded using either dynamite or the Vibroseis technique as energy sources. The Mohorovičić discontinuity shows in this area a characteristic band of reflections [POSGAY et al. 1981; POSGAY et al. 1990]. Given adequate acquisition procedures, reflections even from the sub-Moho range down to the asthenosphere can be observed [POSGAY et al. 1986]. By test measurements at Nikitsch/Burgenland in 1981 it was proved that even under less than optimal conditions, — e.g. observing with analog-seismic equipment and single-fold coverage, good energy transfer exists. Thus, reflections even from the lower crust could be observed although relatively small amounts of explosives (10 – 50 kg) had been used.

From a shot point near Körmend (Hungary), fair quality reflections from the lower crust and the Moho could be observed in the wide angle range along an E-W profile up to a distance of 90.7 km from the shot point. For the reflection seismic identification of the Moho the results of the refraction seismic Alpine profile 1975 are very helpful. This profile was shortly reinterpreted [YAN and MECHIE 1989] and can be used for comparison. It is only 20 km south of the reflection seismic profile presented here.

The Pennine of the Rechnitz schist uplift has a central position in the regional geological analysis of the east end of the Eastern Alps. The reasons for investigating the deeper parts of the crust in this area are mentioned in Section 2. Only for practical reasons was the reflection seismic profile removed into the Tertiary near the crystalline margin. In the near future it is planned to continue the profile to WNW up to the area of Pinkafeld. The actual investigations are an integral part of the working programme of the Commission for Geophysical Research of the Austrian Academy of Sciences.

2. Field measurements

The area between the villages Neuhodis and Rechnitz in the north, and Dürnbach and Schachendorf in the south was selected for the field measurements of 1992. The reasons for selecting this area were: 1) the probability of favourable conditions for the excitation of seismic energy in the transition zone from the Alps to the Pannonian area. 2) The key position of the Penninic schists within the window of Rechnitz for regional geological analysis.

The profile is east-west oriented: it starts somewhere between Rechnitz and Schachendorf and goes towards the west as a fairly straight line up to a point between Neuhodis and Dürnbach. The profile is therefore situated just a few km south of the isolated schist outcrop of Rechnitz and more or less parallel to its southern rim. The basement could therefore be expected at a depth of a few 100 m under the Tertiary overburden. The profile was planned for later continuation up to somewhere west of Pinkafeld.

The measurements were carried out in autumn 1992. A spread of 96 geophone points with a group interval of 50 m leads to a CMP distance of 25 m. The recording instruments were a Sercel 332 HR and a Sercel 338 B in master-slave configuration, each instrument recording on 48 channels. The Sercel 332 HR was appointed to be the master. Two of the traces of each master and slave were connected to geophones with identical positions in the field. By use of this trace overlapping time-break errors of the slave could be eliminated by a cross correlation technique. Neither shot nor receiver arrays were used.

Seven shots with 30 kg explosives each were blasted in 6 boreholes at a depth of 20 to 30 m. The distances between the boreholes were usually 700 m, i.e. 15 geophone points positioned between two shot holes. *Fig. 1* shows the layout of the profile and the position of the shot points in the field.

A refraction survey was carried out on three profiles A, B, C running from north to south to trace the base of the Tertiary, i.e. top crystalline. The basement shows a highly accentuated topography with a general rise to the north, where the basement crops out from the Tertiary. The velocity distribution determined from the refraction seismic data is a valuable supplement to the velocity information deduced from the deep seismic shots. These refraction seismic data were successfully used for the near surface static correction calculation.

3. Processing of the reflection seismic data

The data processing was done with the DISCO package from COGNISEIS Development (Houston, Tx, U.S.A.). The data were originally stored in SEG-B standard format on 9-track tapes. In the first step the tapes were checked and stored on disk after demultiplexing. There were 9 records from both machines, master and slave, shot at 6 different source positions. Each
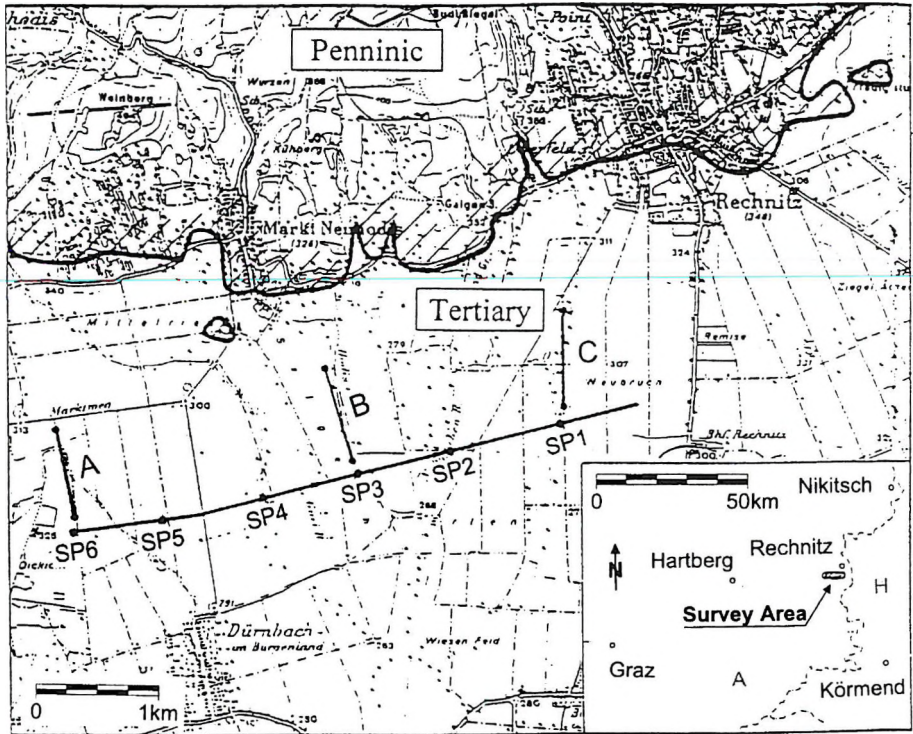
Fig. 1. Location map of the refraction seismic lines A, B and C and of the deep reflection seismic profile (SP1 to SP6)

1. ábra. Az A, B, C refrakciós vonalak és a mélyszeizmikus szelvény (SP1-től SP6-ig) helyszínrajza

record has a total number of 48 channels with a sampling interval of 2 milliseconds. The recording time was 16 to 24 seconds.

Since the analog amplifiers of the master and slave machines are not calibrated, the energy of the slave records had to be corrected. To compensate for the different amounts of explosives, the rms-amplitude of all traces of the combined records was calculated. The ratio of these values to the value of an arbitrarily chosen record led to a gain factor for the compensation of the charge irregularities. For further processing only the combined and gain corrected records were used.

To calculate the static correction values, the records were transferred to SEG-Y standard format and copied to a PC. A refraction analysis of the first breaks was done by the Generalized Reciprocal Method of PALMER [1980], whereby a special refraction analysis package, developed by JOANNEUM

RESEARCH Forschungsgesellschaft mbH, was used. The static correction values were calculated for a datum plane of 200 m above sea level. The next step included the geometry information, muting of the first breaks, and elimination of bad traces. The spherical divergence correction was based on the velocities of the refraction analysis.

A frequency analysis of the records followed. The average amplitude spectrum in a time range of 0 to 16 seconds was calculated. *Fig.* 2 shows a dominant signal frequency of 20 Hertz and a noise frequency (ground roll) of about 5 Hertz. Based on this analysis a filter test was designed. The records
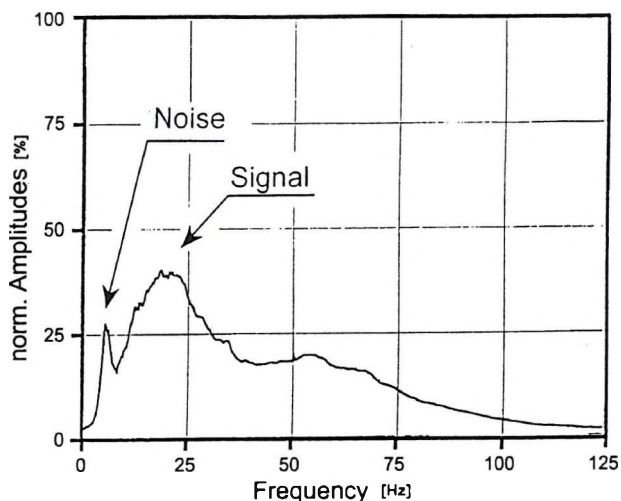
Fig. 2. Spectral analyses in the traveltime range from 0 to 16 seconds

2. *ábra.* A 0–16 s-os menetidő-tartomány amplitúdó–frekvencia analízise

were filtered by zero phase band pass filters with different bandwidths. The result of this filter test helped to optimize the deconvolution parameters. The bandlimited deconvolution gave slightly better results than the spiking deconvolution. For further processing the records were truncated to an adequate time range of 23 seconds.

The next step was collecting the CMP's. Since the field job was designed for a target depth of more than ten kilometers, velocity analysis in the shallow depth range was difficult. Because of this, in this range the velocities obtained by refraction analysis were used for the dynamic correction. In the deeper section, a stacking velocity of about 6000 meters per second was estimated. The following brute stack, based on this velocity model, was used to optimize
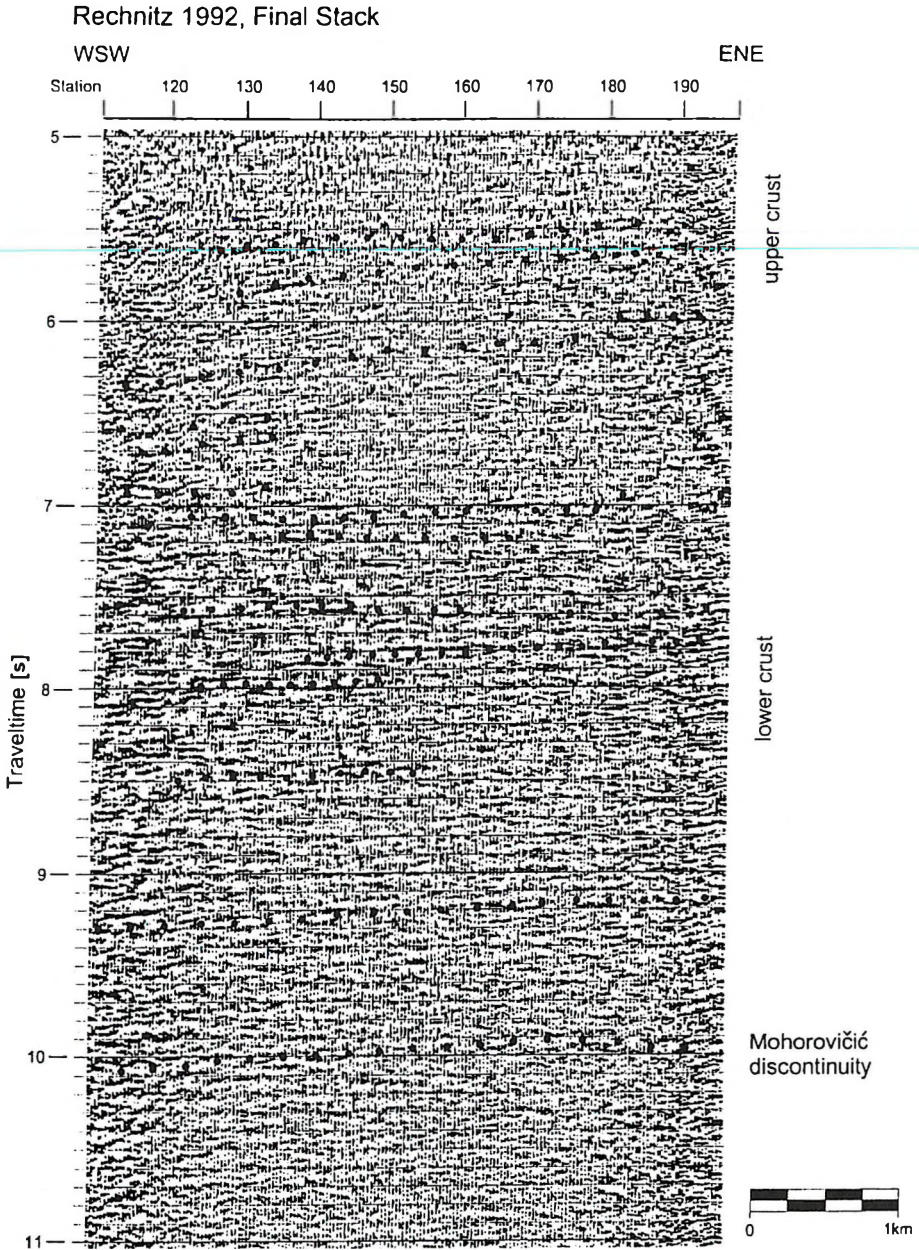
Rechnitz 1992, Final Stack

Fig. 3. Reflection seismic two way traveltime section of the 1992 campaign in the range from 5 to 11 seconds

3. ábra. Az 1992-es mérések kétszeres vertikális menetidő szelvénye az 5–11 s-os tartományról

the input parameters for the residual statics calculation. Application of the residual statics and the stacking operation led to the final stack (*Fig. 3*). Only the deeper part (5 s to 12 s) is shown.

4. Results

The final stack (Fig. 3) contains the total information of the acquisition campaign. It allows the determination of the reflection times. There are strong surface waves which could not be removed totally by filtering. Furthermore one has to consider that at shot holes 4 and 5 shot depths of only 13 m were possible because of the technical problems mentioned above. Thus only charges of 10 and 15 kg were possible. This caused reduced reflection energy in the last part of the profile.

The datum of +200 m above sea level, i.e. about 100 m below the surface, was chosen to keep static corrections small. The base of the Tertiary shows a considerable relief down to 85 m below sea level with a high velocity contrast between Tertiary (1900 – 2000 m/s) and Crystalline (6000 m/s). Calculation of the static corrections was based on these data.

In the range down to 1 s reflection time only sporadic reflections appear over short distances. They can be interpreted as reflections from the Pannonian series.

The upper crust is practically free of reflections, except some short reflection elements at about 3 and 5.1 s. There are some west dipping elements in the time range of 5.4 – 6.4 s. More short reflection elements are down to about 7 s, also dipping west. Starting with a reflection time of 6.96 s at shot point 1 there is a reflection band continuing nearly over the whole profile. Between 7.6 and 8.0 s there are some more reflections with distinct perseverance. Below this are more short reflecting elements. On the western half of the profile is a characteristic band of reflections between 9.2 and 9.3 s, which can be followed to the easternmost part of the profile. At longer times only a few not very characteristic reflection elements exist maintaining the general trend.

At a reflection time of 10 s there are reflections whose rise is less pronounced in the eastern part of the profile compared to the reflections above. Below about 10.2 s no definite reflections exist. Due to this fact the mantle might be indicated.
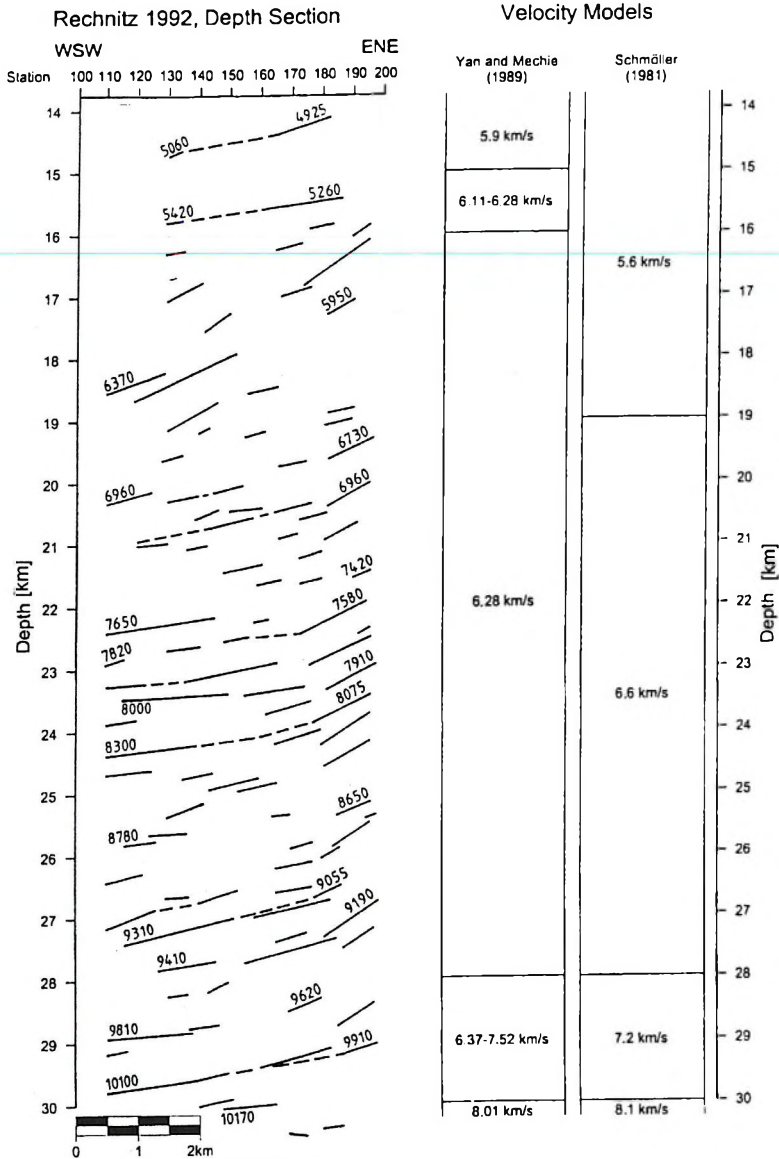
Fig. 4. Depth section of the reflection seismic data of the 1992 campaign (left side) and velocity models 'YAN and MECHIE [1989]' and 'SCHMÖLLER [1981]' deduced from the ALP 75 refraction and wide angle reflection seismic data [YAN and MECHIE 1989; WEBER et al. 1981] (right side)

4. ábra. Az 1992-es reflexiós mérések mélységszelvénye (bal oldalon) és a „YAN and MECHIE [1989]" és „SCHMÖLLER [1981]" féle az ALP 75 szelvény refrakciós és szélesszögű reflexiós adataiból levezetett sebességmodellek [YAN and MECHIE 1989; WEBER et al. 1981] (jobb oldal)

In the lower crust the general trend of the reflections is rising to ENE with an angle of 11 – 15°.

A more detailed correlation of reflections is shown on the depth section *Fig. 4.*

5. Interpretation

5.1. Velocity models derived from ALP 75 seismic measurements

Useful velocity data for the surroundings of the prospecting area exist from the ALP 75-refraction seismic measurements [YAN and MECHIE 1989] and from reflection seismic records in the wide angle range with the shot point near Körmend in western Hungary. Further measurements were performed on the occasions of the International Geodynamic Project 1975 and 1977 [WEBER et al. 1981].

For the section of the ALP 75-profile which is 22 km S of the Rechnitz area YAN & MECHIE [1989] use the following velocity model. In the upper crust at the top of the Crystalline there is a velocity gradient of 0.01 to 0.015 (km/s)/km, dropping to a value of 0.004 (km/s)/km at greater depths. The velocity in the upper crust increases from about 6.0 km/s to 7.0 km/s at a depth of 7 km. From there the velocity is constant down to a depth of 10 km. From 10 to about 15 km a 'low velocity channel' exists, in which the velocity decreases to 5.90 km/s. From the depth of 14 km down to 30 km this velocity model is shown in Fig. 4 as the 'YAN and MECHIE [1989]' model. From theoretical considerations a transition layer of 1 km thickness was assumed in this model at the base of the upper crust. Below this transition layer at a depth of about 16 km follows the boundary between the upper and lower crust. It is characterized by a velocity increase from 6.11 to 6.28 km/s. Because of amplitude and phase relationships, a transition zone with a thickness of 2 km has been built into the model at the base of the lower crust. There the velocity increases from 6.37 km/s to 7.52 km/s. The position of the Mohorovičić discontinuity is defined by a fairly abrupt velocity increase to 8.01 km/s at a depth of about 30 km.

The wide angle reflection seismic data along profile ALP 75 [WEBER et al. 1981] are also of interest for the recognition of the Moho and the reflectivity of the upper and lower crust. At six stations the arrivals of
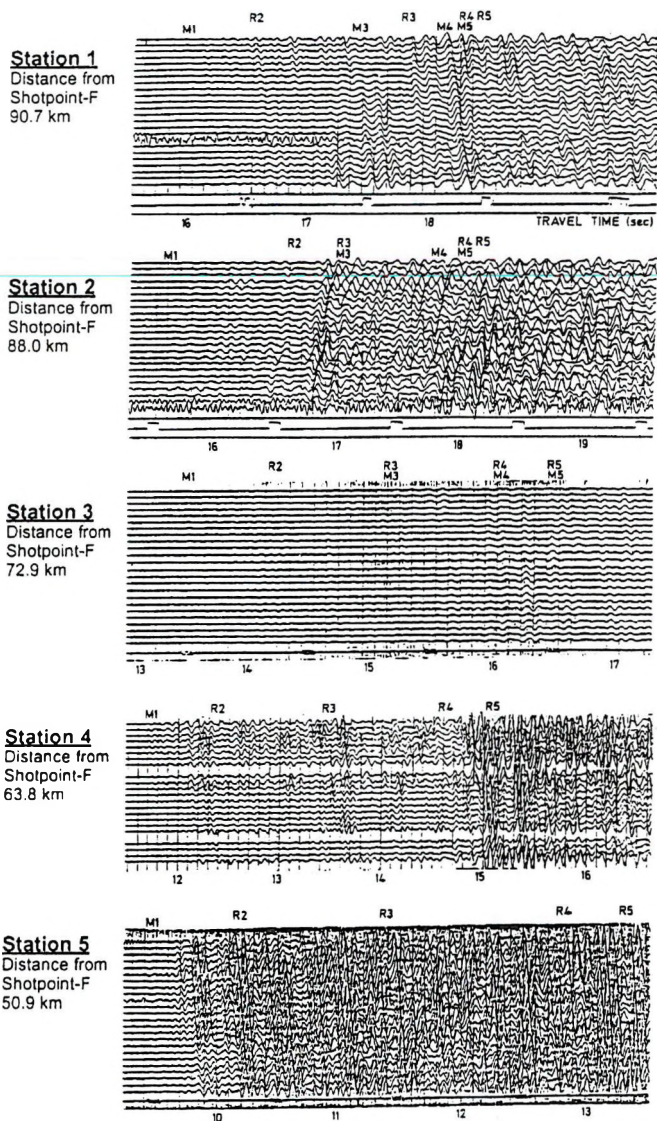
Fig. 5. Wide angle reflection seismic data on the ALP 75 profile from shotpoint near Körmend (Hungary) to recording stations 1—Hartmannsdorf; 2—Eichberg; 3—Commende Wald; 4—Eisenhüttl; 5—Punitzer Wald. M1, M3, M4, M5 are refraction arrivals, R2, R3, R4, R5 are reflection arrivals. The Moho is represented by the reflection band R4 to R5
[from WEBER et al. 1981]

5. ábra. Szélesszögű reflexiós szeizmikus adatok az ALP 75 szelvényen a Körmend (Magyarország) közeli robbantópont és az 1—Hartmannsdorf; 2—Eichberg; 3—Commende Wald; 4—Eisenhüttl; 5—Punitzer Wald közötti szakaszról. M1, M3, M4, M5 refrakciós-, R2, R3, R4, R5 reflexiós beérkezések. A Moho-t az R4-től R5-ig reflexiós köteg képviseli [WEBER et al. 1981]
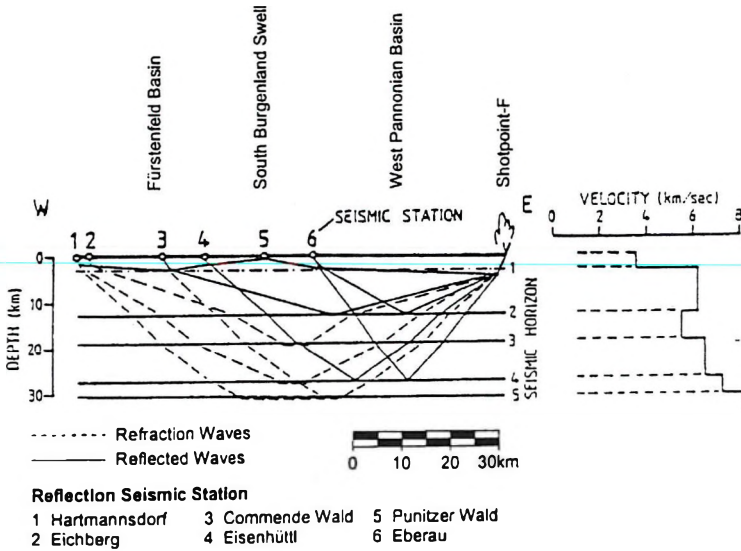
Fig. 6. Velocity model derived from the ALP 75 wide angle reflection seismic data of Fig. 5.
[from WEBER et al. 1981]

6. ábra. Az ALP 75 szélesszögű reflexiós adatokból (5. ábra) származtatott sebesség modell
[WEBER et al. 1981]

shotpoint F could be recorded. The records of five stations (station 1 to station 5) are reproduced in *Fig. 5.* Using the arrivals of these records, with the refracted waves marked by M1, M3, M4, M5 and the reflections marked by R2 to R5, a *P*-wave velocity model was developed by SCHMÖLLER [in WEBER et al. 1981]. It is presented as a profile from shotpoint F in the east to the recording stations 1 to 6 in the west (*Fig. 6*).

Reflections R2 and R3 from the top and base of the 'low velocity channel' exist on the five records. The top of the lower crust is therefore clearly characterized by the reflection seismic data. On each of the 5 wide angle spreads the Moho reflection can be recognized as a band of reflections (R4, R5). However there is some discrepancy in the definition of the Moho given above in that on all wide angle spreads there are events even from below the reflection band defined as the Moho. These reflections probably come from the uppermost part of the mantle. On spread 4 (Eisenhüttl) a characteristic reflection at about 0.3 s below the Moho and on spread 3 a reflection 0.4 s below this level can be identified. This might be an indication for the gradient zone assumed by YAN and MECHIE [1989] with a thickness of up to 6 km in this part of the deep refraction seismic profile. However one has to be cautious

when interpreting these events as sub-Moho reflections. They cannot be
distinguished from diffractions because of the short spread length of 0.69 km.
However, their frequent appearance — especially in the time range up to 2 s
below the Moho — might indicate true reflections.

This velocity model is also shown in Fig. 4 as the 'SCHMÖLLER [1981]'
model. For comparison purposes the horizons corresponding to the main
velocity-discrepancies are marked in both models. The most important
difference is obviously in the low velocity channel: in the model 'YAN and
MECHIE [1989]' this low velocity channel is at a depth between 10 and 15 km;
however, in the 'SCHMÖLLER [1981]' model it is in the depth range 12.5 –
19 km. In other words the top of the lower crust is 2 km deeper than in the
'YAN and MECHIE [1989]' model. The top of the gradient zone above the
Moho of the 'YAN and MECHIE [1989]' model seems to correspond with the
reflection pattern of the wide angle reflection data. The position of the Moho
is about the same in both models, which is in the assumed range of accuracy
of the computed depth profile. So the two models agree in a wide range
although YAN and MECHIE [1989]' model was derived from refraction data
whereas the other model — 'SCHMÖLLER [1981]' — was derived from wide
angle reflection seismic data in combination with refraction data on usual
single 24-channel spreads.

The determination and comparison of real amplitudes of the wide angle
reflection data are not possible because of the use of different analog and
digital reflection seismic instruments during that campaign as well as different
amplification and variable amounts of explosives at shotpoint F (1, 2 and 4
tons).

5.2. Identification of the Mohorovičić discontinuity in the reflection seismic data of 1992

There is some ambiguity in the velocity analysis of the Rechnitz data of
1992 (Figs. 3, 4) because of the relatively short spread of 4.7 km length. The
velocity analysis results in an average stacking velocity of 6.0 km/s.

With reference to the experience in other areas the Moho reflection is
defined as a more or less pronounced band of reflections in the lower crust.
Below the Moho is a zone free of reflections or with only short, sporadic and
weak reflections. No reflection from the sub-Moho range is expected. To get
sub-Moho reflections, greater charges and geophones with lower natural

frequency (4.5 Hz) are necessary, judging from the experience of POSGAY et al. [1981] and POSGAY et al.[1986].

In view of the above, the band of reflections dipping slightly west and with a traveltime of 9.97 s in the east of the profile (Fig. 3) is obviously the Moho reflection. The Moho reflection shows a reflection configuration nearly parallel to the reflections above it; it is characterized by a strong trough between the principal adjacent, nearly equally strong peaks. Below this zone there are only weak reflection elements with maximum horizontal extensions of some 100 m and some sporadic arrivals with questionable reflection character.

No final conclusion on the nature of the Moho in the Rechnitz area can be drawn from the sparse data available. The character and continuity of reflections support the concept accepted by many geophysicists of a laminated lower crust near the Moho. Several reasons for this characteristic Moho reflectivity are possible [MEISSNER and KUSZNIR 1987; WEVER et al. 1987]. A development of magmatic layers by intrusions from the mantle might be a plausible explanation. This is supported by the regional high position of the mantle in this area. POSGAY [1980] points out that the Moho changed its position during geological times. Therefore one could interpret the sub-Moho reflections as an indication of the remnants of an older Moho.

5.3. Comparison with other investigations in the East Styrian Tertiary basin and in the Pannonian area

Using two vertically crossing spreads a deep reflection seismic measurement was performed in the year 1981 at Nikitsch, about 30 km N of the presently investigated area [MAURITSCH et al. 1986]. A reflection band at 9.5 s reflection time was recognized as the deepest coherent reflection event over the full spread length of 1.46 km. Additional reflections from the lower crust were observed in the depth range of 18 – 19.5 km. The work of POSGAY [1980] and POSGAY et al. [1986] is a further basis for comparison studies. In particular, the investigations in western Hungary were useful. The NW–SE running standard profile MK-1 ends near Deutsch-Kreutz and can therefore be compared with the Nikitsch data. The Moho reflection is identified at 7.9 – 8.5 s reflection time, where a transition zone is assumed. The Moho reflection is not continuous and indicates disturbances. Furthermore a good correlation should exist between the Moho depth and the heat flow data. The

conclusion is that there was a partial melting of rocks at the Moho. The extrapolation of the depth lines leads to Moho depths of 27 km in the area south of Rechnitz. On the Hungarian side there is obviously a regional high of the Moho with depth values of 26 km. There might be a closed high in the Szombathely-Köszeg area of Hungary extending to Austria. The Moho's depth value of 27 km near Nikitsch offers a good fit to this hypothesis. Further comparison studies can be done with gravity data based on a fairly dense net of sample points to establish rock densities. ALBU et al. [1989] presented a structure map of the Moho in Austria and Hungary showing a depth of about 31 km in the area south of Rechnitz. The map also shows the postulated high of Köszeg although the top is shifted laterally and 3 or 4 km deeper compared to the results of this deep seismic reflection survey.

6. Acknowledgements

REFERENCES

MAURITSCH H. J., SCHMÖLLER R., WALACH G., WEBER F. 1986: Geophysical investigations of crustal structures in the Eastern Alps and the Alpine-Pannonian Transition zone. *In*: Results of the Austrian Investigations in the Int. Lithosphere Prog. from 1981 to 1985. Arb.a.d.Zentr.anst.Met.u.Geodyn. **67**, Publ.Nr. 306, pp. 27–52

MEISSNER R., KUSZNIR N. 1987: Crustal viscosity and the reflectivity of the lower crust. Annales Geophysicae, **5**, 4, pp. 365–374

PALMER D. 1980: Generalized reciprocal method of seismic refraction interpretation. Soc. Expl. Geophys., Tulsa, 101 p

POSGAY K. 1980: Earth's crust and mantle studies by the seismic reflection method in Hungary. 6th EGS meeting, Vienna, EGS Newsletters No. **16**

POSGAY K., ALBU I., PETROVICS I. and RÁNER G. 1981: Character of the Earth's Crust and Upper Mantle on the Basis of Seismic Reflection Measurements in Hungary. Earth evolution sciences 3–4, pp. 272–279

POSGAY K., ALBU I., RÁNER G. and VARGA G. 1986: Characteristics of the reflecting layers in the Earth's crust and upper mantle in Hungary. *In*: Reflection Seismology: A Global perspective. Geodynamics Series (Eds.: BARAZANGI M. and BROWN L.) **13**, Publ. No. 0112 of the Int.Lithosphere Prog.Washington D.C.

POSGAY K., ALBU I., MAYEROVA M., NAKLÁDALOVÁ Z., IBRMAJER I., BLIŽKOVSKÝ M., ARIC K., GUTDEUTSCH R.: 1989: Contour map of the Mohorovičić discontinuity beneath central Europe. Geophys. Trans. **36**, 1-2, pp. 7–13

POSGAY K., HEGEDŰS E., TIMÁR Z. 1990: The identification of mantle reflections below Hungary from deep seismic profiling. Tectonophysics **173**, pp. 379–385

WEBER F., JANSCHEK H., MAURITSCH H., OBERLADSTÄTTER M., SCHMÖLLER R., WALACH G. 1981: Activities of the Institute of Geophysics of the Mining University Leoben in the International Geodynamics Project. *In*: Results of the Austrian Investigations in the International Geodynamic Project 1972-1979, BMWF, Sektion Forschung, Vienna, pp. 35–57

WEVER Th., TRAPPE H., MEISSNER R. 1987: Possible relations between crustal reflectivity, heat flow, and viscosity of the continents. Annales Geophysicae, **5**, 3, pp. 255–266

YAN Q. Z., MECHIE J. 1989: A final structural section through the crust and lower lithosphere along the axial region of the Alps. Geoph. J. pp. 465–188

Mélyszeizmikus mérések eredményei Rohonctól délre (Burgenland) Ausztriában

Franz WEBER, Rupert SCHMÖLLER, Rudolf K. FRUHWIRTH

1992-ben mélyszeizmikus reflexiós méréseket hajtottak végre Rohonctól délre Burgenlandban. Harminc kg-os tölteteket robbantottak fel egymástól 700 m távolságban lévő 6 robbantólyukban egy 4800 m-es 96 csatornás rögzített terítés mentén. Ez az eljárás 2-3-szoros fedésnek felel meg. A legjobb jelkiemelést a sávkorlátozott dekonvolúció adta. Kis mélységtartományra a dinamikus korrekció refrakció analizis eredménye; 6000 m/s-os összegzési sebességet becsültek a mélyebb szelvényszakaszokra.

A tercier aljzata alatt kb. 280 m-től 5 s-os kétszeres vertikális menetidőig egy reflexió hiányos zóna van. E zóna alatt 7 s-ig a reflexiók elszórtak, míg a 7-8 s-os tartományban a jól felismerhető reflexiók egy átmeneti zónát jeleznek. A Moho mint legmélyebb reflexió 10 s-nál jelenik meg. Mind a Moho, mind a felette lévő reflexiók enyhén Ny-i dőlésűek.

Modelling of S-waves from an area covered with flood-basalt off Lofoten, N. Norway

Rolf MJELDE[*], Benedicte MYHRE[*], Markvard A. SELLEVOLL[*], Hideki
SHIMAMURA[**], Takaya IWASAKI[**],
Toshihiko KANAZAWA[***]

A seismic V_p/V_s model for an area covered with flood-basalt off the north Norwegian coast, has been developed based on previous results from P-wave modelling of data from an Ocean Bottom Seismograph (OBS) study. The horizontal components of the OBS-data reveal abundant presence of S-wave phases, which have been modelled by 2-D ray-tracing. The mean V_p/V_s-ratio for the sediments above the basalt is estimated to be 2.0–2.1. This relatively high value probably indicates a low degree of consolidation in the sediments, and possibly also that the sediments are dominated by shale. The mean V_p/V_s-ratio for the entire crust is estimated to be 1.9 beneath a profile on the seaward side of the Vøring Escarpment (VE), suggesting gabbroic lithology and oceanic origin of the crust. On the landward side of the VE, the modelling suggests a significantly lower V_p/V_s-ratio for the crystalline crust: 1.7–1.75, which indicates granitic/granodioritic lithology and continental origin of the crust.

Keywords: **continental margin, V_p/V_s-ratio, three-component OBSs, northern Norway**

*   Institute of Solid Earth Physics, Allégt. 41, University of Bergen, 5007 Bergen, Norway
** Laboratory for Ocean Bottom Seismology, Geophysical Institute, Hokkaido University, Sapporo 060, Japan
***Earthquake Research Institute, University of Tokyo, Tokyo 113, Japan

1. Introduction

Seismic studies of the Earth's crust have traditionally been restricted to the use of longitudinal P-waves. Such studies generally provide good images of the crustal structures, particularly when multichannel reflection data are combined with wide-angle data [e.g. MJELDE et al. 1993]. These structural images have contributed significantly to our present understanding of the geodynamic forces responsible for the formation and evolution of the crust and upper mantle.

The models obtained from P-wave studies are, however, hampered by some limitations; the most important of these arises from the fact that different lithologies can generally not be distinguished by use of P-waves alone. Such aspects can often be elucidated in more detail by the integrated use of P-waves and (transversal) S-waves [e.g. NEIDELL 1985]. Significant amounts of S-wave energy are frequently generated in surveys employing controlled source seismology, even in marine surveys where P-waves are converted to S-waves at the sea-floor or deeper interfaces [MJELDE 1992]. Efficient use of S-waves in marine surveys requires three-component receivers (geophones) on the sea-floor, since the particle motion of crustal S-arrivals is generally close to the horizontal at the sea-floor.

In order to study the crustal structures of the volcanic margin off Lofoten, N. Norway, and to investigate to what extent S-waves could contribute to an improved understanding of the geological evolution of the area, a large seismic experiment using three-component Ocean Bottom Seismographs (OBSs) was performed in 1988. Strong S-waves were detected on the continental shelf that provided important new insights on lithology and liquid-filled cracks [MJELDE 1992, MJELDE, SELLEVOLL 1993a,b, MJELDE et al. 1995a]. The present paper describes the modelling of the S-waves recorded in the area covered with flood-basalt across the continent–ocean transition and almost to the shelf edge.

2. Geological framework

In the late Silurian to early Devonian the region (*Fig. 1*) was dominated by the compression between Laurentia (Greenland) and Baltica (Norway), resulting in the formation of the Caledonides [BUKOVICS et al. 1984, BØEN
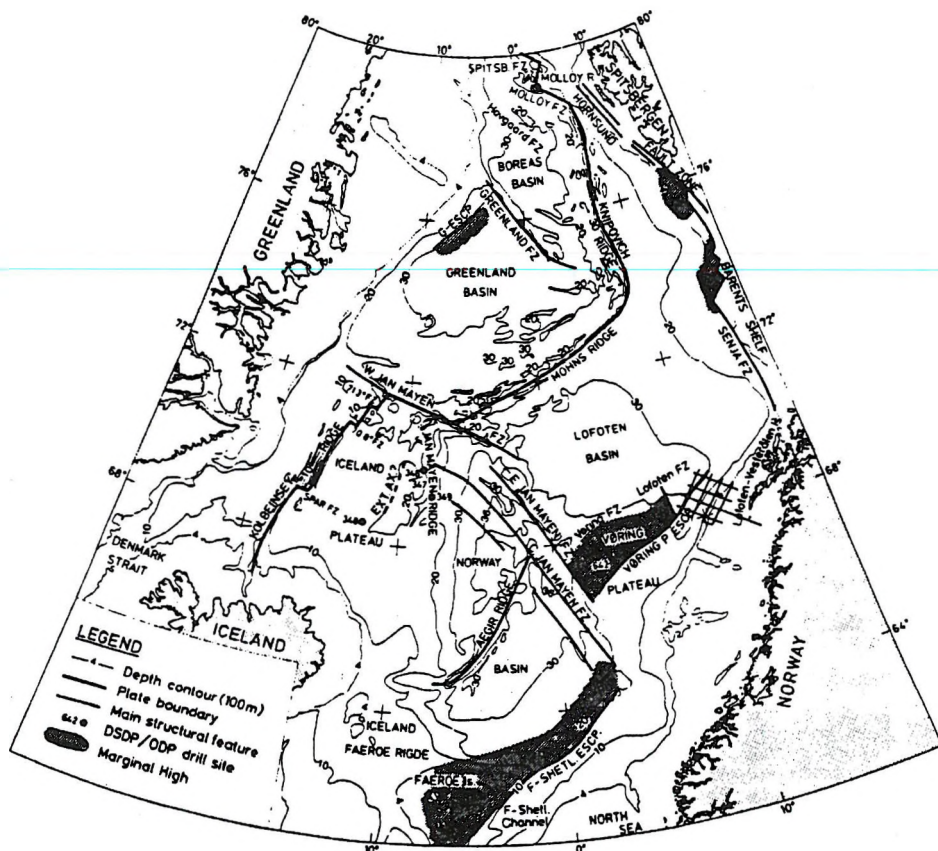
Fig. 1. Regional physiography and structural features of the ocean basins and continental margins in the Norwegian-Greenland Sea. Also indicated ODP drill site 642 and the investigated area off Lofoten. Modified from ELDHOLM et al. [1990]

1. ábra. A Norvég tenger és a Grönlandi tenger kontinentális peremének és óceáni medencéinek szerkezeti jellegzetességei és regionális földrajza. A 642 ODP fúrás helyét és a vizsgált Lofoten peremet is jelöli. ELDHOLM et al. [1990] nyomán

et al. 1984, GAGE, DORE 1986]. In post-Caledonian times, the region has been dominated by extensional tectonics. The most significant tectonic episode was the Late Jurassic—Early Cretaceous extension, which led to major faulting activity [MOKHTARI 1991]. Sedimentary sequences up to 5 km thick of Cretaceous age are preserved on the Lofoten shelf.

The Early Cenozoic extension axis shifted westward with respect to the Jurassic—Cretaceous episode. The Cenozoic extension lasted for about 10 Ma and caused continental separation in the earliest Eocene [SKOGSEID,

ELDHOLM 1989, MJELDE et al. 1995b]. The rifting was associated with high magmatic activity, causing accretion of thick magmatic bodies at the base of the crust, emplacement of sills in the adjacent continental crust and Creta-ceous sediments, as well as extrusive volcanism forming large wedges of flood basalt partially observed as Seaward Dipping Reflectors (SDRs) [ELDHOLM et al. 1989, MJELDE et al. 1995b]. At the Lofoten Margin the 1–2.5 km thick basalt is inferred to extend almost to the shelf edge up to 85 km landward from the marginal high escarpment (Vøring Escarpment - VE) [MJELDE et al. 1992]. The margin from Lofoten to Møre (Fig. 1) is referred to as a volcanic continental margin due to the important presence of magmatic rocks, which may be related to rifting and break up in the vicinity of the Iceland hotspot [e.g. ELDHOLM et al. 1989].

3. Data acquisition, processing and modelling

The experiment was performed in 1988 in cooperation between the Institute of Solid Earth Physics, University of Bergen, Norway, the Labora-tory for Ocean Bottom Seismology, Hokkaido University, Japan, and the Earthquake Research Institute, University of Tokyo, Japan. The scientific programme comprised seismic reflection, seismic refraction, and gravimetric measurements performed simultaneously. *Fig. 2* shows the most important geological features in the investigated area with the position of the seismic reflection/refraction lines and the 19 OBS positions indicated. Acquisition of the OBS data was performed using the University of Bergen's R/V Håkon Mosby. Four Bolt 1500 C air-guns with a total volume of 78.7 1 were used as source. The source was operated at a depth of 21 m, and the shotpoint interval was 240 m (2 min).

The analogue OBS instruments used were developed and built by the geophysical institutes at Hokkaido and Tokyo universities [ASADA et al. 1979, KANAZAWA 1986, SHIMAMURA 1988]. The instruments have three orthogonal components (4.5 Hz gimbal mounted geophones): one vertical and two horizontal. The instruments can record continuously for 14 days within the frequency range from 1 to 30 Hz (-3 dB). For more details concerning the experiment, the reader is referred to SELLEVOLL et al. [1988].

Conversion of the OBS data from analogue to digital form was performed at the universities of Hokkaido and Tokyo. Subsequent processing implies band-pass filtering and deconvolution. The main seismic signal is constrained
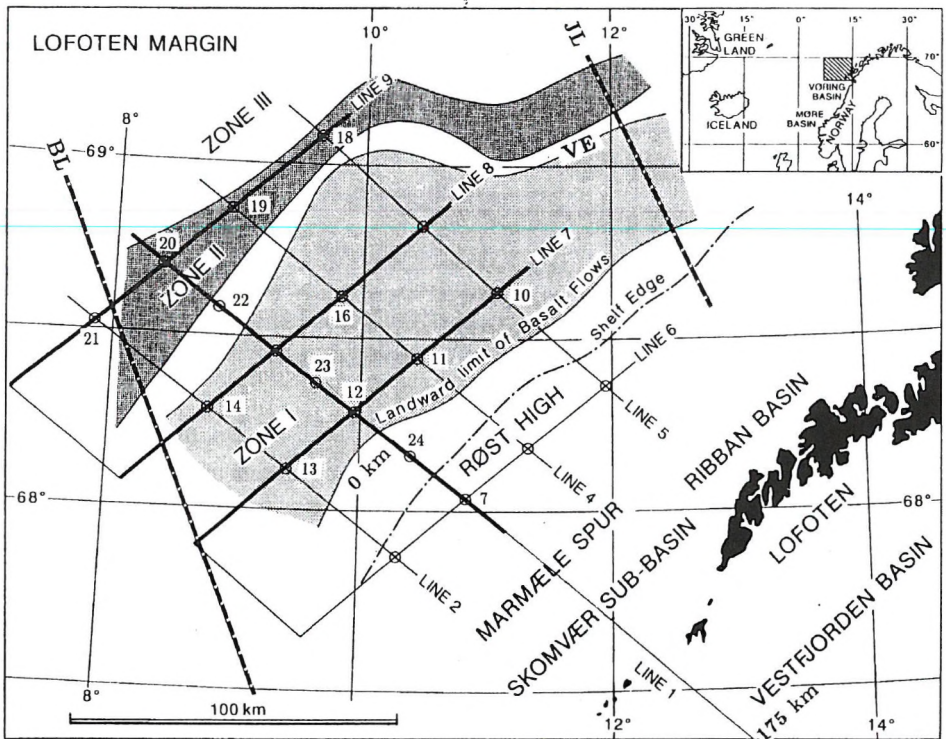
Fig. 2. Main structural elements off Lofoten with position of OBSs (open circles) and seismic reflection and refraction profiles shot during the 1988 survey indicated. The profiles described in this paper are indicated as bold lines. VE=the Vøring escarpment, BL=Bivrost lineament, JL=Jennegga lineament, ZONE I=Early Eocene flood basalt, ZONE II=Seaward dipping reflectors, ZONE III=Oceanic crust. The position of the Vøring and Møre basins are indicated in the upper right corner. Modified from SELLEVOLL et al. [1988]

2. ábra. A Lofoten perem fő szerkezeti jellegzetességei, az OBS-ek helyzetének (üres körök), valamint az 1988 évi szeizmikus reflexiós és refrakciós vonalak feltüntetésével. A dolgozatban tárgyalt szeizmikus vonalakat vastag vonallal jelöltük. VE=a Vøring hasadék, BL=Bivrost lineamens, JL=Jennegga lineamens, ZONE I=korai eocén bazaltfolyás, ZONE II=tenger irányába dőlő reflektáló felület, ZONE III=óceáni kéreg. A Vøring és a Møre medencék helyzete a jobb felső sarokban látható. SELLEVOLL et al. [1988] nyomán

to the 6–13 Hz interval, and the use of a spiking deconvolution operator with 1500 ms length facilitates the interpretation of the *S*-waves. Interpretation of the data is done on displays with travel-times reduced by 8 km/s (for a detailed discussion of the processing, see MJELDE 1992, MYHRE 1995) .

The interval from the seafloor to the top of the basalt is mapped with high resolution from the multichannel reflection data. No deeper interfaces can be inferred with certainty from the reflection data in the area covered with basalt, and thus in this area the seismic crustal model must be based on the OBS-data alone [MJELDE et al. 1992]. These OBS data were modelled by means of 2-D kinematic (travel-time) ray-tracing. The uncertainty in the velocities is estimated to be ±0.1 km/s (both for *P*- and *S*-waves), and the uncertainty in the V_p/V_s -ratio is estimated to be ±0.05.

4. *P*-wave model

The *P*-wave models derived from the vertical components of the OBSs are presented in *Figs. 3, 4,* and discussed in detail by MJELDE et al. [1992]. On the seaward side of the escarpment (Fig. 4), basalts that may be related to the initial phase of sea-floor spreading are observed as two layers with *P*-wave velocities of 4.0 and 5.0 km/s, respectively. The SDRs are constrained to these layers. The vertical velocity increase is probably attributable to increasing alteration of the basalt and formation of secondary minerals filling the pores [FLOVENZ 1980].

The crust below the flood-basalt has been divided into an upper 6.7 km/s layer and a lower crustal 7.3 km/s layer. Detailed modelling of the OBS-data suggests that the velocities in these layers gradually decrease landwards to velocities in the range of 6.0 to 6.8 km/s (upper and lower crust respectively) close to the escarpment [MJELDE et al. 1995b]. This lateral velocity variation is interpreted as being caused by a gradual landward decrease in the amount of high-velocity 'oceanic' intrusions into stretched continental crust *(Fig. 5)*.

On the landward side of the escarpment (Fig. 3), the *P*-wave velocity in the two basaltic layers is estimated to be 4.4 and 5.2 km/s, respectively. Above the crystalline basement a low-velocity layer interpreted as a sequence of pre-opening sedimentary layers, is observed. The velocities of the crystalline portion of the crust are found to be similar to those observed under the continental shelf (6.0 to 6.8 km/s; [MJELDE et al. 1992]), which implies that the crust east of the VE is of continental origin.
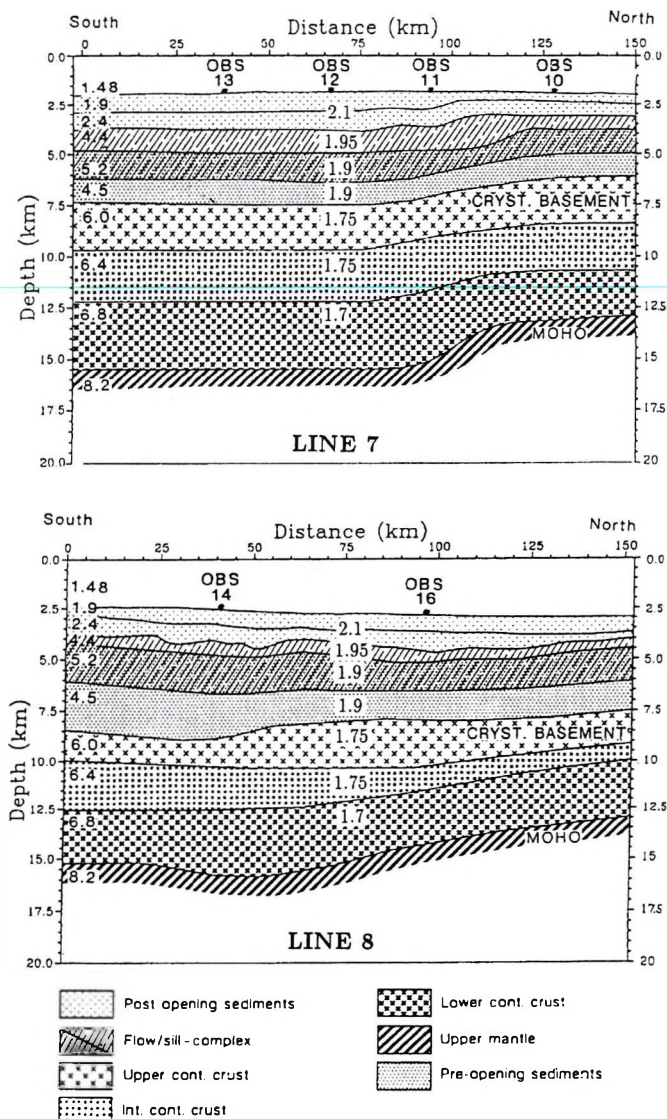
Fig. 3. Velocity models for profiles 7 and 8, landward of the VE. The *P*-wave velocity models are discussed in detail by MJELDE et al. [1992]. The *P*-wave velocities are shown in km/s at the left hand-side of the models, and the V_p/V_s-ratios from this study are indicated in the central part of the models

3. ábra. A 7-es és 8-as szelvények sebesség modellje a VE szárazföld felé eső részére. A *P*-hullám modellt MJELDE et al. [1992] részletesen tárgyalta. A *P*-hullám sebességek a modellek bal oldalán km/s-ban, míg a tanulmányban előforduló V_p/V_s hányadosok a modellek középtáján találhatók
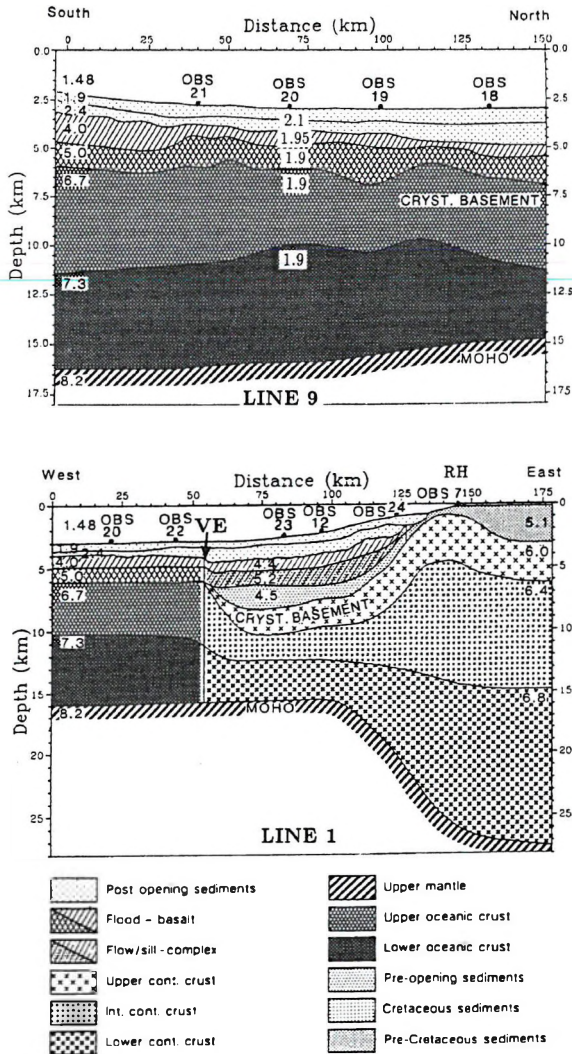
Fig. 4. Velocity models for profiles 9 (on SDRs) and 1 (dip-profile). *P*-wave velocity models are discussed in detail by MJELDE et al. [1992]. The *P*-wave velocities are shown in km/s at the left hand-side of the models as well as in the central part of the model of profile 1. The V_p/V_s-ratios from this study are indicated in the central part of the model of profile 9. The V_p/V_s -ratios along profile 1 are the same as for corresponding layers in the strike-profiles (Fig. 3), with the exception of the sedimentary layers above the basalt where the V_p/V_s-ratio is 2.0

4. ábra. Sebesség modellek a 9 (SDR) és 1 (dőlés irányú) szelvényekre. A *P*-hullám modelleket részleteiben tárgyalja MJELDE et al. [1992]. A *P*-hullám sebességek az ábra bal oldalán, valamint az 1. szelvény középső részén láthatók. A tanulmányban szereplő V_p/V_s hányadosok a 9. szelvény középső részén találhatóak. Az 1. vonal mentén a V_p/V_s hányadosok ugyanazok, mint a csapásirányú vonalak megfelelő rétegére számítottak (3. ábra) azzal a különbséggel, hogy a bazalt feletti üledékes rétegre a V_p/V_s hányadosok értéke 2,0

DISTANCE (km)
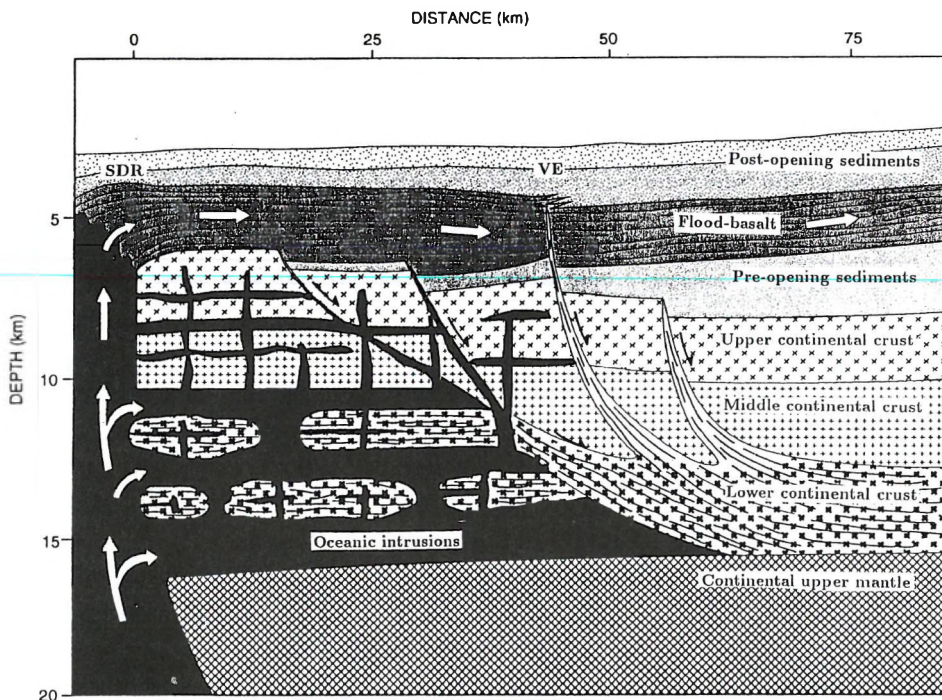
Fig. 5. Geological model of the continent/ocean transition, from MJELDE et al. [1995b]. The arrows indicate flow-lines of magmatic material emplaced during the late rifting/early spreading stage. The interfaces observed in the OBS-data are: the top and bottom of the basalt, the top of the crystalline crust, the top of the lower crust seaward of the VE, and the Moho. The remaining details in the geological model are included to explain the observed lateral variations in seismic velocity

5. ábra. A kontinens/óceán átmenet geológiai modellje MJELDE et al. [1995b] szerint. A nyilak a magmatikus anyag folyásvonalait jelölik, amelyek a késői felszakadás/korai elmozduláskor alakultak ki. Az OBS adatokban észlelt határfelületek a bazalt alja és teteje, a kristályos kéreg teteje, a VE tengerfelőli részén az alsókéreg teteje, és a Moho. A geológiai modell egyéb részletei a szeizmikus sebességben észlelt laterális változásokat indokolják

5. V_p/V_s model and discussion

The *P*-wave models, as presented above, were used as a basis for modelling the *S*-waves, i.e. the interfaces are kept constant in the modelling, and the two unknown parameters are thus the *P*-to-*S* conversion depth and the *S*-wave velocity in each layer.

The *S*-waves were modelled from the horizontal components by use of kinematic ray-tracing. *Fig. 6* demonstrates the differences between the vertical and one horizontal component for a typical OBS landward of VE.

On the vertical component, a strong crustal arrival (head wave; P_g) is observed to about 60 km offset. An even stronger arrival with the same apparent velocity is observed about 2 sec later. This later arrival can be traced to the maximum offset (100 km). On the horizontal component, the P_g-phase is very weak, confirming that this arrival is a near vertically polarized P-wave. The later arrival is very strong also on the horizontal component, proving that this phase corresponds to an S-wave. The high apparent velocity of the arrival shows that the wave has propagated within the crust (near horizontally) as a P-wave that has been converted to an S-wave on the way up.

More examples of horizontal component data, as well as some seismogram sections with calculated travel-time curves superimposed, are shown in *Figs. 6–12*. Only one of the horizontal components is presented since the two components are qualitatively very similar [MJELDE 1992]. The code for the different arrivals is indicated in the various figures: the $P\overline{P}_{7.3}P_{4.0}S$ -phase in Fig. 8, for instance, represents a wave that has propagated downwards to the 7.3 km/s interface as a P-wave, along this interface as a P-wave, upwards to the 4.0 km/s interface as a P-wave, and as an S-wave from this interface to the sea-floor. From Figs. 6–12 it is clear that all major S-wave phases can be modelled either as waves that have propagated near-horizontally as P-waves and P-to-S converted on the way up, or as P-to-S reflections. Attempts have been made to model the arrivals with low apparent velocities as near-horizontally propagating S-waves (S_g-phase), but these attempts have not provided consistent results.

Fig. 6. Comparison between the vertical (above) and one horizontal component (below) of OBS 11, profile 4. On the horizontal component, the P_g-phase is very weak, confirming that this arrival is a near vertically polarized P-wave. The later arrival (*PPS*) is very strong also on the horizontal component, proving that this phase corresponds to an S-wave. The high apparent velocity of the arrival shows that the wave has propagated within the crust (near horizontally) as a P -wave that has been converted to an S-wave on the way up

6. ábra. Az OBS 11 (4. szelvény) vertikális (felül) és egy horizontális (alul) komponensének összehasonlítása. A horizontális komponensben a P_g fázis nagyon gyenge, igazolva azt, hogy ez a beérkezés közel vertikális polarizáltságú P-hullám. A későbbi beérkezés (PPS) horizontális komponense nagyon erős, igazolva, hogy ez a fázis az S-hullámnak felel meg. A beérkezés nagy látszólagos sebessége abból következik, hogy a kéregben közel vízszintesen terjedő P-hullám a felfelé haladó részen S-hullámmá konvertálódott
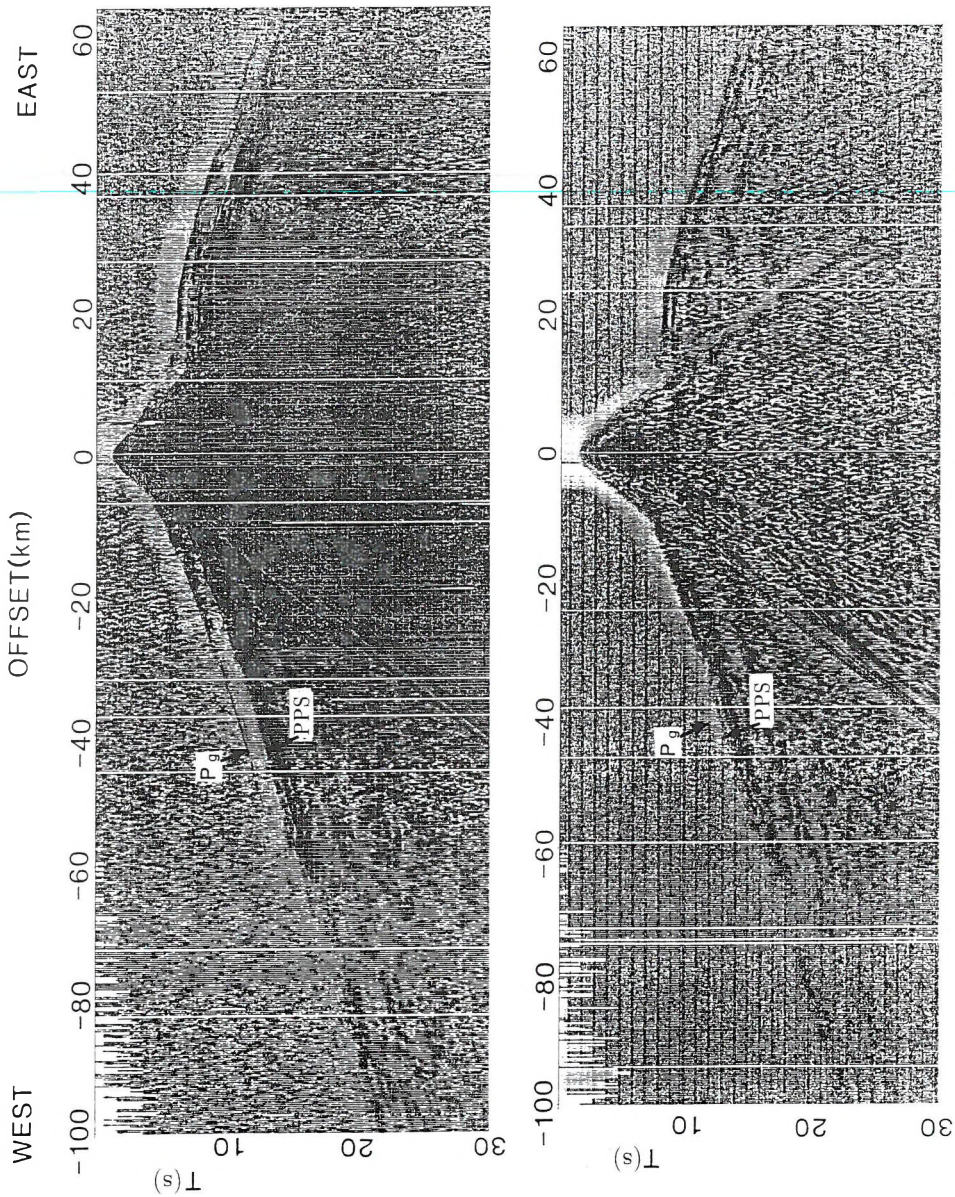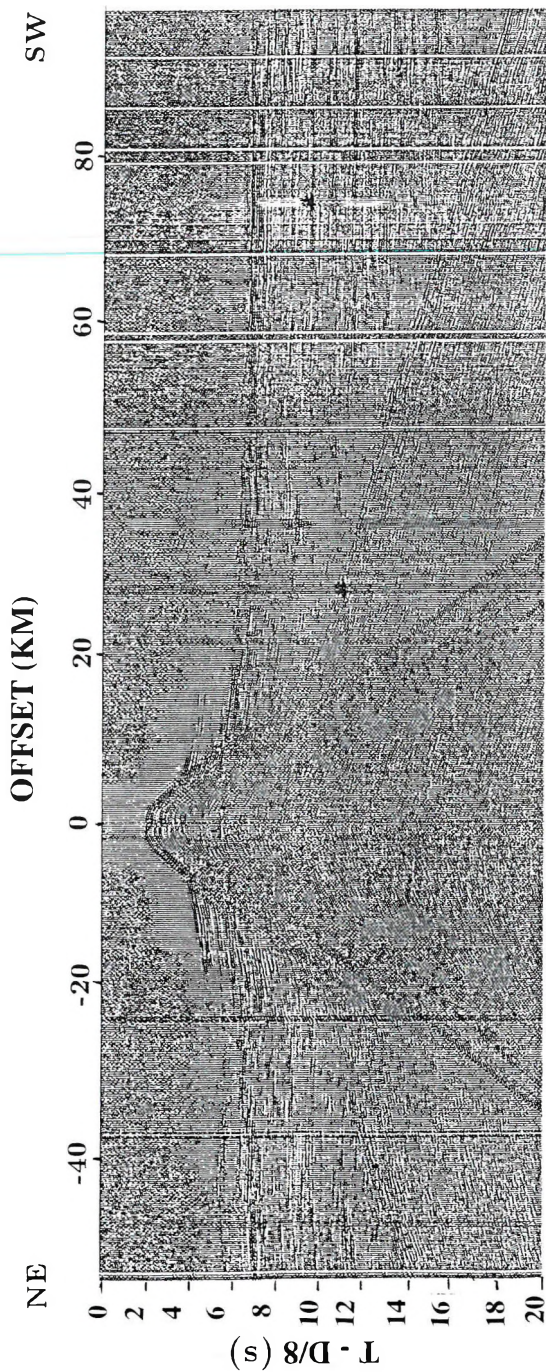
Fig. 7. OBS 19 profile 9 horizontal (high-gain) component (reducing velocity 8.0 km/s). 6–13 Hz band-pass filtered and deconvolved

7. ábra. Az OBF 19 9-es szelvény horizontális (nagy erősítésű) komponense (a redukáló sebesség 8,0 km/s). Sávszűrt (6–13 Hz) és dekonvolvált szelvény
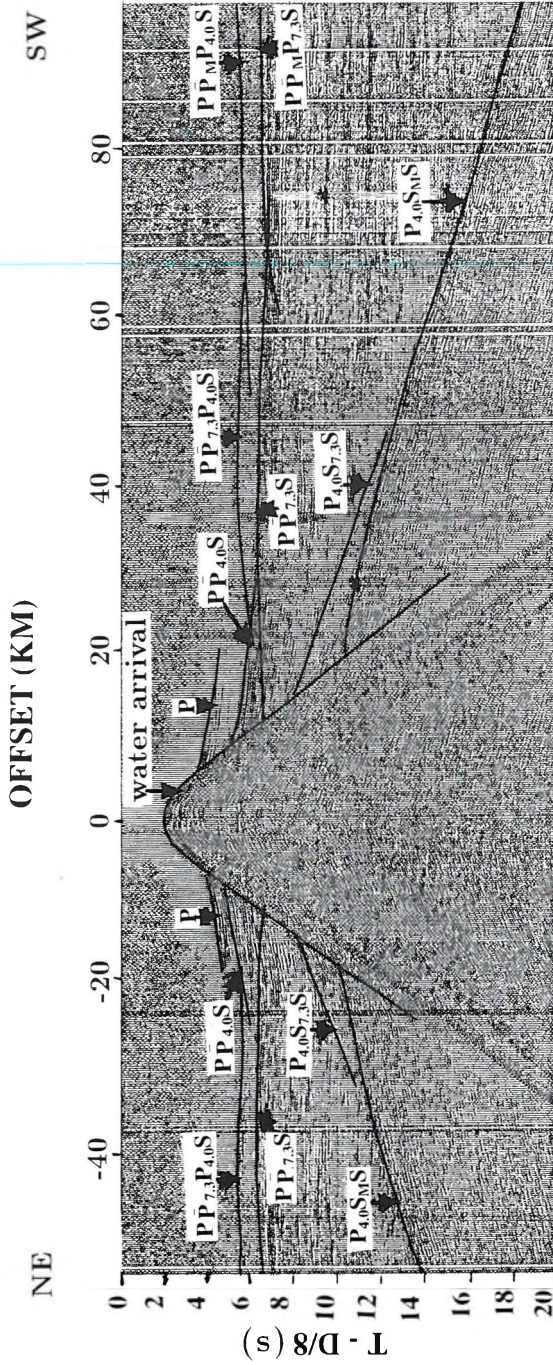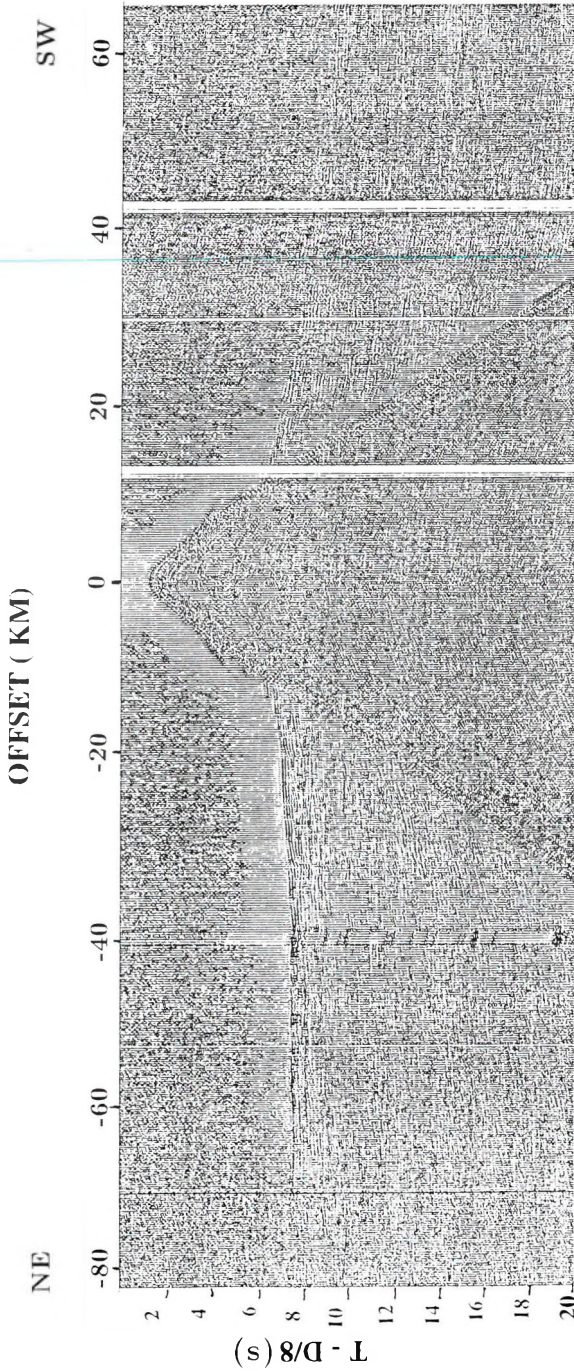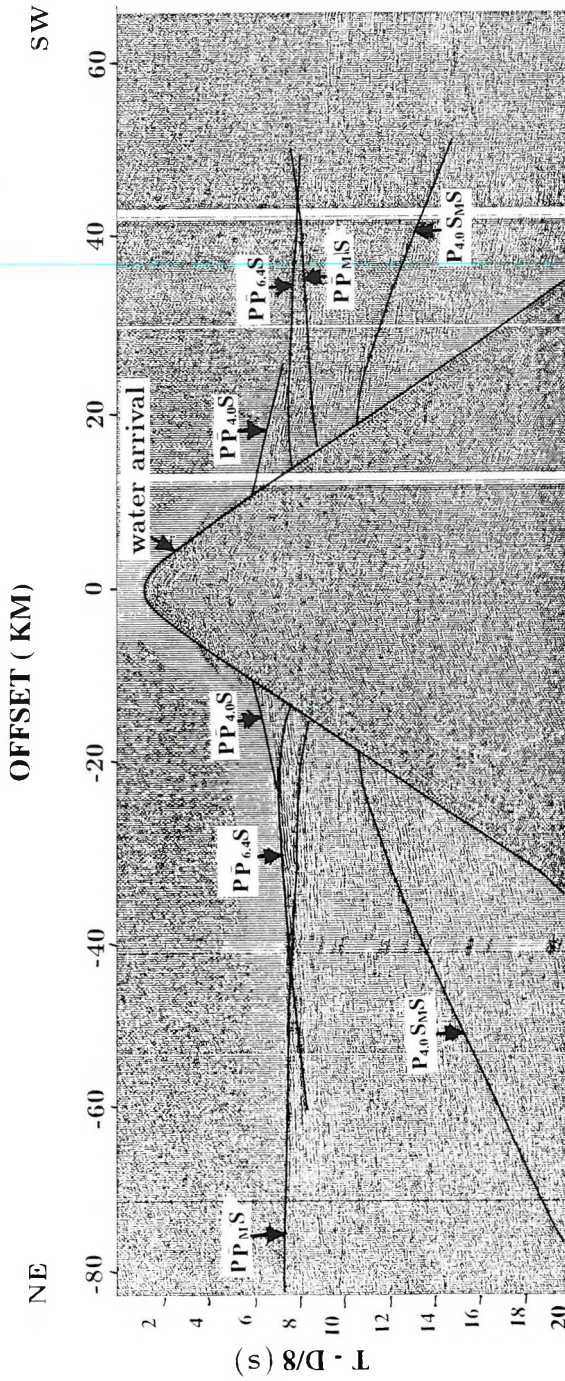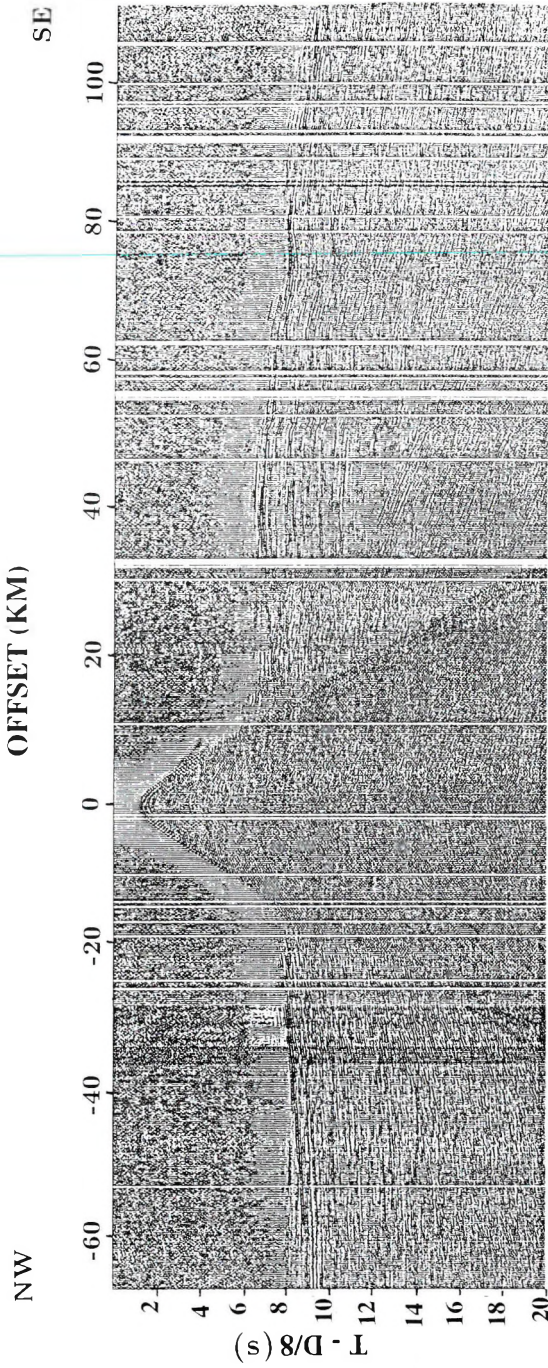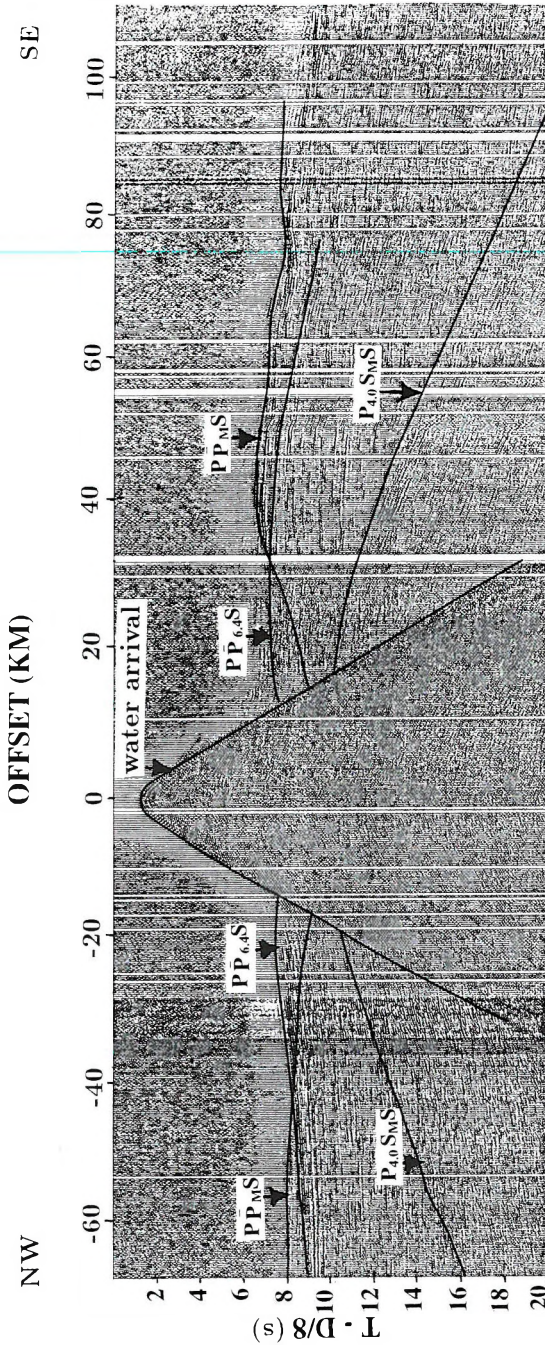
Fig. 8. OBS 19 profile 9 horizontal component with S-wave travel-time curves from the model in Fig. 4 (calculated from 2-D ray-tracing). See text for explanation of the ray-code.

8. ábra. Az OBS 19 9-es szelvény horizontális komponense a 4. ábra modelljéből (2-D sugárkövetéssel) számított S-hullám menetidő görbékkel. A sugárkódok magyarázata a szövegben

Fig. 9. OBS 12 profile 7 horizontal (high-gain) component (reducing velocity 8.0 km/s). 6–13 Hz band-pass filtered and deconvolved
9. ábra. Az OBS12 7-es szelvény horizontális (nagy erősítésű) komponense (a redukáló sebesség 8,0 km/s). Sávszűrt (6–13 Hz) és dekonvolvált szelvény

Fig. 10. OBS 12 profile 7 horizontal component with S-wave travel-time curves from the model in Fig. 3 (calculated from 2-D ray-tracing). See text for explanation of the ray-code

10. ábra. Az OBS12 7-es szelvény horizontális komponense a 3. ábra modelljéből (2-D sugárkövetéssel) számított S-hullám menetidőgörbékkel. A sugárkódok magyarázata a szövegben

Fig. 11. OBS 12 profile 1 horizontal (high-gain) component (reducing velocity 8.0 km/s). 6–13 Hz band-pass filtered and deconvolved

11. ábra. Az OBS12 1-es szelvény horizontális (nagy erősítésű) komponense (a redukáló sebesség 8,0 km/s). Sávszűrt (6–13 Hz) és dekonvolvált szelvény

Fig. 12. OBS 12 profile 1 horizontal component with S-wave travel-time curves from the model in Fig. 4. (calculated from 2-D ray-tracing). See text for explanation of the ray-code

12. ábra. Az OBS12 1-es szelvény horizontális komponense a 4. ábra modelljéből (2-D sugárkövetéssel) számított S-hullám menetidőgörbékkel. A sugárkódok magyarázata a szövegben

The modelling suggests that the P-to-S conversions occur at the top of the basalt for all profiles. In addition, conversions are modelled to occur at the top of the lower crustal 7.3 km/s layer on the seaward side of the VE, and at the top of the middle crustal 6.4 km/s layer on the landward side of the VE. P-to-S conversions at the top of the basalt seem very likely in view of the very strong impedance contrast at this interface. Such conversions have also been observed by KODAIRA et al. [1995] in OBS-data immediately seawards of the present study. The apparent lack of P-to-S conversions at the top of the crystalline crust (6.7 and 6.0 km/s) can probably be explained by the very short offset-range; these arrivals can be expected to be observed as first-arrivals. The mean V_p/V_s-ratios can thus be estimated for three intervals, in the sediments above the basalt for all profiles, in the interval from the top of the basalt to the 7.3 km/s interface, as well as within the lower crust seaward of the VE, and in the interval from the top of the basalt to the 6.4 km/s interface, as well as within the middle and lower crustal interval landward of the VE.

The calculated V_p/V_s-ratios for each profile are indicated in the models in Figs. 3, 4. The mean V_p/V_s-ratio for the sediments is estimated as 2.1 for the three strike profiles 7, 8 and 9, and as 2.0 for the perpendicular profile 1. These values are similar to values obtained for sediments of similar age (Eocene to the present) from OBS-data immediately to the south of the study area [DIGRANES et al. 1995], and to values obtained for the shallow Cretaceous sediments on the Lofoten continental shelf [MJELDE 1992]. These relatively high values may be related to a low degree of consolidation of the sediments, and possibly also to abundant presence of shale.

Along profile 9, situated on the SDRs, the mean V_p/V_s-ratio for the entire crust is estimated to be 1.9, with no significant variations between different layers within the crust (Fig. 4). The V_p/V_s-ratio in the thin uppermost basaltic layer is set to 1.95 since it must be expected that the presence of microcracks in this layer will decrease its shear stiffness. This difference cannot be resolved from the data, however, and geological interpretations must be based on the calculated mean value of 1.9 for the entire crystalline crust. From the modelled P-wave velocities, MJELDE et al. [1992] concluded that the crust along profile 9 was of oceanic origin. This conclusion is strongly supported by the S-wave model since V_p/V_s-ratios of 1.9 for crustal rocks clearly fall within the range of gabbro/amphibolite [e.g HOLBROOK et al. 1992]. The same conclusion was drawn by KODAIRA et al. [1995] for the area immediately

seaward of the present study area, although their estimated V_p/V_s-ratio was somewhat lower: 1.8.

As described above, detailed modelling of the P-waves suggests that the crustal velocities decrease from 'oceanic' beneath profile 9, to 'continental' beneath the VE (Fig. 5). Unfortunately, the resolution of the S-waves is not high enough to constrain this model further.

On the landward side of the VE, the modelling suggests a significantly lower V_p/V_s-ratio for the crystalline crust (Fig. 3). As described above, only the mean V_p/V_s-ratio from the top of the basalt to the top of the middle crust can be estimated. In the presented models we have assumed that the V_p/V_s-ratio of the basalts is similar to what is inferred on the seaward side of the VE. The V_p/V_s-ratio of the upper crystalline crust is assumed to be 1.75, since the V_p/V_s-ratio of the middle and lower crust is calculated to be 1.7–1.75. A higher V_p/V_s-ratio than 1.75 in the upper crust would suggest a more mafic upper crust than that observed in the lower crust, which is geologically very unlikely, and not in accord with the observations from the continental shelf [MJELDE 1992]. These assumptions lead to a V_p/V_s-ratio in the pre-opening sediments (beneath the basalt) of 1.9, which suggests that the sediments are shaly and well consolidated. The P-wave modelling shows, however, that the P-wave velocity in the basalt varies laterally, and it is thus possible that the V_p/V_s-ratio in the sediments might change laterally as well. A higher V_p/V_s-ratio in the basalt would imply a lower ratio in the pre-opening sediments, which could be interpreted in terms of a higher sand/shale ratio, whereas a lower V_p/V_s-ratio in the basalt would imply even more shaly sediments.

As described above, the V_p/V_s-ratio of the middle and lower crust is calculated to be 1.7–1.75. The modelling suggests a slightly lower V_p/V_s-ratio in the lower crust than in the middle crust, but it must be underlined that these differences are at the limit of the resolution in the modelling, and should thus not be interpreted in geological terms. The low mean value indicates that the crystalline crust landward of the VE is of continental origin since the calculated V_p/V_s-ratio suggests abundant presence of felsic rocks such as granite, granodiorite or felsic amphibolite facies gneiss [HOLBROOK et al. 1992]. The modelling of the S-waves thus confirms the main results derived from the P-waves [MJELDE et al. 1992], and it is also in accord with the S-wave model obtained on the continental shelf [MJELDE 1992].

An interesting observation made during the modelling of the S-waves from OBSs located on the continental shelf was the presence of S-wave

anisotropy. The *S*-wave velocity in the sediments on the shelf was estimated to be about 10 % higher along a dip profile than along a strike profile [MJELDE, SELLEVOLL 1993a]. This anisotropy was explained by a model with vertical microcracks aligned vertically along the direction of maximum compressive stress, corresponding to the strike of the dip-profile. Similar anisotropy in accord with this model might be present in the data described in this paper; the modelling suggests that the *S*-wave velocity in the sediments is about 5 % higher along profile 1 than along the three strike-profiles. It must be underlined, however, that this possible anisotropy is at the limit of the resolution in the modelling.

The same anisotropy as described above for the sediments on the shelf, was also observed in the lower crust beneath the shelf [MJELDE 1992, MJELDE et al. 1995a]. This anisotropy was observed as an angle-of-incidence difference in *S*-wave velocity. Such anisotropy cannot be inferred from the present data. This might indicate that the lower crustal anisotropy is restricted to the continental shelf, or it might be related to the somewhat lower quality of the observed *S*-waves seaward of the shelf. The anisotropy on the shelf could be clearly identified because of the unique observation of an *S*-wave reflection from the Moho ($S_M S$-phase) that could be followed almost continuously from vertical incidence to wide-angles. It was clearly stressed by MJELDE [1992] that without this observation the anisotropy would probably not have been discovered.

6. Conclusions

Based on a previously published *P*-wave model off Lofoten, N. Norway, a corresponding V_p/V_s model has been developed based on 2-D ray-tracing of OBS horizontal components. Three strike-profiles and one dip-profile have been modelled in an area where flood-basalts extruded during the early Eocene opening between Norway and Greenland make the conventional multichannel reflection technique inefficient.

Strong *S*-wave energy is observed on the horizontal components of the OB*S*-data. The modelling shows that all major *S*-wave arrivals can be modelled either as waves that propagated near-horizontally as *P*-waves and *P*-to-*S* converted on the way up, or as *P*-to-*S* reflections. The modelling suggests that the *P*-to-*S* conversions occur at the top of the basalt for all profiles. In addition, conversions are modelled to occur at the top of the lower

crustal 7.3 km/s layer on the seaward side of the VE, and at the top of the middle crustal 6.4 km/s layer on the landward side of the VE.

The mean V_p/V_s-ratio for the sediments above the basalt is estimated to be 2.1 for the three strike profiles, and 2.0 for the perpendicular profile. These relatively high values are probably related to a low degree of consolidation of the sediments, and possibly also to the abundant presence of shale. Along the strike-profile situated above the seaward dipping reflectors on the seaward side of the VE, the mean V_p/V_s-ratio for the entire crust is estimated to be 1.9, with no significant variations between different layers within the crust. This high value clearly indicates that the crust is of oceanic origin beneath this profile. On the landward side of the VE, the modelling suggests a significantly lower V_p/V_s-ratio for the crystalline crust. The calculated ratio of 1.7–1.75 suggests that the crust is of continental origin in this part of the area.

The estimated V_p/V_s-ratio for the sediments above the basalt is about 5 % higher along the dip-profile than along the strike-profiles. This apparent S-wave anisotropy is similar to, although smaller than, the anisotropy discovered on the continental shelf [MJELDE, SELLEVOLL 1993a]. This anisotropy was explained by a model with vertical microcracks aligned vertically along the direction of maximum compressive stress. It must be underlined, however, that the possible anisotropy described in the present paper is at the limit of the resolution in the modelling.

Acknowledgements

REFERENCES

ASADA T., KANAZAWA T., SHIMAMURA H. 1979: A pop-up type ocean bottom seismograph. (in Japanese) Prog. Abstr. Seism. Soc. Japan, **2**, 114

BUKOVICS C., SHAW N. D., CARTIER E. G., ZIEGLER P. A. 1984: Structure and development of the mid-Norway continental margin. *In*: SPENCER A. M. et al. (eds.): Petroleum Geology of the North European Margin, pp. 407–423. London, Graham and Trotman

BØEN F., EGGEN S., VOLLSET J. 1984: Structures and basins of the margin from 62–69°N and their development. *In:* SPENCER, A. M. et al. (eds.): Petroleum Geology of the North European Margin, pp. 3–28. London, Graham and Trotman

DIGRANES P. MJELDE R., KODAIRA S., SHIMAMURA H., KANAZAWA T. SHIOBARA, H., BERG, E. W. 1995: 2-D ray-tracing modelling of shear waves in OBS data from the VØRING Margin, N. Norway. Pure and Applied Geophysics. In press

ELDHOLM O., THIEDE J., TAYLOR E. 1989: Evolution of the Vøring Volcanic Margin. Proc. ODP, Sci. Results, 104, pp. 1033–1065. College Station, TX (Ocean Drilling Program)

ELDHOLM O., SKOGSEID, J., SUNDVOR E., MYHRE, A. M. 1990: Norwegian- Greenland Sea. *In*: The Geology of North America, Vol. L, The Arctic Ocean Region, pp. 351–363. The Geological Society of America

FLOVENZ O. G. 1980: Seismic structure of the Icelandic crust above layer three and the relation between body wave velocity and the alteration of the basaltic crust. Journal of Geophysics, **47**, pp. 211–220

GAGE M. S., DORE A. G. 1986: A regional geological perspective of the Norwegian offshore exploration provinces. *In*: Habitat of Hydrocarbons on the Norwegian Continental Shelf, pp. 21–38, Norwegian Petroleum Society, London, Graham and Trotman

HOLBROOK W. S. MOONEY W. D. CHRISTENSEN N. I. 1992: The seismic velocity structure of the deep continental crust. *In*: FOUNTAIN D. M, ARCULUS R., KAY R.W. (eds): Continental lower crust. Elsevier, Amsterdam

KANAZAWA T. 1986: A seven component, a low power consumption and an acoustic commandable ocean bottom seismograph. (in Japanese). Prog. Abstr. Seism. oc. Japan, 2, 240

KODAIRA S., BELLEBERG M., IWASAKI T., KANAZAWA,T., HIRSCHLEBER H. B., SHIMAMURA H. 1995: V_p/V_s-ratio structure of the Lofoten continental margin, N. Norway, and geological implications. Geophysical Journal International. In press

MJELDE R., SELLEVOLL M. A., SHIMAMURA H., IWASAKI T., KANAZAWA T.1992: A crustal study off Lofoten, N. Norway, by use of Ocean Bottom Seismographs. Tectonophysics, **212**, pp. 269–288

MJELDE R., SELLEVOLL M. A., SHIMAMURA H., IWASAKI T., KANAZAWA T. 1993: Crustal structure under Lofoten, N. Norway, from vertical incidence and wide-angle seismic data. Geophysical Journal International, **114**, pp. 116–126

MJELDE R., SELLEVOLL M. A., SHIMAMURA H., IWASAKI T., KANAZAWA T. 1995a: S-wave anisotropy off Lofoten, Norway, indicative of fluids in the lower crust? Geophysical Journal International, **120**, pp. 87–96

MJELDE R., KODAIRA S., HASSAN R. K., GOLDSCHMIDT-ROKITA A., TOMITA N., SELLEVOLL M. A., HIRSCHLEBER H. B., SHIMAMURA H., IWASAKI T., KANAZAWA T. 1995b: The continent/ocean ocean transition of the Lofoten volcanic margin, N. Norway. Journal of Geodynamics. In press

MJELDE R., SELLEVOLL M. A. 1993a: Possible shallow crustal S-wave anisotropy off Lofoten, Norway, inferred from 3-C Ocean Bottom Seismographs. Geophysical Journal International, **115**, pp. 159–167

MJELDE R., SELLEVOLL M. A. 1993b: Seismic anisotropy inferred from wide-angle reflections off Lofoten, Norway, indicative of shear-aligned minerals in the upper mantle. Tectonophysics, **222**, pp. 21–32

MJELDE R. 1992: Shear waves from 3-C Ocean Bottom Seismographs off Lofoten, Norway, indicative of anisotropy in the lower crust. Geophysical Journal International, **110**, pp. 283–296

MOKHTARI M. 1991: Geological model for the Lofoten Continental Margin. Dr. Scient. Thesis, Inst. of Solid Earth Physics, Univ. of Bergen, 190 p

MYHRE B.1995: S-wave modelling from thre-component Ocean Bottom Seismographs off Lofoten. (in Norwegian) Ms. Sc. Thesis. Univ. of Bergen

NEIDELL N. S. 1985: Land applications of S-waves. Geophysics: The leading edge of exploration, pp. 32–44

SELLEVOLL M. A., SHIMAMURA H., GIDSKEHAUG A., JOHNSEN H. 1988: Seismic investigations of the Lofoten Margin and seismic reflection measurements on the Mohn's Ridge, R/V Håkon Mosby, 29 July–19 August, 1988. (in Norwegian) Cruise report, Inst. of Solid Earth Physics, Univ. of Bergen, pp. 19

SHIMAMURA H. 1988: OBS technical description. Annexe to cruise report, see SELLEVOLL et al., 1988, pp. 3

SKOGSEID J., ELDHOLM O. 1989: VØRING Plateau Continental Margin: Seismic interpretation, stratigraphy and vertical movements. *In*: ELDHOLM O., THIEDE J., TAYLOR J., (eds.): Proc. ODP, Sci. Results. **104**, pp. 993–1030. College Station, TX (Ocean Drilling Program)

S-hullámok modellezése bazaltlávával fedett területről Lofoten, É-Norvégia vidékén

R. MJELDE, B. MYHRE, M. A. SELLEVOLL, H. SHIMAMURA, T. IWASAKI, T. KANAZAWA

Lofoten (É. Norvégia) peremen lévő bazalt árral fedett területre szeizmikus V_p/V_s modellt dolgoztak ki, amely egy korábbi Ocean Bottom Seismograph (OBS) vizsgálat adatain végzett P-hullám modellezés eredményein alapszik. Az OBS adatok horizontális komponensei az S-hullám kétségtelen jelenlétére utalnak, amelyet 2-D sugárkövetéssel modelleztek. A bazalt feletti üledékben a V_p/V_s hányados középértékét 2,0–2,1-re becsülték. Ezt a viszonylag nagy értéket az üledékek kismértékű konszolidációjának, valamint az agyagok dominanciájának tulajdonítják. A Vøring Szakadék (VE) tengerparti oldalán lévő szelvényben az egész kéregre becsült V_p/V_s hányados 1,9, amely gabbró kifejlődésre és óceáni eredetű kéregre utal. A modellezés szerint a VE szárazföld felőli oldalán a kristályos kéregre lényegesen kisebb : $V_p/V_s = 1,7–1,75$ hányados becsülhető, amely a kéreg gránit/granodiorit litológiáját és kontinentális eredetét sugallja.

Copyright

Fig. 3. Section PGT-4 with enlarged vertical scale
3. ábra. A kinagyított vertikális léptékű PGT-4 szelvény